

ปฏิบัติการไฮโดรจีนชั้นแบบเลือกเกิดของอะเซทิลีนบนตัวเร่งปฏิบัติการแพลเลเดียม
บนไททานเนียมไดออกไซด์ที่เตรียมโดยวิธีโซลโวลเทอรัมอล



นางสาว ลักษณ์า นัคราเรือง

วิทยานิพนธ์นี้เป็นส่วนหนึ่งของการศึกษาตามหลักสูตรปริญญาวิศวกรรมศาสตรมหาบัณฑิต


สาขาวิชาวิศวกรรมเคมี ภาควิชาวิศวกรรมเคมี
คณะวิศวกรรมศาสตร์ จุฬาลงกรณ์มหาวิทยาลัย

ปีการศึกษา 2547

ISBN: 974-53-1388-2

ลิขสิทธิ์ของจุฬาลงกรณ์มหาวิทยาลัย

SELECTIVE HYDROGENATION OF ACETYLENE ON
PALLADIUM CATALYSTS SUPPORTED ON
SOLVOTHERMAL-DERIVED TITANIUM DIOXIDE



Miss Lakkana Nakkararuang

A Thesis Submitted in Partial Fulfillment of the Requirements
for the Degree of Master of Engineering in Chemical Engineering

Department of Chemical Engineering

Faculty of Engineering

Chulalongkorn University

Academic Year 2004

ISBN: 974-53-1388-2

Thesis Title SELECTIVE HYDROGENATION OF ACETYLENE ON
 PALLADIUM CATALYSTS SUPPORTED ON
 SOLVOTHERMAL-DERIVED TITANIUM DIOXIDE

By Miss Lakkana Nakkararuang

Field of Study Chemical Engineering

Thesis Advisor Joongjai Panpranot, Ph.D.

Thesis Co-advisor Bongkot Ngamsom, Ph.D.

Accepted by the Faculty of Engineering, Chulalongkorn University in Partial
Fulfillment of the Requirements for the Master's Degree

..... Dean of the Faculty of Engineering
(Professor Direk Lavansiri, Ph.D.)

THESIS COMMITTEE

..... Chairman
(Associate Professor Suttichai Assabumrungrat, Ph.D.)

..... Thesis Advisor
(Joongjai Panpranot, Ph.D.)

..... Thesis Co-advisor
(Bongkot Ngamsom, Ph.D.)

..... Member
(Varong Pavarajarn, Ph.D.)

..... Member
(Assistant Professor Seeroong Prichanont, Ph.D.)

..... Member
(Choowong Chaisuk, D.Eng.)

ลักษณะ นัคราเรื่อง: ปฏิริยาไฮโดรจีนชันแบบเลือกเกิดของอะเซทิลีนบนตัวเร่งปฏิริยาแพลเลเดียม บนไททาเนียมไดออกไซด์ที่เตรียมโดยวิธีโซลโวเทอร์มอล (SELECTIVE HYDROGENATION OF ACETYLENE ON PALLADIUM CATALYSTS SUPPORTED ON SOLVOTHERMAL-DERIVED TITANIUM DIOXIDE) อ. ที่ปริกาษา: ดร. จุงใจ ปั้นประณต, อ. ที่ปริกาษา (ร่วม): ดร. บงกช งามสม, 127 หน้า. ISBN 974-53-1388-2

ในงานวิจัยนี้ไททาเนียมไดออกไซด์ที่มีผลึกขนาดนาโนเมตร ถูกเตรียมขึ้นโดยการสลายตัวด้วยความร้อนของไททาเนียมนอร์มอลบิวทอกไซด์ในตัวทำละลายที่แตกต่างกัน 2 ชนิด คือ โทลูอินและ 1,4-บิวเทนไดออล ที่อุณหภูมิ 320 องศาเซลเซียส และนำไปใช้เป็นตัวรองรับของตัวเร่งปฏิริยาแพลเลเดียมและแพลเลเดียม-ซิลเวอร์ สำหรับปฏิริยาไฮโดรจีนชันแบบเลือกเกิดของอะเซทิลีน ไททาเนียมไดออกไซด์ที่ได้จากการเตรียมในตัวทำละลายทั้ง 2 ชนิด พบเพียงเฟสอะนาเทสเพียงอย่างเดียว และมีขนาดผลึกและพื้นที่ผิวใกล้เคียงกัน อย่างไรก็ตามจากการศึกษาผลของอิเล็กตรอน สปิน เรโซแนนซ์ (Electron Spin Resonance) พบว่าไททาเนียมไดออกไซด์ที่เตรียมในโทลูอินจะมีค่า Ti^{3+} หรือผลึกที่ไม่สมบูรณ์ของไททาเนียมไดออกไซด์มากกว่าผลึกที่เตรียมใน 1,4-บิวเทนไดออล เมื่อใช้ไททาเนียมไดออกไซด์อะนาเทสเฟสที่มีค่า Ti^{3+} สูงเป็นตัวรองรับของตัวเร่งปฏิริยาแพลเลเดียม ในปฏิริยาไฮโดรจีนชันแบบเลือกเกิดของอะเซทิลีน พบว่าให้ค่าความว่องไวและค่าการเลือกเกิดเป็นเอทิลีนต่ำกว่า อย่างไรก็ตาม ไม่พบผลดังกล่าวในตัวเร่งปฏิริยาแพลเลเดียมที่เสริมด้วยโลหะซิลเวอร์

สถาบันวิทยบริการ จุฬาลงกรณ์มหาวิทยาลัย

ภาควิชา.....วิศวกรรมเคมี
สาขาวิชา.....วิศวกรรมเคมี
ปีการศึกษา.....2547

ลายมือชื่อนิสิต.....
ลายมือชื่ออาจารย์ที่ปริกาษา.....
ลายมือชื่ออาจารย์ที่ปริกาษาร่วม.....

4670462421 : MAJOR CHEMICAL ENGINEERING

KEYWORDS: NANOCRYSTALLINE TITANIA/ SOLVOTHERMAL METHOD/
ACETYLENE HYDROGENATION/ SUPPORTED PALLADIUM CATALYSTS

LAKKANA NAKKARARUANG: SELECTIVE HYDROGENATION OF
ACETYLENE ON PALLADIUM CATALYSTS SUPPORTED ON
SOLVOTHERMAL-DERIVED TITANIUM DIOXIDE. THESIS
ADVISOR: JOONGJAI PANPRANOT, Ph.D., THESIS CO-ADVISOR:
BONGKOT NGAMSOM, Ph.D. 127 pp. ISBN: 974-53-1388-2

In this study, nanocrystalline titanias have been prepared by thermal decomposition of titanium (IV) *n*-butoxide in two different solvents (toluene and 1,4-butanediol) at 320°C and employed as supports for Pd and Pd-Ag catalysts for selective acetylene hydrogenation. The titania products obtained from both solvents showed only anatase phase with similar crystallite sizes and BET surface areas. However, due probably to the different crystallization pathways, the number of Ti³⁺ defective sites as shown by ESR results of the titania prepared in toluene were much higher than the ones prepared in 1,4-butanediol. It was found that the use of anatase titania with higher Ti³⁺ defective sites as a support for Pd catalysts resulted in lower activity and ethylene selectivity in selective acetylene hydrogenation. However, this effect was suppressed by Ag promotion.

Department	Chemical Engineering	Student's signature
Field of Study	Chemical Engineering	Advisor's signature
Academic year	2004	Co-advisor's signature

ACKNOWLEDGEMENTS

The author would like to express her sincere gratitude and appreciation to her advisor, Dr. Joongjai Panpranot, for her invaluable suggestions, encouragement during her study, useful discussions throughout this research and especially, giving her the opportunity to present her research at RSCE conference in Thailand. Without the continuous guidance and comments from her co-advisor, Dr. Bongkot Ngamsom, this work would never have been achieved. In addition, the author would also be grateful to Associate Professor Suttichai Assabumrungrat, as the chairman, and Dr. Varong Pavarajarn, Dr. Choowong Chaisuk, and Assistant Professor Seeroong Prichanont, as the members of the thesis committee. The financial supports of the Thailand Research Fund (TRF), TJTTP-JBIC, and the Graduate School of Chulalongkorn University are gratefully acknowledged.

Most of all, the author would like to express her highest gratitude to her parents who always pay attention to her all the times for suggestions and listen her complain. The most success of graduation is devoted to my parents.

The author would like to acknowledge with appreciation to Miss Patta Soisuwan, Dr. Okorn Mekasuwandumrong, and Dr. Bunjerd Jungsomjit for their kind suggestions on her research without hesitation.

Finally, the author wishes to thank the members of the Center of Excellence on Catalysis and Catalytic Reaction Engineering, Department of Chemical Engineering, Faculty of Engineering, Chulalongkorn University for friendship and their assistance especially Mr. Kongkiat Suriye. To the many others, not specifically named, who have provided her with support and encouragement, please be assured that she thinks of you.

CONTENTS

	Page
ABSTRACT (IN THAI)	iv
ABSTRACT (IN ENGLISH)	v
ACKNOWLEDGMENTS	vi
CONTENTS	vii
LIST OF TABLES	x
LIST OF FIGURES	xi
CHAPTER	
I INTRODUCTION	1
II LITERATURE REVIEWS	3
2.1 Synthesis of nanocrystalline titania by solvothermal method	4
2.2 Supported Pd catalyst in selective hydrogenation reaction.....	5
2.3 Role of titania in the selective hydrogenation on Pd catalysts...	10
2.4 Comments on the previous studies.....	13
III THEORY	14
3.1 Titanium	14
3.2 Titanium (IV) oxide	15
3.3 Acetylene Hydrogenation Reaction.....	19
3.4 Promoters	22
IV EXPERIMENTS	23
4.1 Chemicals	23
4.2 Equipment.....	25
4.2.1 Autoclave reactor.....	25
4.2.2 Temperature program controller.....	26
4.2.3 Electrical furnace (Heater).....	26
4.2.4 Gas controlling system.....	26
4.3 Catalyst Preparation.....	27
4.3.1 Preparation of titanium dioxide support.....	27
4.3.2 Palladium loading.....	28
4.4 Catalyst Characterization.....	29

4.4.1 Atomic Absorption Spectroscopy (AAS).....	29
4.4.2 X-ray diffraction	29
4.4.3 BET Surface Area	29
4.4.4 Thermalgravimetric Analysis (TGA).....	29
4.4.5 CO-pulse chemisorption	30
4.4.6 Scanning electron microscopy (SEM)	33
4.4.7 Transmission electron microscopy (TEM)	33
4.4.8 CO ₂ Temperature Programmed Desorption (CO ₂ -TPD)...	33
4.4.9 Electron Spin Resonance (ESR.).....	33
4.4.10 Temperature Programmed Desorption.....	34
4.4.10 Temperature Programmed Oxidation.....	34
4.5 Reaction study in acetylene hydrogenation	38
V RESULTS AND DISCUSSION	42
5.1 Solvothermal-derived titania	42
5.1.1 Formation of titanium dioxide synthesized in 1,4-butanediol.....	42
5.1.2 Formation of titanium dioxide synthesized in toluene.....	43
5.1.3 Support structure and morphology	44
5.2 1%Pd over Titanium (IV) oxide catalyst.....	56
5.2.1 Catalyst Characterisation (fresh catalyst).....	56
5.2.2 Reaction Study in the Selective hydrogenation of Acetylene.....	61
5.2.3 Catalyst Characterisation (spent catalyst).....	69
5.3 1%Pd-3%Ag over Titanium (IV) oxide catalyst.....	70
5.3.1 Catalyst Characterisation(fresh catalyst).....	70
5.3.2 Reaction Study in the Selective hydrogenation of acetylene.....	75
5.3.3 Catalyst Characterisation (spent catalyst).....	78
5.4 Temperature Programmed Study.....	80
5.4.1 Temperature programmed desorption after ethylene adsorption for 3 h.....	80

5.4.2 Determination of the effluent gases during temperature programmed desorption.....	83
5.4.3 Proposed mechanism for selective acetylene hydrogenation on the solvothermal TiO ₂ supported Pd and Pd-Ag catalysts.....	85
VI CONCLUSIONS AND RECOMMENDATIONS.....	87
6.1 Conclusions.....	87
6.2 Recommendations.....	88
REFERENCES.....	89
APPENDICES	
APPENDIX A: CALCULATION FOR CATALYST PREPARATION.....	96
APPENDIX B: CALCULATION FOR THE CRYSTALLITE SIZE.....	98
APPENDIX C: CALCULATION FOR METAL ACTIVE SITES AND DISPERSION.....	101
APPENDIX D: CALIBRATION CURVES.....	102
APPENDIX E: CALCULATION OF CONVERSION AND SELECTIVITY..	105
APPENDIX F: LIST OF PUBLICATIONS.....	106
VITA.....	127

LIST OF TABLES

TABLE		Page
3.1	Thermal data for changes of state of titanium compounds.....	15
3.2	Crystallographic properties of anatase, brookite, and rutile.....	17
4.1	Chemicals used in the experiment.....	24
4.2	Reactants used for the synthesis of titania.....	25
4.3	Operating conditions of gas chromatograph (GOW-MAC).....	31
4.4	Operating conditions of gas chromatograph (GC-8A).....	36
4.5	Operating conditions of gas chromatograph for selective hydrogenation of acetylene.....	40
5.1	Average crystallite size and surface area of titania products.....	45
5.2	Dielectric constant	48
5.3	BET surface area of 1%Pd/TiO ₂	56
5.4	Results from Pulse CO Chemisorption of 1%Pd/TiO ₂	58
5.5	Average palladium oxide crystallite sizes of 1%Pd/TiO ₂	67
5.6	BET Surface area of 1%Pd-3%Ag/TiO ₂	70
5.7	Results from Pulse CO Chemisorption of 1%Pd-3%Ag/TiO ₂	72

LIST OF FIGURES

FIGURE		Page
2.1	Reaction between a species (G^*) and an adsorbed molecule R.....	6
3.1	Crystal structure of TiO_2	16
3.2	Major reaction path of acetylene hydrogenation system.....	21
4.1	Autoclave reactor.....	26
4.2	Diagram of the reaction equipment for the catalyst preparation.....	27
4.3	Flow diagram of CO chemisorption measurement.....	32
4.4	Flow diagram of measurement of Temperature Programmed Oxidation.....	37
4.5	A schematic of acetylene hydrogenation system.....	41
5.1	Mechanism of solvothermal reaction for the anatase formation.....	43
5.2	Mechanism of reaction in toluene for the titania product.....	44
5.3	XRD patterns of titania products.....	46
5.4	SEM images of titania products synthesized in BG	49
5.5	SEM images of titania products synthesized in toluene	50
5.6	The TGA profile of titania.....	52
5.7	Temperature Programmed Desorption of CO_2 of titania products	53
5.8	ESR results of titania products.....	55
5.9	XRD patterns of 1%Pd/ TiO_2	57
5.10	TEM micrograph of 1%Pd/ TiO_2 (fresh catalyst).....	60
5.11	Reaction result on 1%Pd/ TiO_2 in acetylene hydrogenation (H_2 /acetylene = 2, temperature = $50^\circ C$).....	64
5.12	Reaction result on 1%Pd/ TiO_2 in acetylene hydrogenation (H_2 /acetylene = 2, balance N_2 , total flow 200 cc/min).....	66

5.13	TEM micrograph of 1%Pd/TiO ₂ (spent catalyst).....	68
5.14	Temperature programmed oxidation profiles.....	69
5.15	XRD patterns of 1%Pd3%Ag/TiO ₂	71
5.16	TEM micrograph of 1%Pd-3%Ag/TiO ₂ (fresh catalyst).....	74
5.17	Reaction result on 1%Pd3%Ag/TiO ₂ in acetylene hydrogenation (H ₂ /acetylene = 2, balance N ₂ , total flow 200 cc/min).....	76
5.18	Reaction result on various catalyst in acetylene hydrogenation (H ₂ /acetylene = 2, balance N ₂ , total flow 200 cc/min).....	77
5.19	TEM micrograph of 1%Pd-3%Ag/TiO ₂ (spent catalyst).....	79
5.20	Temperature programmed desorption study.....	82
5.21	Temperature programmed profile of carbon dioxide.....	84
5.22	Temperature programmed profile of methane.....	84
5.23	The mechanisms of the selective hydrogenation of acetylene to ethylene.....	86

CHAPTER I

INTRODUCTION

The solvothermal method has been used to successfully synthesize various types of nanosized metal oxides with large surface area, high crystallinity, and high thermal stability (Inoue *et al.*, 1988; Inoue *et al.*, 1992; Inoue *et al.*, 1993; Kominami *et al.*, 1999; Kongwudthiti *et al.*, 2003; Mekasuwandumrong *et al.*, 2003 and Payakgul *et al.*, 2005). For example, thermal decomposition of titanium (IV) *n*-butoxide in organic solvents yields nano-sized pure anatase titania without bothersome procedures such as purification of the reactants or handling in an inert atmosphere. These nanocrystalline titanias have been shown to exhibit high photocatalytic activities (H. Kominami *et al.*, 2001 and Ohtani *et al.*, 1995). However, thermal stability as well as photocatalytic activity of the solvothermal-derived titania were found to be strongly dependent on the organic solvent used as the reaction medium during crystallization (Payakgul *et al.*, 2004). The titania products synthesized in toluene showed lower thermal stability and lower photocatalytic activities than the ones synthesized in 1,4-butanediol. The authors suggested that the amount of defect structures in the titania prepared by this method was different depending on the solvent used due to the different crystallization pathways.

Due to their unique properties, it is interesting to investigate the characteristics and catalytic properties of the solvothermal-derived nanocrystalline titania supported noble metal catalysts as another exploitation of such materials

Supported palladium catalysts are widely used for selective acetylene hydrogenation to ethylene (Shin *et al.*, 1998; Kim *et al.*, 2003 and Ngamsom *et al.*, 2004). The commonly used supports for palladium are α -alumina and silica. However, it has recently been reported that Pd/TiO₂ catalysts exhibited higher activities and selectivities in selective acetylene hydrogenation than Pd/Al₂O₃ catalyst (Chu *et al.*,

2004). It is well known that metal catalyst supported on titania exhibits “the strong metal-support interaction” (SMSI) phenomenon after reduction at high temperatures due to the decoration of the metal surface by partially reducible metal oxides (Santos *et al.*, 1983 and Raupp *et al.*, 1985) or by an electron transfer between the support and the metals (Herrmann *et al.*, 1987 and Chou *et al.*, 1987). Recently, J. H. Kang *et al.* (2002) reported that during the selective hydrogenation of acetylene to ethylene on Pd/TiO₂ catalysts, charge transfer from Ti species to Pd weakened the adsorption strength of ethylene on the Pd surface hence higher ethylene selectivity was obtained.

In this study, nanocrystalline titania were synthesized by the solvothermal method in two different solvents (1,4-butanediol and toluene) and employed as supports for Pd and Pd-Ag catalysts. The nature of the titania supports and its effect on the characteristics of the catalysts were the main focuses. Moreover, the effect of defective structures in titania on the catalytic performances of the titania supported Pd and Pd-Ag catalysts in acetylene hydrogenation was investigated. The study has been scoped as follows:

1. Preparation of titanium dioxide using solvothermal technique in two different solvents (toluene and 1,4-butanediol).
2. Preparation of titanium dioxide supported Pd (1wt%Pd) and Pd-Ag catalysts (1wt%Pd-3wt%Ag) using the incipient wetness impregnation method.
3. Characterization of the catalyst samples using atomic absorption spectroscopy (AAS), X-ray diffraction (XRD), BET surface area, thermogravimetric analysis (TGA), scanning electron microscopy (SEM), transmission electron microscopy (TEM), pulse CO chemisorption, electron spin resonance (ESR) and temperature programmed study.
4. Reaction study of the catalyst samples in selective acetylene hydrogenation at 40-90°C and 1.01 bar using a fixed-bed quartz reactor.

CHAPTER II

LITERATURE REVIEWS

Titanium dioxide has been widely applied in many applications i.e., electronic materials, cosmetic materials, photocatalysis, etc. The development of TiO₂ synthesis route has been extensively investigated. Now nanocrystalline titania can be synthesized via different preparation techniques such as sol gel processing and solvothermal method. These nanocrystalline titanias have been shown to exhibit high photocatalytic activities. However, less is known about applications of these titanias as catalyst supports.

Selective hydrogenation of acetylene to ethylene is a well-known catalytic reaction used to purify ethylene feedstocks for the production of polyethylene. Typically, supported palladium catalyst is employed for this process due to its good activity and selectivity. Nevertheless, various factors have shown to affect the performance of Pd catalysts for the selective hydrogenation of acetylene such as addition of a second metal, pretreatment with oxygen-containing compounds, H₂ spill-over and support effects.

This chapter summarizes the recent reports about (1) synthesis of nanocrystalline titania using solvothermal method, (2) supported Pd catalysts in selective hydrogenation reaction, and (3) role of titania in the selective hydrogenation on Pd catalysts which are given in section 2.1-2.3, respectively. Comments on the previous studies are also given in section 2.4

2.1 Synthesis of nanocrystalline titania by solvothermal method

Solvothermal method (Kominami *et al.*, 1999) has been developed for synthesis of metal oxide and binary metal oxide by using solvent as the reaction medium. Use the solvent instead of the water in the hydrothermal method produce the different forms of intermediate phase and the stability of such intermediate phase was not strong. Instability of the intermediate phase gives a large driving force to the formation of product under quite mild condition.

C. S. Kim *et al.* (2003) synthesized TiO₂ nanoparticles in toluene solutions with isopropoxide (TIP) as precursor by a solvothermal synthetic method. Weight ratios of precursor to solvent prepared in the mixture are 5/100, 10/100, 20/100, 30/100 and 40/100. At the weight ratio of 10/100, 20/100 and 30/100, TiO₂ nanocrystalline particles were obtained after synthesis at 250°C for 3 h in an autoclave. TiO₂ particles are formed and they have a uniform anatase structure with average particle size below 20 nm. As the composition of TIP in the solution increases, the particle size of TiO₂ powder tends to increase. For the products obtained from the solution of 5/100 and 40/100, crystalline particles cannot be obtained. The 5/100 of TIP in the mixture may be too small amount to synthesize TiO₂ nanoparticles at 250°C and longer time is also needed to obtain adequate size of the particle. In the mixture of 40/100 TIP the synthetic process of TiO₂ particles may be hindered by agglomeration of the reactants due to surplus of precursor.

H. Kominami *et al.* (2003) studied thermal treatment of titanium (IV) butoxide dissolved in 2-butanol at 573K under autogenous pressure (alcoholthermal treatment) yielded microcrystalline anatase-type titanium (IV) oxide (TiO₂). Thermal treatment of oxobis (2,4-pentanedionato-O,O') titanium (TiO(acac)₂) in ethylene glycol (EG) in the presence of sodium acetate and a small amount of water at 573K yielded microcrystalline brookite-type TiO₂. Tungsten (VI) oxide (WO₃) powders of monoclinic crystal structure with high crystallinity were synthesized by hydrothermal treatment (HTT), at 523 or 573 K, of aqueous tungstic acid (H₂WO₄) solutions prepared from sodium tungstate by ion-exchange (IE) with a proton-type resin. Anatase and brookite TiO₂ products were

calcined at various temperatures and then used for photocatalytic mineralization of acetic acid in aqueous solutions under aerated conditions and dehydrogenation of 2-propanol under deaerated conditions. Almost all the anatase-type TiO_2 samples showed the activities more than twice higher than those of representative active photocatalysts, Degussa P-25 and Ishihara ST-01 in both reactions. A brookite sample with improved crystallinity and sufficient surface area obtained by calcination at 973K exhibited the hydrogen evolution rate almost equal to P-25. HTT WO_3 powders with various physical properties were used as photocatalyst for evolution of oxygen (O_2) from an aqueous silver sulfate solution. WO_3 powder of high crystallinity, e.g., IE-HTT- WO_3 synthesized at 573 K, gave much higher O_2 yield than commercially available WO_3 samples.

Payakgul *et al.* (2005) synthesized titania using thermal decomposition of titanium (IV) n-butoxide (TNB) in organic solvents yields nanosized anatase titania without the contamination of other phases. From the characteristic, it is suggested that anatase titania synthesized in 1,4-butanediol is the result from direct crystallization while titania synthesized in toluene is transformed from precipitated amorphous intermediate. Thermal stability of products investigated by calcination at various temperatures and photocatalytic activity evaluated from ethylene decomposition reaction suggest that amount of defect structures in titania synthesized depends upon the solvent used.

2.2 Supported Pd catalyst in selective hydrogenation reaction

Sárkány and coworker (A. Sárkány *et al.*, 1984) studied the hydrogenation of a mixture of 0.29 mole% C_2H_2 , 0.44 mole% H_2 and C_2H_4 up to 100%, a so-call tail-end mixture, on palladium black and several Pd/ Al_2O_3 catalysts. Hydrogenation of C_2H_4 increased with time on stream for all the Al_2O_3 -supported catalysts; the opposite behaviour was noted with palladium black. Polymer formation was noted for all catalysts studied and also increased with time. It was recognized that a small number of C_2H_4 hydrogenation sites were located on the metal but the majority were on the polymer-covered support. The authors proposed that C_2H_4 adsorbed on the support and was hydrogenated there. Spill-over hydrogen was tentatively identified as the source of

hydrogen. Because of the parallelism between polymer formation and ethylene hydrogenation, it was proposed that the surface polymer served as a hydrogen pool or facilitated diffusion of hydrogen from Pd to the support.

Hydrogen spill-over (B. K. Hodnett *et al.*, 1986) is the deal of evidence used to suggest the surface-mobile species. It can play a role in catalytic reaction involving hydrogen. However, spill-over hydrogen is elusive it has never been detected by physico-chemical means under condition similar to those prevailing during catalysis. It is therefore difficult to determine the real role of this species in catalytic hydrogenation, hydrogenolysis and other hydrotreating reactions. The effects attributed to spill-over are usually chemical effect, e.g., hydrogenation by spill-over hydrogen of species adsorbed on a support, removal of carbonaceous deposits, occurrence or enhancement of a given reaction and, more generally, change in catalytic activity. These phenomena are frequency anomalous and can often be explained only by invoking surface mobility and spill-over from one phase to another. The hydrogen spill-over phenomenon is described in Figure 3.2. Essentially a hydrogen species is formed on one phase (usually a metal) and spilled over to react on the other phase.

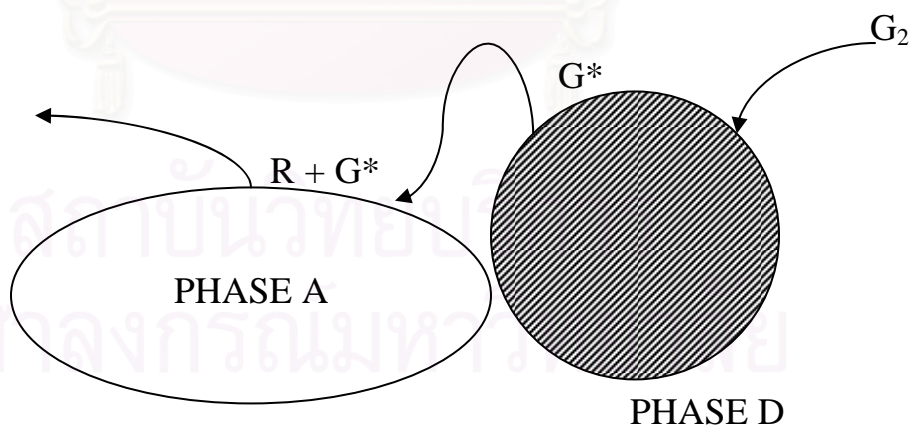


Figure 2.1 Reaction between a species (G^*), formed on phase D, and then transferred to phase A by spill-over and surface diffusion, where it reacts with an adsorbed molecule R . (re-drawn from B. K. Hodnett *et al.*, 1986)

S. Asplund (1996) studied the catalyst aging by coke formation for the selective hydrogenation of acetylene in the presence of excess ethylene on supported palladium catalyst. He found that the deposited coke have a substantial influence on the effective diffusivity, which decreased about one order of magnitude during 100 h of operation. He also observed previously the selectivity for the undesired ethane was higher on aged catalysts, while the activity for acetylene hydrogenation was almost constant. However, these effects were strongly dependent on the catalyst particle size, although the behavior of fresh catalysts was unaffected by mass transfer limitations. When the catalyst used was Pd/Al₂O₃ the change in selectivity with aging could be explained solely as a consequence of the increased diffusion resistance. The mass transfer effects were important also on Pd/Al₂O₃, but on this catalyst there was an additional increase in ethane selectivity that could not be attributed to diffusion limitations. Calculations and experimental tests showed that the observed phenomena are relevant also for the shell-type catalysts normally used industrially. The coke formation itself was about four to five times faster on Pd/ α -Al₂O₃ compared to the α -Al₂O₃ supported catalyst. The coke was generally concentrated towards the pellet periphery showing the influence of diffusion resistance also on the coke-forming reactions.

E. W. Shin *et al.* (1998) synthesized supported Pd catalysts modified with Si deposited on the support by silane decomposition when used in acetylene hydrogenation; the Si-modified catalysts show higher selectivity for ethylene and produce less amount of green oil than the unmodified Pd catalysts. They suggested that Si covers the Pd surface as Si or SiO₂ patches. The Pd surface is diluted with the deposited Si. However, the electronic property of the Pd surface seems to be unaffected by the Si species. They conclude that improved performance of the Si modified catalysts comes mostly from geometric modification of the Pd surface by Si.

J. H. Kang *et al.* (2000) studied the effect of transition-metal oxides as promoters of the Pd catalyst for acetylene hydrogenation. Transition-metal oxides added to Pd/SiO₂ improve significantly the activity and the ethylene selectivity of the catalyst in acetylene hydrogenation, which is caused by the interaction between the oxides and the Pd surface

similar to the case of the oxide-supported catalysts. They confirmed that metal oxide spread on and modify both geometrically and electronically the Pd surface after the catalyst is reduced at 500°C. Such a behavior of metal oxides in the catalyst is correlated well with their promotional effect on the catalyst performance. They found that the oxide on the Pd surface retard the sintering of the dispersed Pd particles, suppresses the adsorption of ethylene in the multiply-bound mode, and facilitates the desorption of ethylene produced by acetylene hydrogenation. Among the three metal oxides examined in this study, titanium oxide is found to have the most promotional effect.

Q. Zhang *et al.* (2000) studied an alloy of palladium and silver dispersed on Al₂O₃ for the selective hydrogenation of acetylene. They reported that the activity of Pd–Ag catalyst is lower than that of pure metal Pd catalyst. But the selectivity of Pd–Ag catalyst is higher and less impaired by temperature increase than that of Pd catalyst. They also found that metal Pd and Ag can form an alloy on the surface of alumina. There is a synergetic effect in the hydrogenation of acetylene over Pd–Ag catalyst. Addition of Ag to Pd catalyst decreases the quantity of absorption hydrogen, and reduces absorption hydrogen spill over from the bulk of the metals to react with acetylene, which increases the selectivity of acetylene hydrogenation to ethylene.

A Sárkány *et al.* (2002) investigated acetylene hydrogenation and formation of surface deposits on two series of Pd and Pd–Au/SiO₂ catalysts differing in metal particle size ($D = 0.47$ and 0.08). Gold was deposited via ionization of pre adsorbed hydrogen over pre-reduced Pd/SiO₂ in order to ensure selective poisoning of the Pd surface. The non-steady-state regime of operation and the accumulation of hydro carbonaceous over layer were tested in pulse-flow experiments. They determined concentration of surface hydro carbonaceous deposits accumulated during different treatments by temperature programmed oxidation (TPO). They also observed hydrocarbon over layer to form immediately and its presence appeared to be a necessary requisite to get steady-state conversion and selectivity data. They suggested that a large excess of hydrogen suppressed the formation of carbonaceous lay down and increased the over-hydrogenation of acetylene. Presence of Au decreased the carbon coverage and

improved the ethene selectivity. Decoration of Pd by Au and the morphology of particles explain the ethene selectivity improvement.

E. W. Shin *et al.* (2002) studied the origin of the selectivity improvement over the supported Pd catalyst modified with Si, which is deposited selectively on Pd by silane decomposition and subsequently oxidized in oxygen, by observing the adsorption and desorption behavior of acetylene, ethylene, and hydrogen on the Pd surface. They reported that the adsorption strength of ethylene on Pd becomes weak and the amount of adsorbed hydrogen decreases when the Pd catalyst is modified with Si. The Si modification also reduces the amounts of surface hydrocarbons or carbonaceous species that are deposited on the catalyst either during the temperature programmed desorption (TPD) of ethylene or by surface reactions between co adsorbed acetylene and hydrogen. The hydrocarbon species deposited on the Si modified catalyst have a shorter chain length than those produced on the Pd-only catalyst. All these results are consistent with the improvement in ethylene selectivity on the Si-modified Pd catalyst, which has been explained based on the reaction mechanism of acetylene hydrogenation.

A. Sárkány *et al.* (2003) synthesized Pd/SiO₂ (1.08 wt.%) catalyst via sol-derived route using poly(diallyldimethylammonium chloride) (PDDA) polycation as ionic stabiliser. The immobilised sol (monomer/Pd²⁺ = 1.25) fixed at pH = 8.5 onto Aerosil 200 contains Pd particles of 3.1 nm number-mean diameter. The immobilised sol showed good thermal stability but oxidation of PDDA to get “polymer free” sample causes sintering of Pd particles. They reported that the immobilized sample even in “as prepared state” possesses hydrogenation activity. Treatments at different temperatures in H₂ or Ar enhance the catalytic activity suggesting an increase in space around the metal particle. They suggested that the PDDA modified sample exhibits better competition selectivity than the “polymer free” sample pointing to surface structure variations caused by geometric/steric effects.

W. J. Kim *et al.* (2003) studied the deactivation behavior of Si-modified Pd catalysts in acetylene hydrogenation. They reported that TGA and IR analyses of green

oil produced on the catalyst indicate that it is produced in smaller amounts and its average chain length is shorter on a Si-modified catalyst than on an unmodified one. The above findings are due to deposition of Si species on the Pd surface; such deposits effectively block multiply-coordinated adsorption sites on the catalyst and suppress the formation of green oil on the catalyst surface, specifically on or in the vicinity of Pd. The Si species also retard the sintering of Pd crystallites during the regeneration step and allow for the slow deactivation of the catalyst during acetylene hydrogenation, after regeneration. They also suggested that the improvement in the deactivation behavior of the Si-modified catalyst is believed to arise from the geometric modification of the Pd surface with small clusters of the Si species.

2.3 Role of titania in the selective hydrogenation on Pd catalysts

J. H. Kang *et al.* (2002) investigated the performance of TiO₂-modified Pd catalysts, containing TiO₂ either as an additive or as a support, in the selective hydrogenation of acetylene was investigated using a steady-state reaction test. They reported that the TiO₂ added Pd catalyst reduced at 500°C (Pd-Ti/SiO₂/500°C) showed a higher selectivity for ethylene production than either the Pd/TiO₂ or Pd/SiO₂ catalyst. The amounts of chemisorped H₂ and CO were significantly reduced and, in particular, the adsorption of multiply coordinated CO species was suppressed on Pd-Ti/SiO₂/500°C, which is characteristic of the well-known strong-metal-support-interaction (SMSI) phenomenon that has been observed with the TiO₂-supported Pd catalyst reduced at 500°C, Pd/TiO₂/500°C. Moreover, XPS analyses of Pd-Ti/SiO₂/500°C suggested an electronic modification of Pd by TiO₂, and the TPD of ethylene from the catalyst showed the weakening in ethylene adsorption on the Pd surface. The 1,3-Butadiene was produced in smaller amounts when using Pd-Ti/SiO₂/500°C than when using Pd/SiO₂/500°C, indicating that the polymerization of C₂ species leading to catalyst deactivation proceeds at slower rates on the former catalyst than on the latter. They also suggested that the enhanced ethylene selectivity on Pd-Ti/SiO₂/500°C may be explained by correlating the catalyst surface properties with the mechanism of acetylene hydrogenation.

W. J. Kim *et al.* (2004) studied the deactivation behavior of a TiO₂-added Pd catalyst, reduced at 773 K, for the selective hydrogenation of acetylene showed that the added TiO₂ to a Pd catalyst, reduces the amount of green oil deposited on and in the vicinity of Pd sites and maintains the average number of carbon atoms per green oil molecule was smaller for the TiO₂-added catalyst than for the Pd-only catalyst because multiply coordinated Pd sites were suppressed on the TiO₂-added catalyst so TiO₂ improved the lifetime of the catalyst. Accordingly, the TiO₂-added Pd catalyst becomes deactivated at slower rates than the Pd-only catalyst and the deactivation of the former catalyst was nearly unaffected by the regeneration.

Y. Li *et al.* (2003) investigated in situ EPR by using CO as probe molecules shows that even prerduced by H₂ at lower temperature results in SMSI for anatase titania supported palladium catalyst, but not for rutile titania supported palladium catalyst, which is attributed that the Ti³⁺ ions produced by reduction of Ti⁴⁺ by the dissociatively chemisorbed hydrogen on palladium diffusing from Pd to TiO₂ are fixed in the surface lattice of TiO₂, as rutile titania is more thermodynamically and structurally stable than anatase titania so that the Ti³⁺ ions fixed in the surface lattice of anatase TiO₂ is easier to diffuse to surface of palladium particle than one in the surface lattice of rutile TiO₂. The reason why the pre-reduction of both anatase and rutile supported palladium catalyst at higher temperature results in SMSI between Ti³⁺ and Pd is attributed that the thermal diffusion of produced Ti³⁺ ion at higher temperature is much easier than at lower temperature so that it could overcome the binding of surface lattice of both anatase and rutile titania to move to the surface or surrounding of palladium particle. The very different catalytic properties between 0:075%Pd/TiO₂ (R) and 0:075%Pd/TiO₂ (A) catalyst pre-reduced at lower temperature, and the rapid change of conversion and selectivity of 0:075%Pd/TiO₂ (A) and 0:075%Pd/TiO₂ (R) with the elevation of pre-reduction temperature further confirm the presence of SMSI both for anatase titania supported palladium catalyst pre-reduced at lower temperature, and titania (rutile and anatase) supported palladium catalyst pre-reduced at higher temperature.

W. J. Kim *et al.* (2004) investigated the effect of potassium (K) addition on the performance of a TiO₂-modified Pd catalyst in the hydrogenation of acetylene. When potassium was added to Pd-Ti/SiO₂, the resulting catalyst showed an improved selectivity for ethylene production over a wide range of conversions, when the catalyst was reduced at 300°C. This is in contrast with the case of K-free Pd-Ti/SiO₂, which showed an improved selectivity only when the catalyst was reduced at high temperatures, e.g. 500°C. They found that k-containing Pd surface is modified with the Ti species after the catalyst is reduced at relatively low temperatures. The origin of the facilitated modification is the formation of potassium titanates, which have a lower melting point than that of TiO₂ and therefore migrate onto the Pd surface after the catalyst, is reduced at lower temperatures compared to the case of TiO₂.

Y. Li. *et al.* (2004) investigated in situ EPR and IR by using CO as probe molecules show that even pre-reduced by H₂ at lower temperature results in SMSI for anatase titania supported palladium catalyst, but not for rutile titania supported palladium catalyst. This deference is attributed that the Ti³⁺ ions produced by reduction of Ti⁴⁺ are fixed in the surface lattice of TiO₂, as rutile titania is more thermodynamically and structurally stable than anatase titania so that the Ti³⁺ ions fixed in the surface lattice of anatase TiO₂ is easier to diffuse to surface of palladium particle than one in the surface lattice of rutile TiO₂. The reason why the pre-reduction of both anatase and rutile supported palladium catalyst at higher temperature results in SMSI between Ti³⁺ and Pd is attributed that the thermal diffusion of produced Ti³⁺ ion at higher temperature is much easier than at lower temperature so that it could overcome the binding of surface lattice of both anatase and rutile titania to move to the surface or surrounding of palladium particle. The anatase titania supported palladium catalyst 0.075%Pd/TiO₂ (A) reduced at lower temperature has higher selectivity of alkenes than rutile titania supported palladium catalysts 0.075%Pd/TiO₂ (R). For titania (rutile or anatase) supported palladium catalysts, the elevation of pre-reduction temperature from 200 to 450°C gives rise to sharp change of catalytic properties, especially for selectivity of alkenes. The very different catalytic properties between 0.075%Pd/TiO₂ (R) and 0.075%Pd/TiO₂ (A) catalyst pre-reduced at lower temperature, and the rapid change of conversion and selectivity of 0.075%Pd/TiO₂

(A) and 0.075%Pd/TiO₂ (R) with the elevation of pre-reduction temperature are reasonably explained by the presence of SMSI both for anatase titania supported palladium catalyst pre-reduced at lower temperature, and titania (rutile and anatase) supported palladium catalyst pre-reduced at higher temperature.

2.4 Comments on the previous studies

From the previous studies it was found that titanias synthesized using solvothermal method has large surface areas and high thermal stability (Kominami *et al.*, 1999). There is no report on the use of these solvothermal-derived titanias as supports for Pd and Pd-Ag catalyst for selective hydrogenation reaction. However, addition of TiO₂ into Pd/SiO₂ catalysts has shown to improve the reactivity for selective hydrogenation of acetylene due to the decoration of Pd surface by Ti species lower the adsorption strength of ethylene on Pd (Shin *et al.*, 2002). Moreover, Li *et al.* (2003) and Li *et al.* (2004) have shown the effect of Ti³⁺ ions in TiO₂ particles on the catalytic properties of Pd/TiO₂ catalysts in selective hydrogenation of long chain alkadienes. Thus, it is interesting to study the synthesis, characteristic, and catalytic properties of Pd and Pd-Ag catalysts supported on the titania synthesized by solvothermal method in a well-known selective hydrogenation reaction.

CHAPTER III

THEORY

3.1 Titanium (Ti)

Titanium (atomic number 22; ionization potentials: first 6.83 eV, second 13.67 eV, third 27.47 eV, fourth 43.24 eV) is the first member of Group IVB of the periodic chart. It has four valence electrons, and Ti (IV) is most stable valence state. The lower valence states Ti (II) and Ti (III) exist, but these are readily oxidized to the tetravalent state by air, water, and other oxidizing agent. The ionization potentials indicate that the Ti^{4+} ion would not be expected to exist and, indeed, Ti (IV) compounds are generally covalent. Titanium is able to expand its outer group of electrons and can form a large number of addition compounds by coordination other substances having donor atom, e.g., oxygen or sulfur. The most important commercial forms are titanium (IV) oxide and titanium metal.

Thermochemical data

Thermochemical data of titanium (IV) oxide and other titanium compounds are described. Data relating to changes of state of selected titanium compounds are listed in Table 3.1.

Table 3.1 Thermal data for changes of state of titanium compounds

Compound	Properties	Temperature,°C	$\Delta H, \text{kJ/mol}$
TiCl ₄	melting point	-23.95	9.966
	Boiling point	136	35.77
TiCl ₃	sublimation temperature	831.1	166.15
TiCl ₂	sublimation temperature	1318.5	248.5
TiI ₄	melting point	155	19.23±0.63
	Boiling point	379.6	56.48±2.09
TiF ₄	sublimation temperature	285.6	97.78±0.42
TiBr ₄	melting point	38.4	12.89
	Boiling point	231.1	45.19
TiO ₂	phase change (anatase to rutile)		ca-12.6

3.2 Titanium (IV) oxide (Othmer, 1991 and Fujishima *et al.*, 1999)

Physical and chemical properties

Titanium dioxide may take on any of the following three crystal structures: rutile, which tends to be more stable at high temperatures and thus is sometimes found in igneous rocks, anatase, which tends to be more stable at lower temperatures (both belonging to the tetragonal crystal system), and brookite, which is usually found only in minerals and has a structure belonging to the orthorhombic crystal system. The titanium dioxide use in industrial products, such as paint, is almost a rutile type. These crystals are substantially pure titanium dioxide but usually amount of impurities, e.g., iron, chromium, or vanadium, which darken them. A summary of the crystallographic properties of the three varieties is given in Table 3.2.

Although anatase and rutile are both tetragonal, they are not isomorphous (Figure 3.1). The two tetragonal crystal types are more common because they are easy to make. Anatase occurs usually in near-regular octahedral, and rutile forms slender prismatic

crystal, which are frequently twinned. Rutile is the thermally stable form and is one of the two most important ores of titanium.

The three allotropic forms of titanium dioxide have been prepared artificially but only rutile, the thermally stable form, has been obtained in the form of transparent large single crystal. The transformation from anatase to rutile is accompanied by the evolution of ca. 12.6 kJ/mol (3.01 kcal/mol), but the rate of transformation is greatly affected by temperature and by the presence of other substance which may either catalyze or inhibit the reaction. The lowest temperature at which conversion of anatase to rutile takes place at a measurable rate is ca. 700°C, but this is not a transition temperature. The change is not reversible; ΔG for the change from anatase to rutile is always negative (see Tables 3.1 and 3.2 for thermodynamic data)

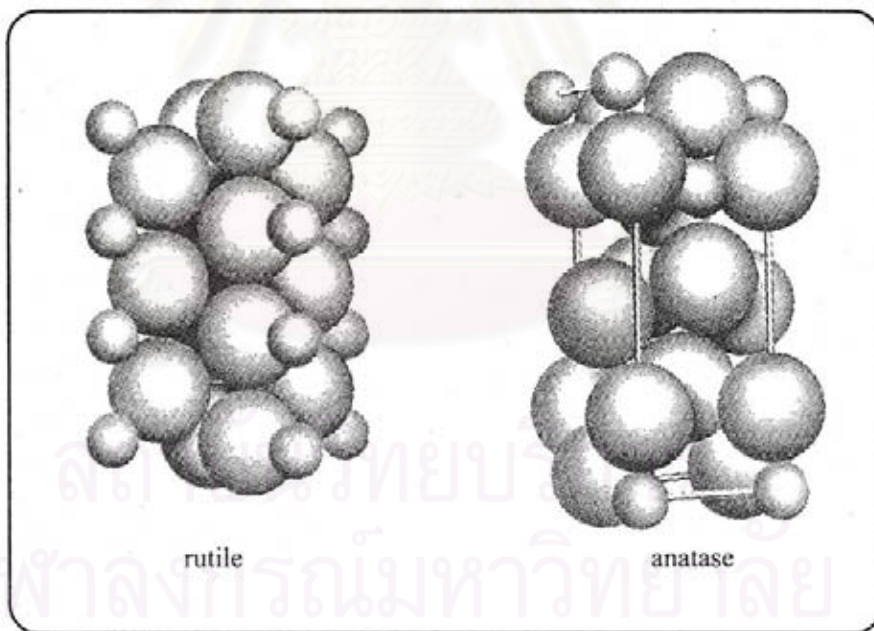


Figure 3.1 Crystal structure of TiO₂. (Fujishima *et al.*, 1999)

Heating amorphous titanium (IV) oxide, prepared from alkyl titanates of sodium titanate with sodium or potassium hydroxide in an autoclave at 200 to 600°C for several days has produced brookite. The important commercial forms of titanium dioxide are anatase and rutile, and these can readily be distinguished by X-ray diffraction spectrometry.

Since both anatase and rutile are tetragonal, they are both anisotropic, and their physical properties, e.g. refractive index, vary according to the direction relative to the crystal axes. In most applications of these substances, the distinction between crystallographic direction is lost because of the random orientation of large numbers of small particles, and it is mean value of the property that is significant.

Table 3.2 Crystallographic properties of anatase, brookite, and rutile.

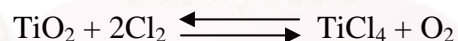
Properties	Anatase	Brookite	Rutile
Crystal structure	Tetragonal	Orthorhombic	Tetragonal
Optical	Uniaxial, negative	Biaxial, positive	Uniaxial, negative
Density, g/cm ³	3.9	4.0	4.23
Hardness, Mohs scale	5 ^{1/2} – 6	5 ^{1/2} – 6	7 – 7 ^{1/2}
Unit cell	D _{4h} ¹⁹ .4TiO ₂	D _{2h} ¹⁵ .8TiO ₂	D _{4h} ¹² .3TiO ₂
Dimension, nm			
a	0.3758	0.9166	0.4584
b		0.5436	
c	0.9514	0.5135	2.953

Measurement of physical properties, in which the crystallographic directions are taken into account, may be made of both natural and synthetic rutile, natural anatase crystals, and natural brookite crystals. Measurements of the refractive index of titanium dioxide must be made by using a crystal that is suitably orientated with respect to the

crystallographic axis as a prism in a spectrometer. Crystals of suitable size of all three modifications occur naturally and have been studied. However, rutile is the only form that can be obtained in large artificial crystals from melts. The refractive index of rutile is 2.75. The dielectric constant of rutile varies with direction in the crystal and with any variation from the stoichiometric formula, TiO_2 ; an average value for rutile in powder form is 114. The dielectric constant of anatase powder is 48.

Titanium dioxide is thermally stable (mp 1855°C) and very resistant to chemical attack. When it is heated strongly under vacuum, there is a slight loss of oxygen corresponding to a change in composition to $\text{TiO}_{1.97}$. The product is dark blue but reverts to the original white color when it is heated in air.

Hydrogen and carbon monoxide reduce it only partially at high temperatures, yielding lower oxides or mixtures of carbide and lower oxides. At ca. 2000°C and under vacuum, carbon reduces it to titanium carbide. Reduction by metal, e.g., Na, K, Ca, and Mg, is not complete. Chlorination is only possible if a reducing agent is present; the position of equilibrium in the system is

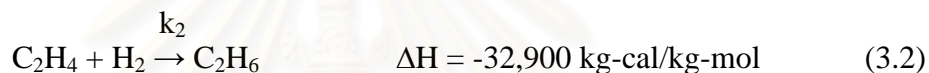
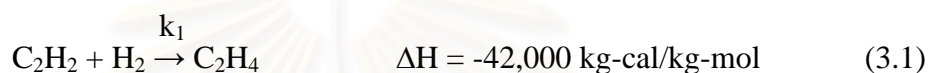


The reactivity of titanium dioxide towards acids is very dependent on the temperature to which it has been heated. For example, titanium dioxide that has been prepared by precipitation from a titanium (IV) solution and gently heated to remove water is soluble in concentrated hydrochloric acid. If the titanium dioxide is heated to ca. 900°C , then its solubility in acids is considerably reduced. It is slowly dissolved by hot concentrate sulfuric acid, the rate of salvation being increased by the addition of ammonium sulfate, which raises the boiling point of the acid. The only other acid in which it is soluble is hydrofluoric acid, which is used extensively in the analysis of titanium dioxide for trace elements. Aqueous alkalies have virtually no effect, but molten sodium and potassium hydroxides, carbonates, and borates dissolve titanium dioxide

readily. An equimolar molten mixture of sodium carbonate and sodium borate is particularly effective as is molten potassium pyrosulfate.

3.3 Acetylene Hydrogenation Reaction

Generally, there are two primary reactions proceeding during acetylene hydrogenation:



The first reaction (3.1) is the desired reaction whereas the second reaction (3.2) is an undesired side reaction due to the consumption of ethylene product. There is also a third reaction occurring during normal operation, which adversely affects the catalyst performance, i.e., the polymerization reaction of C_2H_2 with itself to form a longer chain molecule, commonly called “green oil”.



According to the above reactions involving acetylene hydrogenation, two influencing parameters on the desired reaction can be assigned. The first parameter is reaction temperature, which has a direct relationship with the kinetics of the system. However, it affects not only the reaction rate of the desired reaction (k_1), but also the rate of ethylene hydrogenation (k_2). The rate of polymerisation (k_3) also increases with temperature and the resulting green oil can affect catalyst activity by occupying active sites. When the catalyst is new or has just been regenerated, it has high activity. With time on stream, activity declines as the catalyst becomes fouled with green oil and other contaminants. By the end-of-run (EOR), the inlet temperature must be increased (25-

40°C) over start-of-run (SOR) inlet temperature in order to maintain enough activity for complete acetylene removal. In order to selectively hydrogenate acetylene to ethylene, it is critical to maintain the differential between the activation energies of reaction (eq. 3.1) and (eq. 3.2). However, it is desirable that the ethylene remains intact during hydrogenation. Once energy is supplied to the system over a given catalyst by increasing the temperature, the differential between the activation energies disappears and complete removal of acetylene, which generally has the lower partial pressure, becomes virtually impossible. In other words, higher temperature reduces selectivity; more hydrogen is used to convert ethylene to ethane, thereby increasing ethylene loss. The inlet temperature should therefore be kept as low as possible while still removing acetylene to specification requirements. Low temperatures minimise the two undesirable side reactions and help optimise the converter operation.

Another crucial parameter affecting the selectivity of the system is the ratio between hydrogen and acetylene ($H_2:C_2H_2$). Theoretically, the $H_2:C_2H_2$ ratio would be 1:1, which would mean that no hydrogen would remain for the side reaction (eq. 3.2) after acetylene hydrogenation (eq. 3.1). However, in practice, the catalyst is not 100% selective and the $H_2:C_2H_2$ ratio is usually higher than 1:1 to get complete conversion of the acetylene. As hydrogen is one of the reactants, the overall acetylene conversion will increase with increasing hydrogen concentration. Increasing the $H_2:C_2H_2$ ratio from SOR to EOR can help offset the decline in catalyst activity with time on stream. However, this increased acetylene conversion with a higher $H_2:C_2H_2$ ratio can have a cost in selectivity which leads to ethylene loss. Typically, the $H_2:C_2H_2$ ratio is between 1.1 and 2.5 (Derrien *et al.*, 1986 and Molnár *et al.*, 2001).

The mechanism of acetylene hydrogenation involves four major paths as shown in Fig. 3.2. Path I is the partial hydrogenation of acetylene to ethylene, which is either desorbed as a gaseous product or further hydrogenated to ethane via Path II. It previously was proposed that Path I proceeds mostly on Pd sites, which are covered to a great extent with acetylene under typical industrial reaction conditions, and Path II occurs on support sites, particularly those covered with polymer species.

Consequently, selectivity may be improved by reducing both the strength of ethylene adsorption on Pd and the amount of polymer, which accumulates on the catalyst. One of the methods for improving selectivity is to maintain a low H_2 /acetylene ratio in the reactant stream such that the low hydrogen concentration on Pd retards the full hydrogenation of the ethylenic species on the Pd surface. However, this method has the drawback of accelerating the polymer formation and therefore the H_2 /acetylene ratio must be managed deliberately or sometimes controlled in two steps. Path III, which allows for the direct full hydrogenation of acetylene, becomes negligible at high acetylene coverage and low hydrogen partial pressures. Ethylidyne was suggested as an intermediate in Path III but was later verified to be a simple spectator of surface reactions. Path IV, which allows for the dimerization of the C_2 species, eventually leads to the production of green oil and the subsequent deactivation of the catalyst. Polymer formation lowers ethylene selectivity because it consumes acetylene without producing ethylene and, in addition, the polymer species, which is usually located on the support, acts as a hydrogen pool, thus promoting ethane formation (Kang *et al.*, 2002).

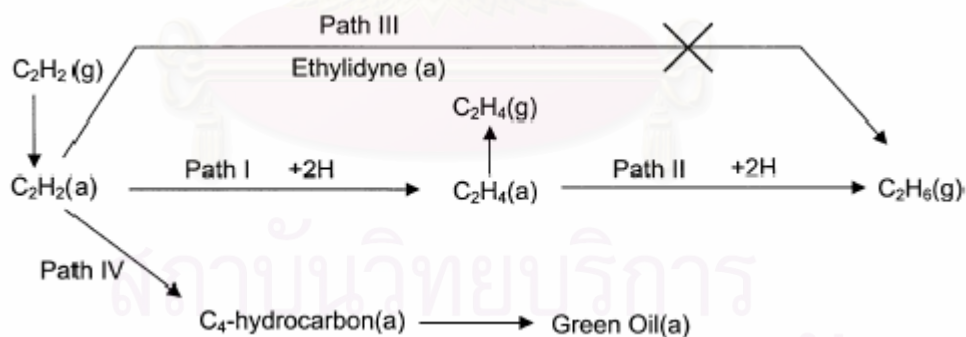


Figure 3.2 Major reaction path of acetylene hydrogenation (Kang *et al.*, 2002)

Considering the mechanism of acetylene hydrogenation described above, it was found that ethylene selectivity is improved when the C_2 species produced by Path I is

readily desorbed from the catalyst surface and the other paths are simultaneously retarded.

3.4 Promoters

There are two kinds of promoters such as textural and chemical promoters. Textural promoters are used to facilitate the dispersion of metal phase during preparation and/or reaction conditions. Chemical promoters are used to enhance the activity and/or selectivity of catalysts. Generally, noble, alkali and alkaline earth metals are considered to be chemical promoters, which play important roles on catalyst performance to date.

The effect of promoter such as Ag (Praserthdam *et al.*, 2002 and Ngamsom *et al.*, 2004), K (Kim *et al.*, 2004), Si (Shin *et al.*, 1998; Shin *et al.*, 2002 and Kim *et al.*, 2003), Au (Sárkany *et al.*, 2002), Ti (Kang *et al.*, 2000; Lee *et al.*, 2003; Kim *et al.*, 2004 and Kang *et al.*, 2002), Nb (Kang *et al.*, 2000), Ce (Kang *et al.*, 2000) incorporated into palladium catalysts for the selective acetylene hydrogenation reaction were studied. They reported that these metal promoters can improve activity and selectivity of acetylene hydrogenation catalysts.

CHAPTER IV

EXPERIMENTAL

This chapter consists of experimental systems and procedures used in this work which is divided into five parts. The chemicals and the reaction apparatus are shown in sections 4.1 and 4.2, respectively. Section 4.3 describes the procedures for catalyst preparation including preparation of titania support, palladium loading, and palladium-silver loading. The fourth part (section 4.4) explains the details of catalyst characterization by various techniques such as AAS, XRD, BET surface area, TGA, CO-pulse chemisorption, SEM, TEM, CO₂-TPD, ESR, C₂H₄-TPD and TPO. The last part (section 4.5) describes the catalyst evaluation in term of catalytic activity measurement in selective acetylene hydrogenation.

4.1 Chemicals

The details of chemicals and synthesis mixtures used in this experiment are shown in Table 4.1 and 4.2, respectively.

สถาบันวิทยบริการ
จุฬาลงกรณ์มหาวิทยาลัย

Table 4.1 Chemicals used in the experiment

Chemical	Supplier
Titanium (IV) tert-butoxide (97% TNB, $\text{Ti}[\text{O}(\text{CH}_2)_3\text{CH}_3]_4$)	Aldrich
1,4-butanediol (1,4-BG, $\text{HO}(\text{CH}_2)_4\text{OH}$)	Aldrich
Toluene ($\text{C}_6\text{H}_5\text{CH}_3$)	APS Finechem
Methyl alcohol	Aldrich
Palladium (II) nitrate hydrate	Aldrich
Silver nitrate (AgNO_3)	APS Finechem
Acetylene : instrument grade : 99.5%	TIG
Ultra high purity hydrogen : 99.999%	TIG
High purity nitrogen : 99.99%	TIG

สถาบันวิทยบริการ
จุฬาลงกรณ์มหาวิทยาลัย

Table 4.2 Reagents used for the synthesis of titania

Reagents	Weight/Volume
TNB (various starting material concentrations)	25 g
Organic solvents (1,4-BG, toluene)	
In the synthesis mixtures	100 cm ³
In the gap	30 cm ³

For catalytic activity measurements:

Reactant gas : Pure acetylene

: Hydrogen

: Nitrogen

Pressure operation : 1 bar

Reaction temperature : 40-90°C

Space velocity : 28819.36 h⁻¹

4.2 Equipments

All equipments used in this study are consisted of:

4.2.1 Autoclave reactor

- Made from stainless steel
- Volume of 1000 cm³
- 10 cm inside diameter
- Maximum temperature of 350°C
- Pressure gauge in the range of 0-140 bar
- Relief valve used to prevent runaway reaction
- Iron jacket was used to reduce the volume of autoclave to be 300 cm³
- Test tube was used to contain the reagent and glycol

The autoclave reactor is shown in Figure 4.1

4.2.2 Temperature program controller

A temperature program controller CHINO DB1000F was connected to a thermocouple with 0.5 mm diameter located inside the autoclave.

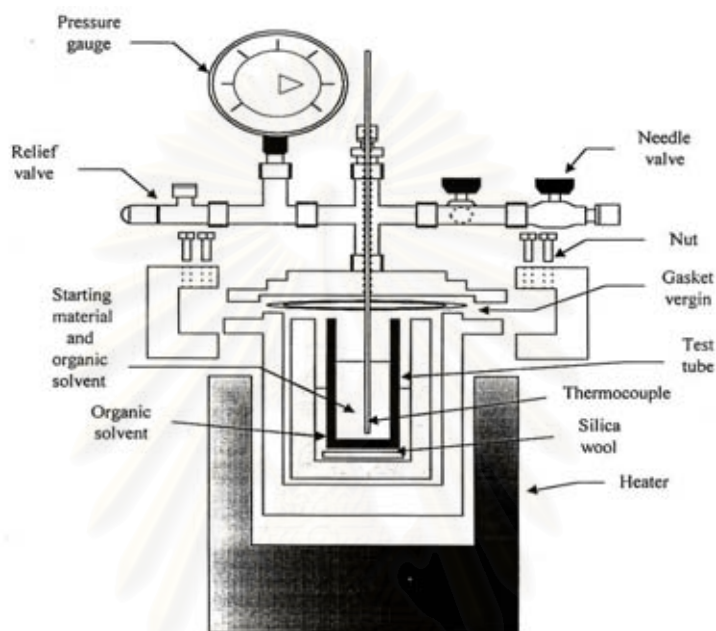


Figure 4.1 Autoclave reactor

4.2.3 Electrical furnace (Heater)

Electrical furnace was used to supply the required heat to the autoclave for the reaction.

4.2.4 Gas controlling system

Nitrogen was set with a pressure regulator (0-150 bar) and needle valves are used to release gas from autoclave.

The diagram of the reaction equipment is shown in Figure 4.2

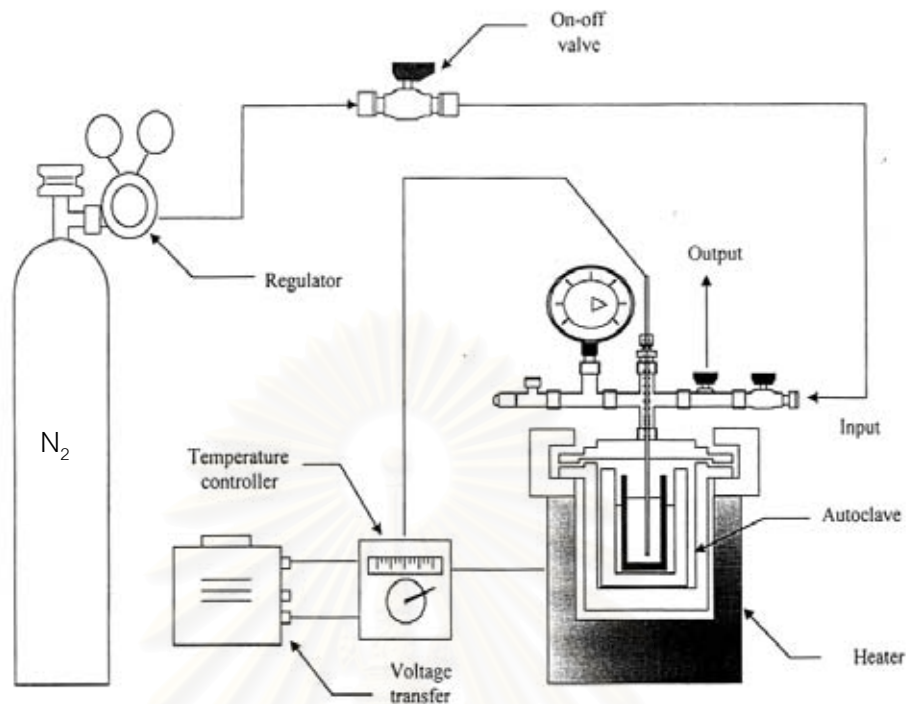


Figure 4.2 Diagram of the reaction equipment for the catalyst preparation.

4.3 Catalyst Preparation

4.3.1 Preparation of titanium dioxide support

Titanium dioxide was prepared using 25 g of TNB. The starting material was suspended in 100 ml of solvent (1,4-butanediol or toluene) in a test tube and then set up in an autoclave. In the gap between the test tube and autoclave wall, 30 ml of solvent was added. After the autoclave was completely purged with nitrogen, the autoclave was heated to the desired temperature (320°C) at a heating rate of $2.5^{\circ}\text{C min}^{-1}$ and held at that temperature for 6 h. Autogeneous pressure during the reaction gradually increased as the temperature was raised. After reaction, the autoclave was cooled to room temperature. The resulting powder was collected after repeated washing with methanol by centrifugation. They were then air-dried at room temperature.

4.3.2 Palladium loading

1wt%Pd and 1wt%Pd-3wt%Ag over TiO₂ supports were prepared by the sequential impregnation technique detailed as follows:

1. Titanium dioxide supports were impregnated with an aqueous solution of palladium nitrate by the incipient impregnation wetness technique. Using the water capacity measurement obtained previously for the titanium dioxide particles, a sufficient amount of the palladium salt was added to obtain a 1% by weight of palladium.

2. The impregnated support was left to stand for 6 h to assure adequate distribution of the metal complex. The support was subsequently dried at 110°C in air overnight.

3. The dried impregnated support was calcined under 60 ml/min nitrogen with the heating rate of 10°C/min until the temperature reached 500°C. A 100 ml/min of flowing air was then switched into the reactor to replace nitrogen and the temperature was held at 500°C for 2 h.

4. The palladium impregnated sample was re-impregnated with silver complex using a similar procedure except that the calcination were performed at 500°C and held at the temperature for 1 h.

5. The calcined sample was finally cooled down and stored in a glass bottle in a desiccator for later use.

4.4 Catalyst Characterization

4.4.1 Atomic Absorption Spectroscopy (AAS)

AAS was performed to determine the composition of elements in the bulk of catalysts. The elemental content of the catalysts was collected using Varian, Spectra A8000 at the Department of Science Service Ministry of Science Technology and Environment.

4.4.2 X-Ray Diffraction (XRD)

XRD was performed to determine the bulk phase of the catalysts by SIEMENS D 5000 X-ray diffractometer using $\text{CuK}\alpha$ radiation with Ni filter in the 2θ range of 20-80 degrees with resolution of 0.04°

4.4.3 BET Surface Area

This method was a physical adsorption of nitrogen gas on the surface of catalyst to find the total surface area. BET surface areas of these catalyst were measured by Micromeritics ASAP 2000 of Chemical Laboratory of Department of Engineering, Chulalongkorn University.

4.4.4 Thermalgravimetric Analysis (TGA)

TGA was used to determine weight loss pattern and reducibility of the catalysts by Shimadzu TGA model 50. The catalyst sample of 10-20 mg was used in the operation and temperature ramping from 35°C to 800°C at $10^\circ\text{C}/\text{min}$ was used. The carrier gas was ultra high purity N_2 .

4.4.5 CO-Pulse Experiment

Metal active sites were measured using CO chemisorption technique where a known amount of CO was pulsed into the catalyst bed at room temperature. The number of metal active sites was measured in the basic assumption that only one CO molecule adsorbed on one metal active site (Vannice *et al.*, 1981; Anderson *et al.*, 1985; Ali *et al.*, 1998 and Mahata *et al.*, 2000). Carbon monoxide that was not adsorbed was measured using thermal conductivity detector. Pulsing was continued until no further carbon monoxide adsorption was observed. Calculation details of %metal dispersion are given in Appendix C.

a) Materials

Ultrahigh purity helium and ultrahigh purity hydrogen were used as carrier gas and reducing agent, respectively. Pure carbon monoxide was used as an adsorbent gas. All gases used in this experiment were supplied by the Thai Industrial Gas Co., Ltd.

b) Apparatus

The amount of carbon monoxide adsorbed on the metal surface was measured by a thermal conductivity detector within a gas chromatograph (GOW-MAC). The operating conditions of the gas chromatograph are shown in Table 4.3. The extensive diagram of the instruments used for measurement of the metal active sites is illustrated in Figure 4.3.

c) Procedure

1) 0.2 g of the catalyst sample was packed in a stainless steel tubular reactor. Helium gas was introduced into the reactor at the flow rate of 30 ml/min for 10 min in order to remove remaining air. The system was switched to 100 ml/min of hydrogen and

heated at an increasing rate of 10°C/min until the temperature reached 500°C and held at that temperature for 1 h.

2) The reactor was cooled down to room temperature.

3) The catalyst was then ready to measure metal active sites; 50 µl of purity carbon monoxide gas was injected into the injection port to adsorb on the metal surface of the catalyst sample. CO was repeatedly injected until the sample did not any longer adsorbed CO.

4) The amount to metal active sites of fresh catalyst was calculated by the amount of adsorbed CO gas according to the description in Appendix C.

Table 4.3 Operating conditions of gas chromatograph (GOW-MAC) for CO chemisorption measurement

Model	GOW-MAC
Detector type	TCD
Carrier gas	Ultra high purity helium
Carrier gas flow rate (ml/min)	30
Detector temperature (°C)	80
Detector current (mA)	80

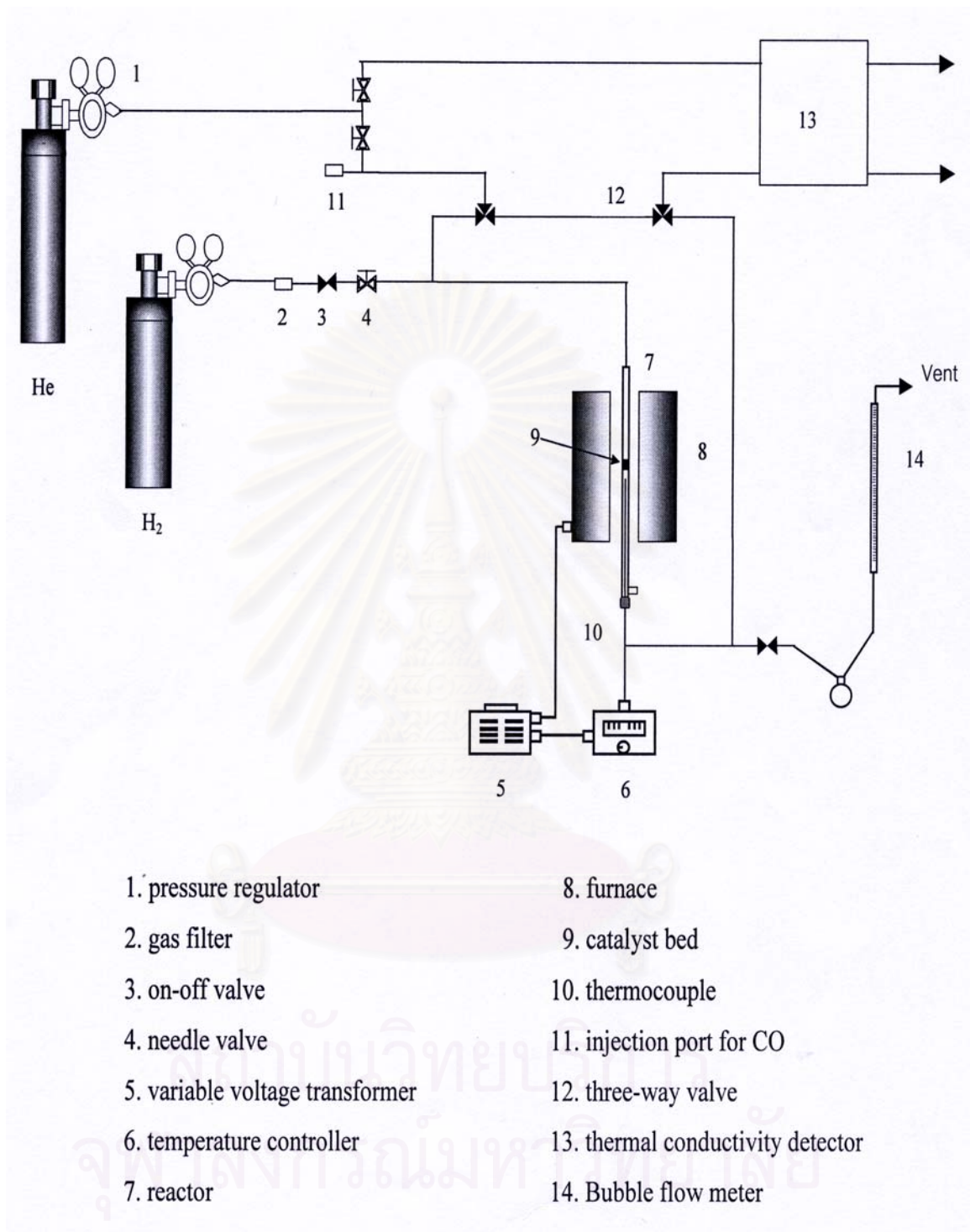


Figure 4.3 Flow diagram of CO chemisorption measurement

4.4.6 Scanning Electron Microscopy (SEM)

Catalyst granule morphology and elemental distribution were obtained using a JEOL JSM-35F scanning electron microscope. The SEM was operated using the back scattering electron (BSE) mode at 20 kV at the Scientific and Technological Research Equipment Center, Chulalongkorn University (STREC).

4.4.7 Transmission Electron Microscopy (TEM)

The palladium oxide particle size and distribution of palladium on silica supported were observed using JEOL-JEM 200CX transmission electron microscope operated at 100kV.

4.4.8 CO₂ Temperature Programmed Desorption (CO₂-TPD)

CO₂-TPD was used to determine the amount of Ti³⁺ in titanium dioxide. 0.05 g of catalyst was used in the operation temperature from 35°C to 800°C. The carrier gas was He. Prior to CO₂-TPD, the catalyst was adsorbed at liquid nitrogen temperature with CO₂ (3 ml/min) for 1 h and the sample was purged with helium. CO₂-TPD was operated until the TCD signal was constant.

4.4.9 Electron Spin Resonance (ESR)

ESR was performed using a JEOL model JES-RE2X at the Scientific and Technological Research Equipment Center, Chulalongkorn University (STREC).

4.4.10 Temperature Programmed Desorption

a) Apparatus

The amount of C_2H_4 , adsorbed on the surface was determined by temperature programmed desorption with a temperature heating rate of $10^\circ C/min$. The thermal conductivity detector was used to measure the amount of C_2H_4 . The operating conditions are the same as CO chemisorption summarized in Table 4.3.

b) Procedures

1) 0.2 g of catalyst was packed in the reactor and reduced by hydrogen flowing over catalyst at the rate of 100 ml/min. The reactor was heated up from room temperature to $500^\circ C$ and maintain at this temperature for 1 h.

2) The reactor was cooled down from $500^\circ C$ to the room temperature by helium flow and heat to $70^\circ C$ then subsequently switched ethylene into the reactor for 3 h. The catalyst adsorbing ethylene was subsequently purged with helium at the same temperature to remove physisorbed hydrogen.

3) The C_2H_4 -TPD experiment was carried out in quartz reactor from room temperature to $800^\circ C$ at a heating rate of $10^\circ C/min$.

4.4.11 Temperature Programmed Oxidation (TPO)

a) Materials

1% vol oxygen in helium gas mixture supplied by Thai Industrial Gas was used as oxidizing agent. Ultra high purity helium was used for purging the system.

b) Apparatus

Temperature programmed oxidation was used to study the amount of coke deposition on the catalysts. Approximately 0.1 g of spent catalyst was packed in the middle of the quartz reactor (8 mm O.D.) located in a tube furnace. The furnace temperature was controlled by a microprocessor base temperature controller (PC 600, Shinko). A gas mixture of 1 vol% oxygen in helium was used as an oxidizing gas. The oxidation process began by heating the catalyst with a flow rate of 5°C/min until the temperature reached 800°C. During the oxidation, the amount of CO₂ in the effluent gas was first analyzed when the catalyst temperature reached 35°C using a gas chromatograph (SHIMADZU 8 AIT) equipped with a gas sampling valve (1.5 ml sampling loop) and a thermal conductivity detector. Figure 4.4 illustrates the flow diagram of the oxidation system. Table 4.4 shows the operating condition of gas chromatograph of the oxidation system.

c) Procedure

- 1) The spent catalyst was packed in the middle of the quartz reactor before placing the reactor in the furnace and pretreated by helium flowing over catalyst at the rate of 100 ml/min. The reactor was heated up from room temperature to 500°C and maintain at this temperature for 1.5 h.

- 2) The 1 vol% oxygen in helium gas was flowed through the system at a flow rate 30 ml/min.

- 3) The temperature programmed oxidation of coke was started. The temperature was raised to 900°C at heating rate of 5°C/min. When the temperature was 35°C, the effluent stream was sampled every 7 min by the on-line gas sample.

- 4) The amount of oxygen consumed and carbon dioxide produced was measured.

5) After the catalyst temperature reached 900°C, the 1 vol% oxygen in helium gas was changed to ultra high purity helium and the reactor was cooled down.

Table 4.4 Operating conditions of gas chromatograph (GC-8A) for Temperature Programmed Oxidation

Model	GC-8 AIT (SHIMADZU)
Detector	TCD
Packed column	Porapack QS (200x0.32 cm)
Helium flow rate	85 ml/min
Column temperature	90°C
Detector/injection temperature	110°C
Detector current	90 mA

สถาบันวิทยบริการ
จุฬาลงกรณ์มหาวิทยาลัย

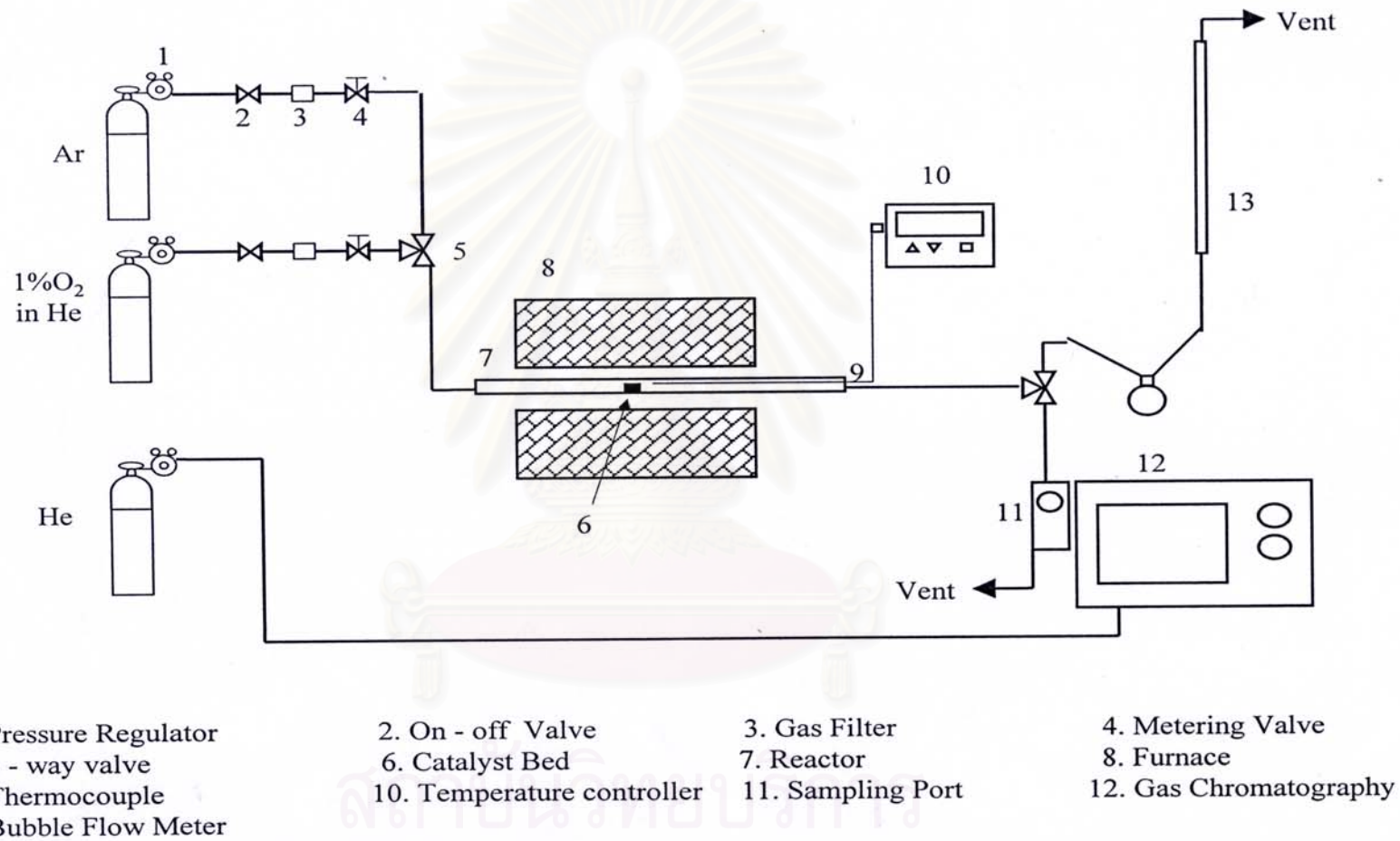


Figure 4.4 Flow diagram of measurement of Temperature Programmed Oxidation

4.5 Reaction study in acetylene hydrogenation

The performance of the catalysts for selective hydrogenation of acetylene was investigated using a GHSV of 28819.36 h⁻¹. A temperature programmed reaction was conducted from 40 to 90°C in order to cover the industrial window operation that is 65-85°C (Cosyns *et al.*, 1984 and Boitiaux *et al.*, 1985). Materials, apparatus, and operating procedures are detailed as below:

a) Materials

The reactant gases used for selective acetylene hydrogenation were a gas mixture of 0.996 vol % acetylene in ethylene and a pure acetylene gas. Ultra high purity hydrogen was used for reactant and reduction process. High purity argon and high purity nitrogen were used for cooling and balance process, respectively. All gases were manufactured by the Thai Industrial Gas Co., Ltd. (TIG).

b) Apparatus

The catalytic test was performed in a flow system as shown diagrammatically in Figure 4.5. The apparatus consisted of a quartz tubular reactor, an electrical furnace and as automation temperature controller. The instruments used in this system are listed and explained as follows:

1) Reactor

The reaction was performed in a conventional quartz tubular reactor (inside diameter = 0.9 cm) at atmospheric pressure.

2) Automation Temperature Controller

This unit consisted of a magnetic switch connected to a variable transformer and a RKC temperature controller series connected to a thermocouple attached to the catalyst bed in a reactor. A dial setting established a set point at any temperature within the range between 0 to 999°C. The accuracy was $\pm 2^\circ\text{C}$.

3) Electrical Furnace

The furnace supplied the required temperature to the reactor which could be operated from room temperature up to 800°C at maximum voltage of 220 volts.

4) Gas Controlling System

The reactants (hydrogen, nitrogen and carrier gas) for the system were separately equipped with a pressure regulator and an on-off valve. The gas flow rates were adjusted by using metering valves and mass flow meters.

5) Gas Chromatograph

The products and feeds were analyzed by a gas chromatograph equipped with a FID detector (SHIMADZU FID GC 9A, carbosieve column S-2) for separating CH_4 , C_2H_2 , C_2H_4 and C_2H_6 . H_2 was analyzed by a gas chromatograph equipped with a TCD detector (SHIMADZU TCD GC 8A, molecular sieve 5A). The operating conditions for each instrument are summarized in Table 4.5.

c) Procedures

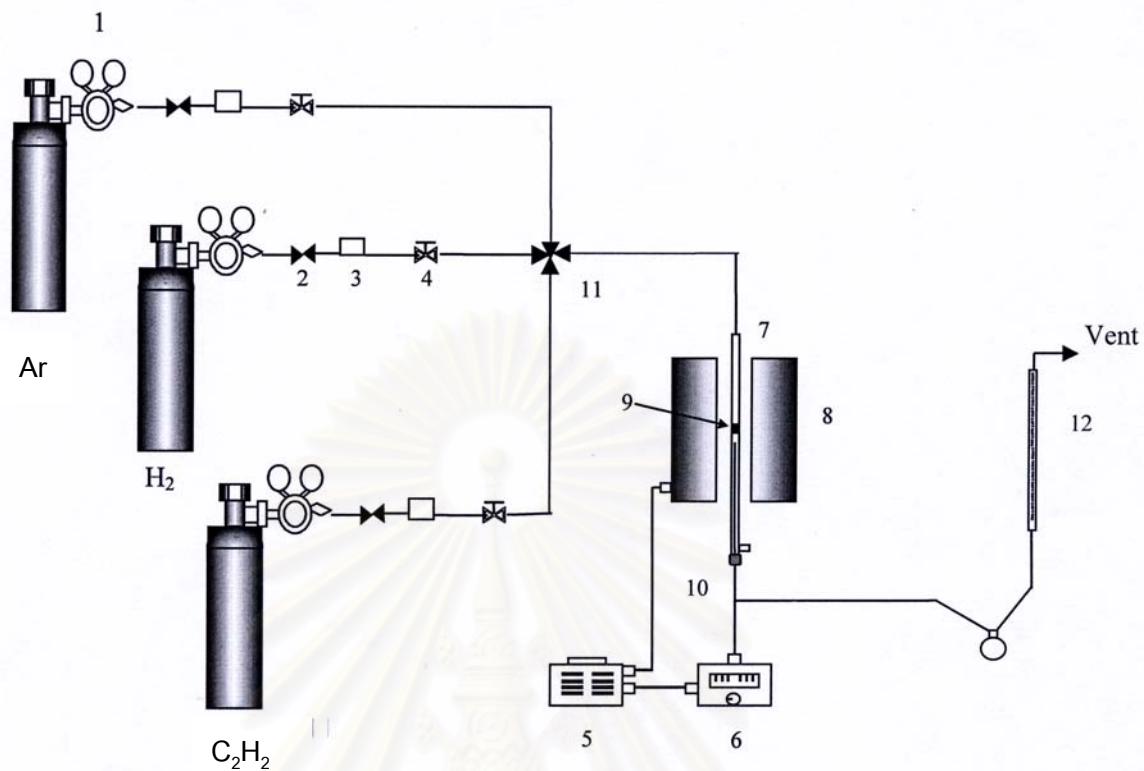
0.2 g of catalyst was packed in a quartz tubular down flow reactor. The catalyst bed length was about 0.6 cm. The reactor was placed into the furnace and argon was introduced into the reactor in order to remove remaining air. Prior to reaction, the

catalyst was reduced with 100 ml/min hydrogen flow at a temperature of 500°C and held at that temperature for 1 h. Afterwards, argon was switched in to replace hydrogen and held at that temperature for 10 min in order to remove the remaining hydrogen.

The reactant was introduced at elevated temperature from 40 to 90°C and 1 atm, sampling was undertaken when the steady state of the system was reached, which was approximately within 2 h. Effluent gases were sampled to analyze the concentration of CH₄, C₂H₂, C₂H₄ and C₂H₆ using GC-9A equipped with a carbosieve S-II column, whereas H₂ concentration was analyzed by GC-8A equipped with a molecular sieve 5A column. Details of the calculation of the catalyst activity to convert acetylene and the selectivity are given in Appendix E.

Table 4.5 Operating conditions of gas chromatograph for selective hydrogenation of acetylene.

Gas Chromatograph	SHIMADZU FID GC 9A	SHIMADZU TCD GC 8A
Detector	FID	TCD
Packed column	Carbosieve column S-II	Molecular sieve 5A
Carrier gas	Ultra high purity He	Ultra high purity Ar
Carrier gas flow rate (ml/min)	30	30
Injector temperature (°C)	185	80
Detector temperature (°C)	185	80
Initial column temperature (°C)	100	50
Initial holding time (min)	50	-
Programmed rate (°C/min)	10	-
Final column temperature (°C)	180	50
Initial final holding time (min)	160	-
Current (mA)	-	70
Analyzed gas	CH ₄ , C ₂ H ₂ , C ₂ H ₄ , C ₂ H ₆	H ₂



- | | |
|---------------------------------|-----------------------|
| 1. pressure regulator | 7. reactor |
| 2. on-off Valve | 8. furnace |
| 3. gas filter | 9. catalyst bed |
| 4. needle valve | 10. thermocouple |
| 5. variable voltage transformer | 11. 4-way joint |
| 6. temperature controller | 12. bubble flow meter |

Figure 4.5 A schematic of acetylene hydrogenation system

CHAPTER V

RESULTS AND DISCUSSION

The different titania supported palladium catalysts prepared and evaluated in this study are consisted of 1%Pd/TiO₂ and 1%Pd-3%Ag/TiO₂ in which the titania used has been synthesized from titanium (IV) tert-butoxide (TNB) mixed with an organic solvent (1,4-butanediol or toluene) in an autoclave under autogenous pressure. The results in this chapter are divided into four parts. The first part (section 5.1) describes the characteristics of the titania prepared in different solvents. The second part (section 5.2) explains the characteristics of titania supported Pd catalysts (1%Pd/TiO₂) and their catalytic behaviors in selective hydrogenation. Effect of Ag promotion on the catalytic properties of Pd/TiO₂ catalysts is illustrated in section 5.3 and the final part (section 5.4) reports temperature programmed study of the TiO₂ and the TiO₂-supported Pd and Pd-Ag catalysts.

5.1 Solvothermal-derived titania

5.1.1 Formation of titanium dioxide synthesized in 1,4-butanediol

Titanium dioxide was synthesized in 1,4-butanediol by the solvothermal method at 320°C for 6 h. Under solvothermal conditions, titanium (IV) tert-butoxide (TNB) was easily converted to glycoxide. Thermal decomposition of the glycoxide molecule was occurred by intramolecular participation of the remaining hydroxyl group of glycol moiety and subsequently a $\equiv\text{Ti-O}^-$ anion was formed. The nucleophilic attack of this titanate ion on another ion and crystallization of titanium (IV) oxide were taken place (Sornnarong Theinkeaw, 2000: 70). The mechanism of TNB in 1,4-butanediol can be depicted in Figure 5.1.

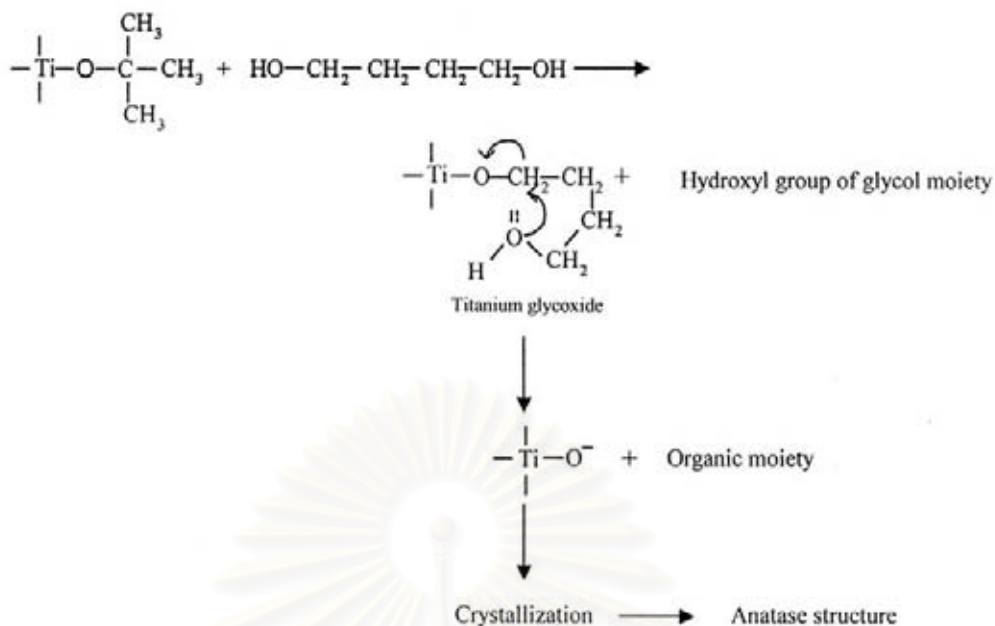


Figure 5.1 Mechanism of solvothermal reaction for the anatase formation

5.1.2 Formation of titanium dioxide synthesized in toluene (Sornnarong Theinkeaw, 2000: 71).

Titanium dioxide was also synthesized in toluene at 320°C for 6 h. Unlike synthesis in 1,4-butanediol, thermal decomposition of TNB in toluene occurred under inert organic solvent condition, yielding a $\equiv\text{Ti}-\text{O}^-$ anion. The nucleophilic attack of the titanate ion on another ion and crystallization was taken place, finally yielding the anatase titania (Sornnarong Theinkeaw, 2000: 70). The mechanism of TNB in toluene can be depicted as shown in Figure 5.2.

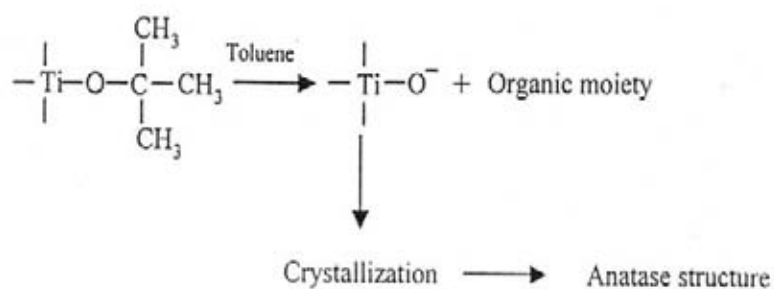


Figure 5.2 Mechanism of reaction in toluene for the titania product (Sornnarong Theinkeaw, 2000: 71).

5.1.3 Support structure and morphology

5.1.3.1 Specific surface area and crystallite site diameter (nm)

The most common procedure for determining surface area of a solid and is based on adsorption and condensation of nitrogen at liquid nitrogen temperature using static vacuum procedure. This method is also called BET (Brunauer Emmett Teller) method.

The BET surface areas and the average crystallite sizes of the titanium dioxide prepared in this study are shown in Table 5.1. There was no significant differences in BET surface area of titania products synthesized in different solvents.

The average crystallite sizes of titania products synthesized in different solvents were determined from the half-height width of the 101 diffraction peak of anatase titania using Sherrer's equation (Kominami *et al.*, 1997 ; Yang *et al.*, 2001 and Iwamoto *et al.*, 2001). The average crystallite sizes of the titania supports prepared in different solvents were found to be ca. 9-10 nm.

Table 5.1 The average crystallite size and BET surface area of the titania products synthesized in 1,4-butanediol and toluene

sample	BET surface area (m ² /g)	Average crystallite size diameter (nm)
TiO ₂ (1,4-butanediol)	59.1	9.4
TiO ₂ (toluene)	64.3	10.1

5.1.3.2 X-ray diffraction (XRD)

The phase identification of titania is based on the results from X-ray diffraction. The XRD patterns of the titania prepared in different solvents in the 2θ ranges from 20° to 80° are shown in Figure 5.3. XRD spectra of the titania show strong diffraction peaks at 25.3° , 37.8° , 48.1° , 54.0° , 55.2° , 62.8° , 68.0° , 71.9° and $76.2^\circ 2\theta$. All of those peaks can be attributed to titania anatase phase. Thus, nanocrystalline pure anatase titania can be produced by the solvothermal technique without any contamination of other phases.

สถาบันวิทยบริการ
จุฬาลงกรณ์มหาวิทยาลัย

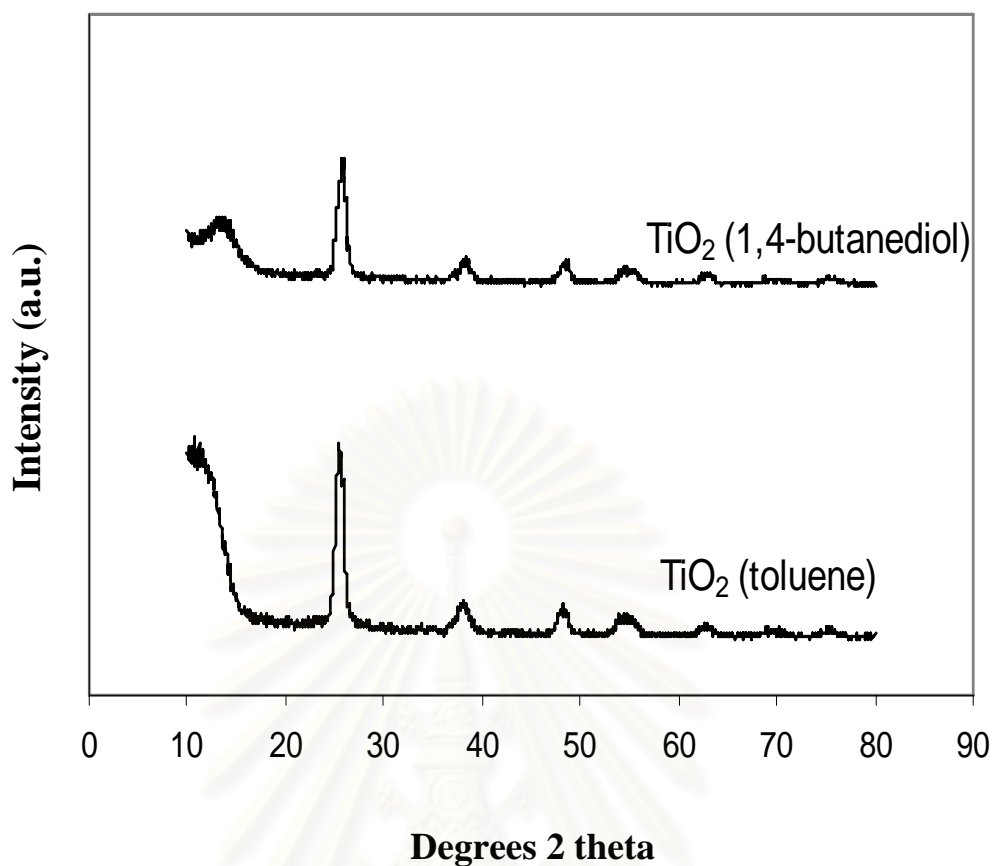


Figure 5.3 XRD patterns of the titania products synthesized in 1,4-butanediol and toluene at 320°C for 6 h.

5.1.3.3 Scanning Electron Microscopy (SEM)

Scanning electron microscopy (SEM) is a powerful tool for observing directly surface texture, morphology and particle granule size of catalyst materials. In the backscattering mode (SEM), the electron beam focused on the sample is scanned by a set of deflection coil. Backscattered electrons or secondary electrons emitted from the sample are detected.

The SEM micrographs of titania products synthesized in 1,4-butanediol for 2 and 6 h are shown in Figure 5.4 (A) and (B), respectively. The morphology of the titania particles was found to be irregular shape and was not changed with increasing reaction time.

The SEM micrographs of titania products synthesized in toluene for 2 and 6 h are shown in Figure 5.5 (A) and (B), respectively. The morphology from SEM showed the formation of large spherical shape which appeared to agglomerate with increasing reaction time.

Thus, it was found that morphology of titania products synthesized in the two solvents was different, the titania synthesized in toluene was micron-size spherical particle but that synthesized in 1,4-butanediol was irregular fine particle. Park *et al.* (1997) synthesized titania in thermal hydrolysis of TiCl_4 . They found that the particle shape depended on the dielectric constant of solvent and the particle potential. The particle synthesized in low dielectric constant solvent, the particle was spherical shape. Moreover, they proposed that the crystal growth after nucleation can also be affected by the kind of solvent because the particle interaction potential is different in each solvent. Table 5.2 shows the dielectric constant of the two solvents used in this study. The results confirmed that morphology of the titania products is dependent on dielectric constant of the solvent. The effect of reaction medium on the synthesis of TiO_2 nanocrystals by solvothermal method has recently been reported by Payakgul *et al.* (2005). The crystallization mechanism of titania particle in the two solvents was found to be different. It was suggested that anatase titania synthesized in 1,4-butanediol resulted from direct crystallization while titania synthesized in toluene was transformed from precipitated amorphous intermediate.

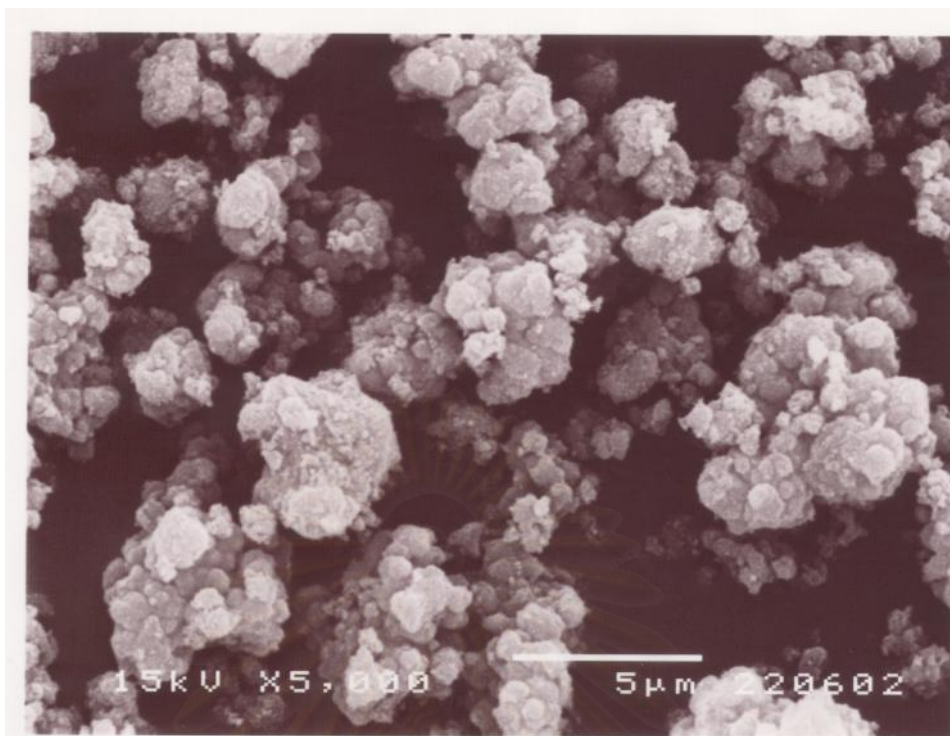
It should be noted that besides the SEM micrographs, all of the other characterization techniques were carried out on the titania particles that synthesized using 6 h reaction time.

Table 5.2 Dielectric constant of the two solvents (Dean *et al.*, 1999)

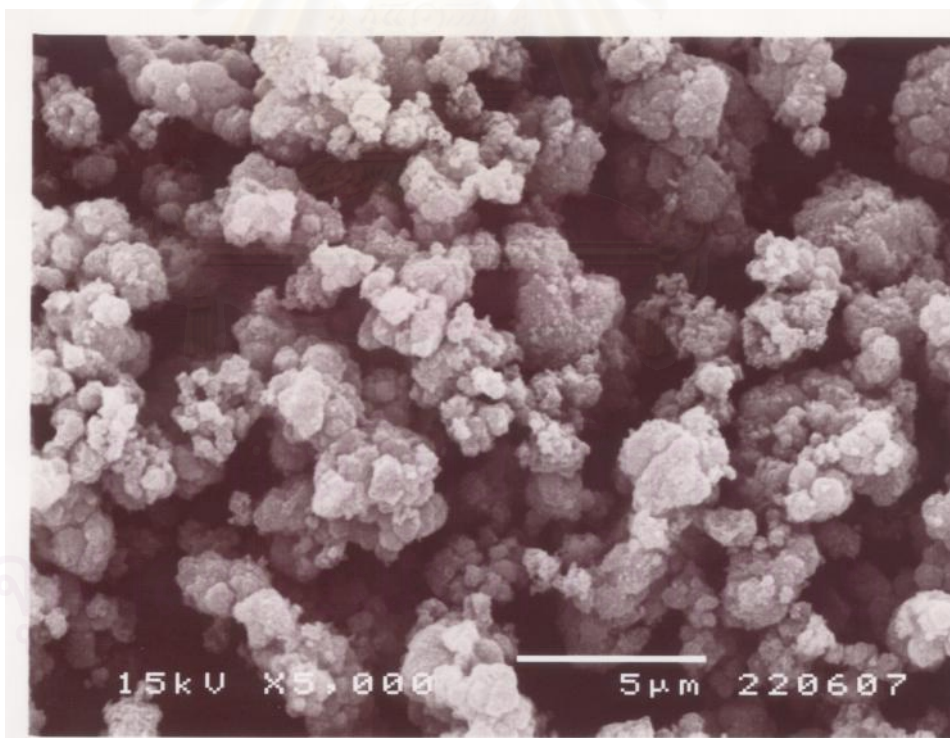
Substances	Dielectric Constant, ϵ (25°C)
1,4-butanediol	32
Toluene	2.4



สถาบันวิทยบริการ
จุฬาลงกรณ์มหาวิทยาลัย

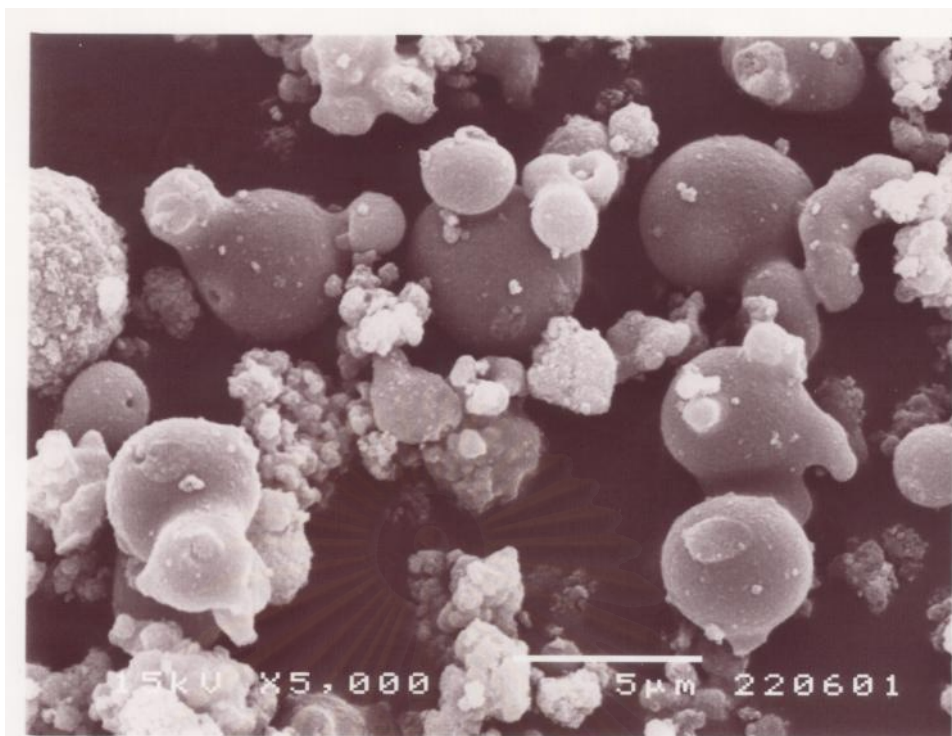


(A) 2 h

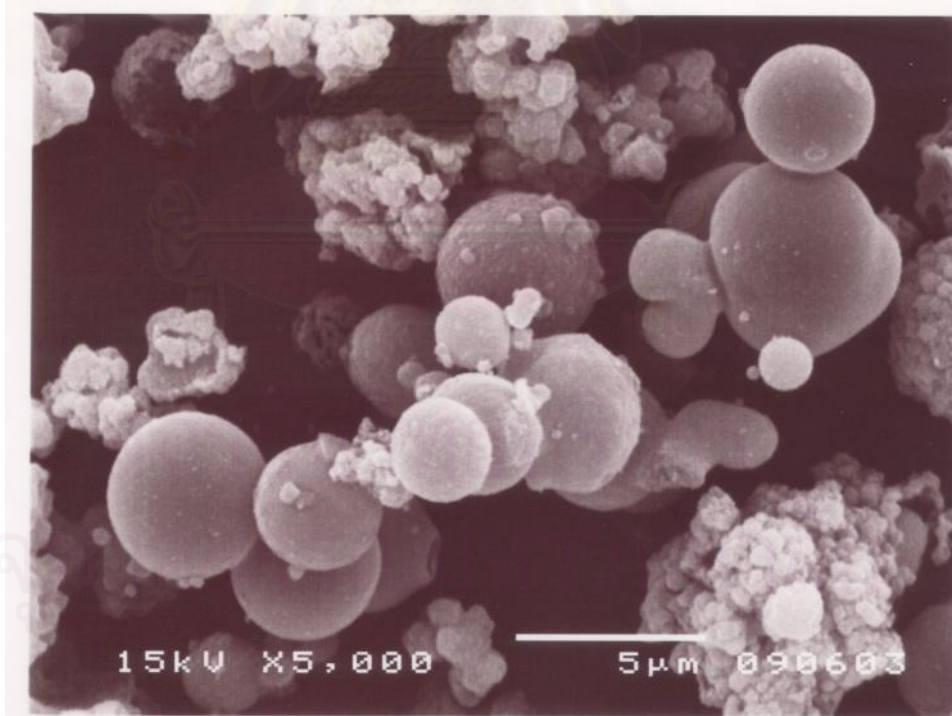


(B) 6 h

Figure 5.4 SEM images of titania products synthesized in 1,4-butanediol for various reaction times.



(A) 2 h



(B) 6 h

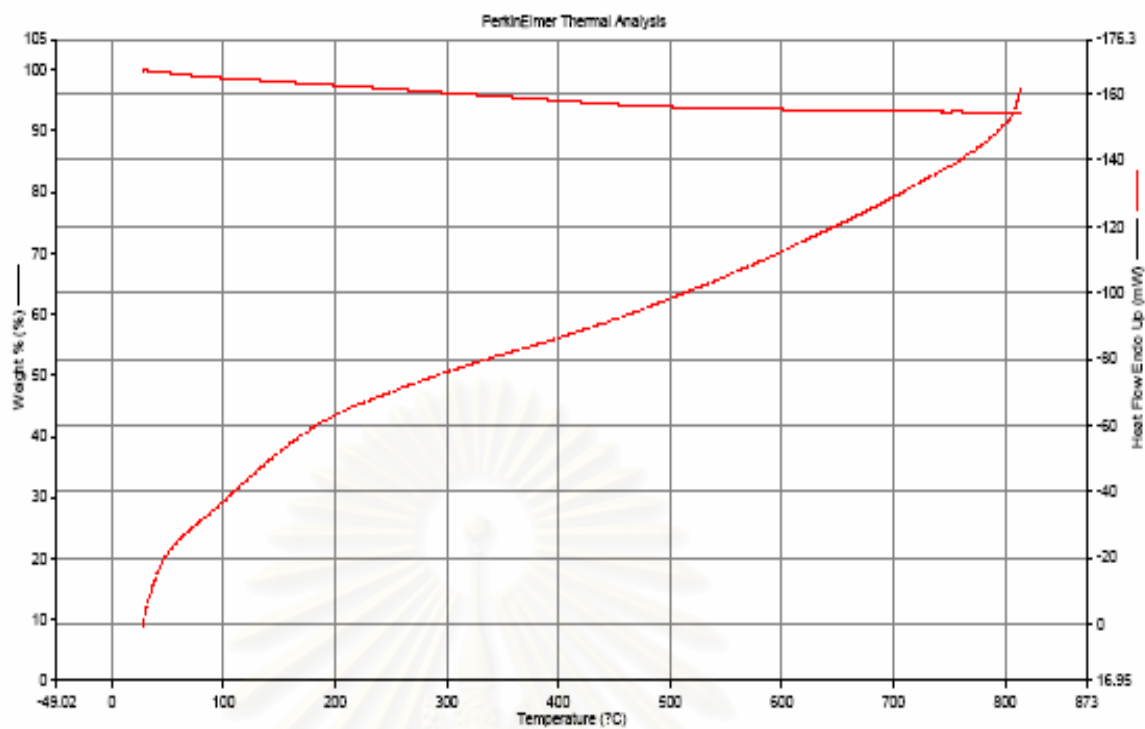
Figure 5.5 SEM images of titania products synthesized in toluene for various reaction times.

5.1.3.4 Thermal gravimetric analysis (TGA)

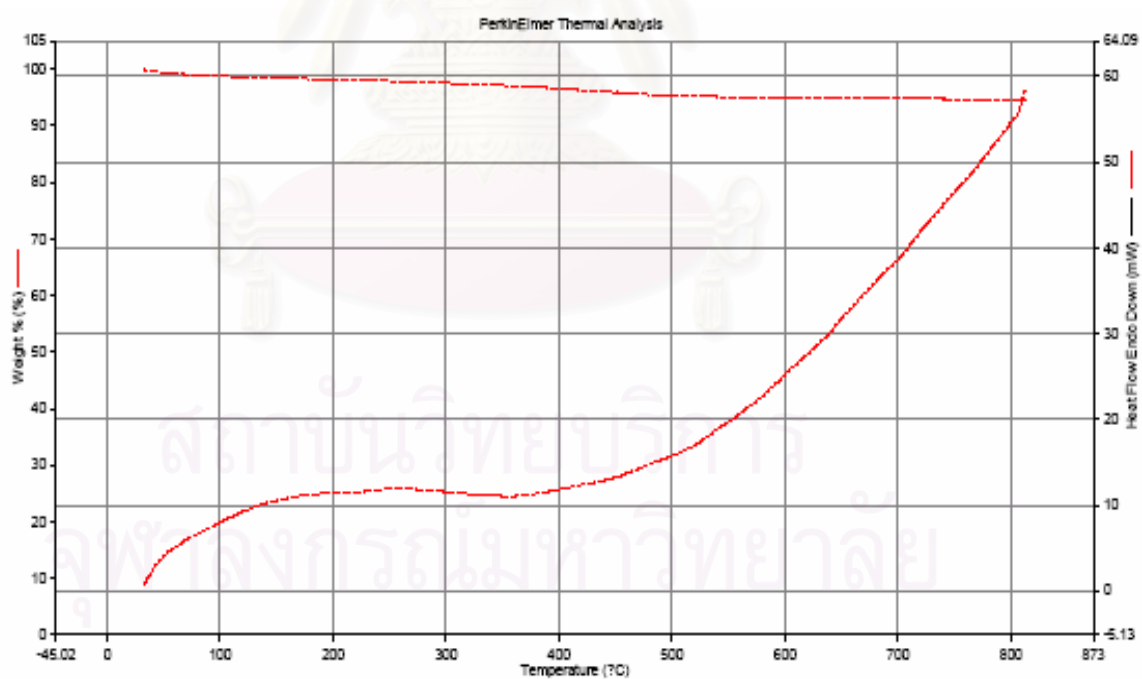
Thermal gravimetric analysis is the most common procedure for determining the change of phase of catalyst. TGA experiments were performed on the titania supports in order to examine the decomposition of titania during heat treatment. The TGA profiles of titania synthesized in 1,4-butanediol and toluene under nitrogen flow 100 cc/min from 35-800°C are reported in Figure 5.6(A) and (B), respectively. No titania phase change was observed when it was heated in nitrogen from 35-800°C.



สถาบันวิทยบริการ
จุฬาลงกรณ์มหาวิทยาลัย



(A) 1,4-butanediol



(B) toluene

Figure 5.6 The TGA profiles of titania synthesized in (A) 1,4-butanediol and (B) toluene.

5.1.3.4 Temperature Programmed Desorption of CO₂ (CO₂-TPD)

CO₂-TPD has been found to be an effective tool for detecting the Ti³⁺ defects in titania. Recently, Tracy et al. reported that based on CO₂-TPD study, surface of titania has two structures which one attributing to CO₂ molecules bound to regular five-coordinate Ti⁴⁺ site considered as the perfected titania structure and the other considered as the CO₂ molecules bound to Ti³⁺ referred to the defective titania structure. Thermal desorption spectra of CO₂ from surface of titania synthesized in 1,4-butanediol and toluene are shown in Figure 5.7.

The peak at -110°C resulted from desorption of CO₂ molecules adsorbed at oxygen vacancy sites on titania. It was suggested that these adsorbed molecules formed CO₂ species as a result of charge transfer from the defects (Ti³⁺ site) to the carbon atom of CO₂. From CO₂ TPD results, it was observed that the titania prepared in toluene have more CO₂ desorption peak area of Ti³⁺ defective site than that of the one prepared in 1,4-butanediol.

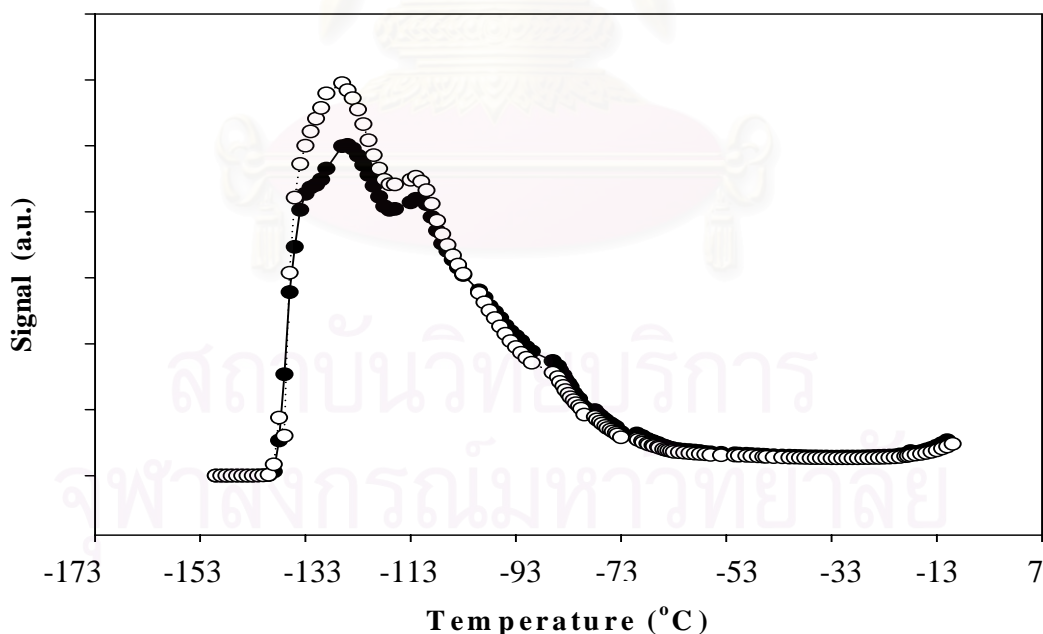
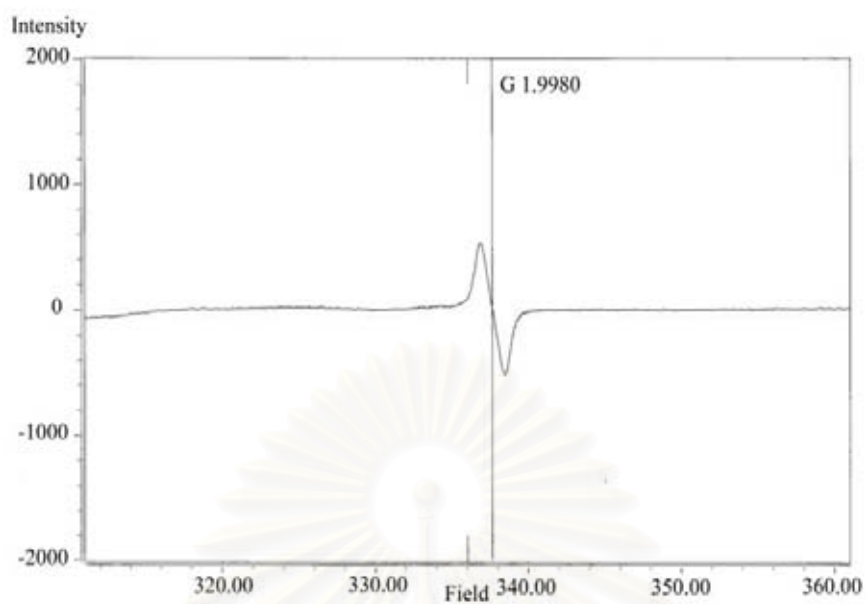


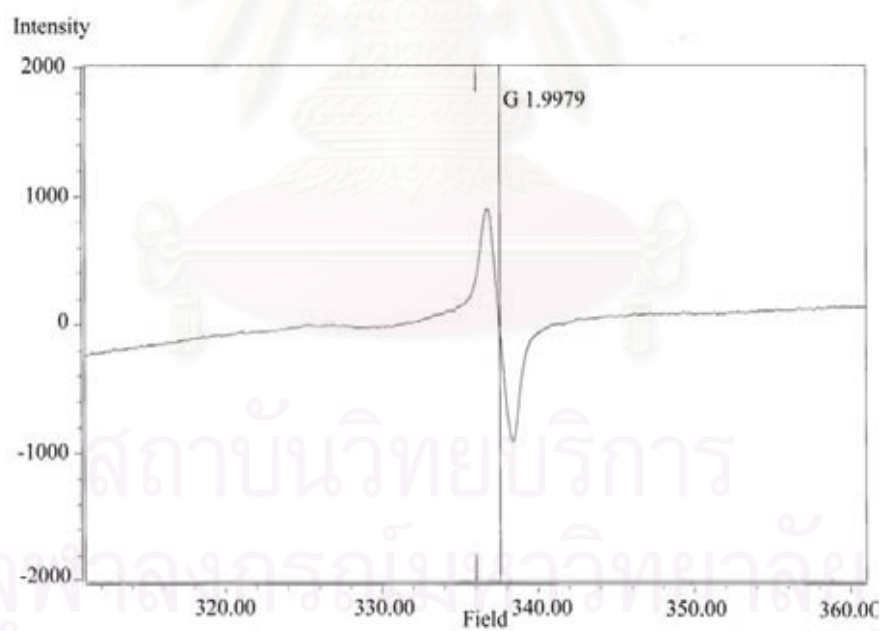
Figure 5.7 Temperature programmed Desorption of titania products synthesized in 1,4-butanediol (●) and toluene (○).

5.1.3.4 Electron Spin Resonance Spectroscopy (ESR)

The number of Ti^{3+} defective sites of titania particles can also be determined using electron spin resonance spectroscopy technique. The ESR results are shown in Figure 5.8. Such Ti^{3+} species are produced by trapping of electrons at defective sites of TiO_2 and the amount of accumulated electrons may therefore reflect the number of defective sites (Ikeda *et al.*, 2003). The signal of g value less than 2 was assigned to Ti^{3+} ($3d^1$) (Salama *et al.*, 1993 and R.F. Howe *et al.*, 1985). Both TiO_2 synthesized in 1,4-butanediol and TiO_2 synthesized in toluene show Ti^{3+} ESR signal at $g = 1.9979$ - 1.9980 with TiO_2 synthesized in toluene exhibited much higher intensity. The results clearly show that the TiO_2 synthesized in toluene possessed more Ti^{3+} defective sites than the one synthesized in 1,4-butanediol.



(A)



(B)

Figure 5.8 ESR results of the titania products synthesized in (A) 1,4-butanediol and (B) toluene.

5.2 1%Pd over Titanium (IV) oxide catalyst

5.2.1 Catalyst Characterization (fresh catalyst)

5.2.1.1 Specific Surface Area

BET surface area of the titania supported palladium catalysts determined by N₂ physisorption measurement are shown in Table 5.3. It was found that BET surface area of the titania synthesized in 1,4-butanediol was slightly less than that of titania synthesized in toluene. Compared the BET surface area of the pure titania supports and the titania supported palladium catalysts, it was found that BET surface areas of the titania supports were slightly decreased after impregnation of Pd suggesting that the metals were deposited in some of the pores of titania.

Table 5.3 BET surface area

sample	BET surface area(m ² /g)	d _p Pd ⁰ (nm)	PdO(nm)
1%Pd/TiO ₂ (1,4-butanediol)	51.8	11.2	10.5
1%Pd/TiO ₂ (toluene)	60.6	13.5	13.2

5.2.1.2 Catalyst Structure and Particle Size Distribution

The phase structure of the prepared catalysts was characterized by X-ray diffraction technique. The XRD diffractograms of the titania supported palladium catalysts are shown in Figure 5.9. From the XRD results of 1%Pd/TiO₂, diffraction peaks for palladium oxide (PdO) were detectable at 33.8°2θ. It was also found that titania support did not undergo structural changes during palladium impregnation and calcination because the XRD analysis only exhibited titania anatase phase for both catalysts.

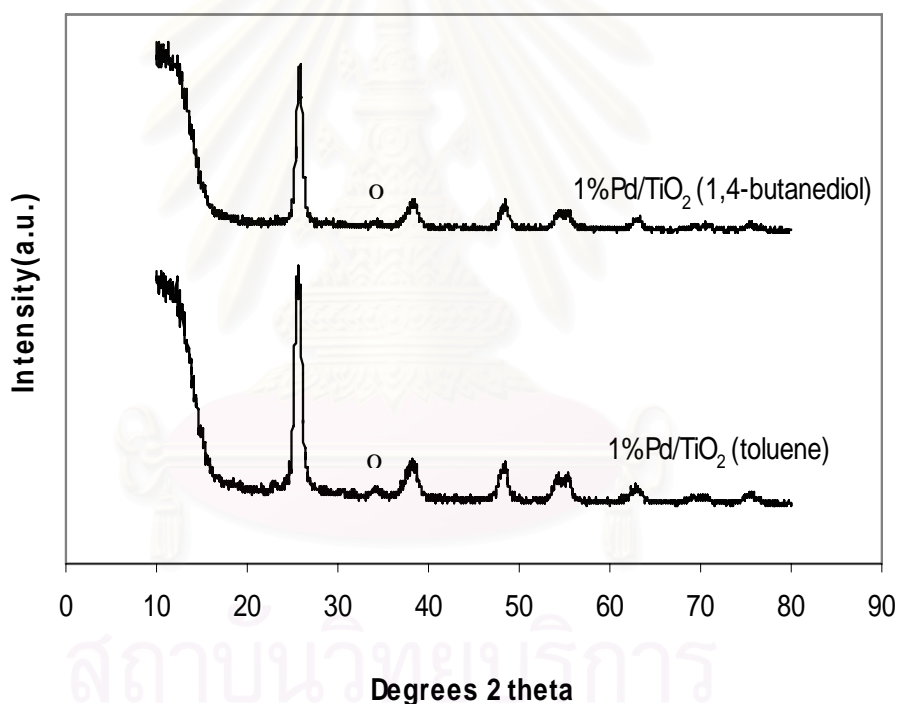


Figure 5.9 XRD patterns of 1%Pd/TiO₂ products synthesized in 1,4-butanediol and toluene at 320°C for 6 h.

5.2.1.3 Metal Active Sites

Chemisorption is the relatively strong, selective adsorption of chemically reactive gases on available metal sites or metal oxide surfaces at relatively higher temperatures (i.e. 25-400°C); the adsorbate-adsorbent interaction involves formation of chemical bonds and heats of chemisorption in the order of 50-300 kJ mol⁻¹.

The pulse CO chemisorption technique was based on the assumption that one carbon monoxide molecule adsorbs on one palladium site (Vannice *et al.*, 1981; Anderson *et al.*, 1985; Ali *et al.*, 1998 and Mahata *et al.*, 2000).

The amounts of CO chemisorption on the catalysts and the percentages of palladium dispersion are given in Table 5.4. It was found that Pd/TiO₂ synthesized in 1,4-butanediol exhibited higher amount of CO chemisorption than Pd/TiO₂ synthesized in toluene. Since both TiO₂ supports possess similar BET surface areas and crystallite sizes, the differences in the amount of active surface Pd were probably induced by the different degrees of crystallinity of the TiO₂ particles.

Table 5.4 Results from Pulse CO Chemisorption

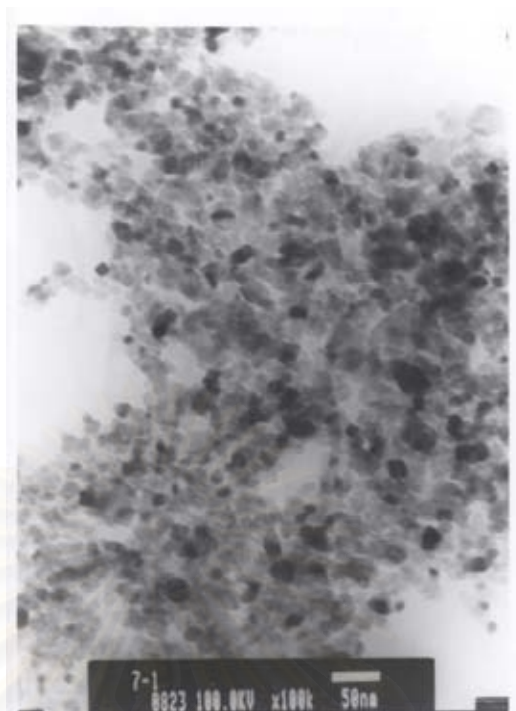
sample	active site (site/g catalyst)	%Pd dispersion
1%Pd/TiO ₂ (1,4-butanediol)	2.54x10 ¹⁸	10.0
1%Pd/TiO ₂ (toluene)	2.1x10 ¹⁸	8.3

5.2.1.4 Transmission Electron Microscopy (TEM)

TEM is a useful tool for determining crystallite size and size distribution of supported metals. It allows determination of the micro-texture and microstructure of electron transparent samples by transmission of a focused parallel electron beam to a fluorescent screen with a resolution presently better than 0.2 nm.

TEM micrographs of fresh titania supported palladium catalysts are shown in Figure 5.10. TEM micrographs were taken in order to physically measure the size of the palladium oxide particle and/or palladium clusters. Since the metal loading is low and the surface area of the sample is very high, in principle it is quite difficult to observe metal dispersion by TEM. However, a large number of pictures were collected from different portion of the samples in order to obtain further evidence about the dispersion of the palladium. The particle size of PdO particles measured from TEM images was found to be in accordance with the results from XRD. The average palladium oxide crystallite sizes calculated from TEM are given in Table 5.3. TEM images show that there is no difference in bulk structure of the fresh titania supported palladium catalysts synthesized in the different solvents.

(A)



(B)

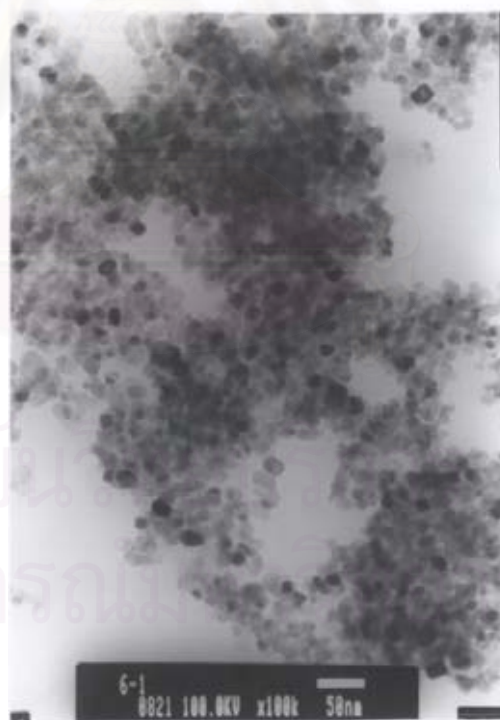


Figure 5.10 TEM micrographs of 1%Pd supported on TiO₂ synthesized in (A)1,4-butanediol and (B) toluene.

5.2.2 Reaction Study in Selective Acetylene Hydrogenation

5.2.2.1 Selective acetylene hydrogenation using a gas mixture of 0.996 vol% acetylene in ethylene

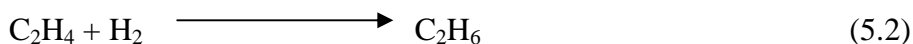
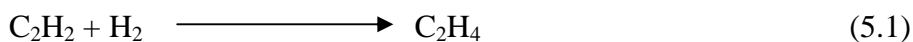
The performance of the catalysts in selective hydrogenation of acetylene was determined in terms of acetylene conversion and selectivity towards ethylene. Acetylene conversion is defined as moles of acetylene converted with respect to acetylene in the feed. Selectivity is the ratio of the amount of acetylene converted to ethylene and total amount of acetylene converted. Ideally, there should be one acetylene molecule converted to ethylene for every hydrogen molecule consumed, or 100% selectivity, since all of the acetylene is converted into ethylene. In actual practice, some hydrogen will always be consumed in the side reaction of ethylene conversion to ethane.

In this study, selective hydrogenation of acetylene was carried out under various reaction conditions. For the first study, we used a gas mixture containing 0.996 vol% acetylene in ethylene as reactant feed for the selective hydrogenation of acetylene. It was found that all of the acetylene was converted to ethane and ethylene selectivity was 0%. The selectivity can be measured by observing the change in ethane and ethylene from the inlet and the outlet. The performance of the catalyst in this study was therefore reported in terms of acetylene conversion and ethylene gain observed from acetylene and hydrogen concentrations as detailed below:

Conversion of acetylene is the ratio of acetylene converted and acetylene in the feed:

$$\text{C}_2\text{H}_2 \text{ conversion (\%)} = 100 \times \frac{\text{acetylene in feed} - \text{acetylene in product}}{\text{acetylene in feed}}$$

Ethylene gain is considered from the following reaction scheme:



Ethylene gain is defined as the ratio of those parts of acetylene that are hydrogenated to ethylene to the amount of totally hydrogenated acetylene:

$$\text{C}_2\text{H}_4 \text{ gain (\%)} = 100 \times \frac{\text{C}_2\text{H}_2 \text{ hydrogenated to C}_2\text{H}_4}{\text{totally hydrogenated C}_2\text{H}_2} \quad (i)$$

Where total hydrogenated acetylene is the difference between moles of acetylene in the product with respect to those in the feed ($d\text{C}_2\text{H}_2$). In other words, acetylene hydrogenated to ethylene is the difference between the total hydrogenated acetylene ($d\text{C}_2\text{H}_2$) and the ethylene being loss by hydrogenation to ethane (equation 5.2). Regarding the difficulty in precise measurement of the ethylene change in the feed and product, the indirect calculation using the difference in the hydrogen amount (hydrogen consumed: $d\text{H}_2$) was used.

The ethylene being hydrogenated to ethane is the difference between all the hydrogen consumed and all the acetylene totally hydrogenated.

$$\text{C}_2\text{H}_4 \text{ gain (\%)} = 100 \times \frac{[d\text{C}_2\text{H}_2 - (d\text{H}_2 - d\text{C}_2\text{H}_2)]}{d\text{C}_2\text{H}_2} \quad (ii)$$

As shown in equation (5.1) and (5.2), 2 moles of hydrogen were consumed for the acetylene lost to ethane, but only 1 mole of hydrogen for the acetylene gained as ethylene. The overall gain can also be written as:

$$\text{C}_2\text{H}_4 \text{ gain (\%)} = 100 \times \left[2 - \frac{d\text{H}_2}{d\text{C}_2\text{H}_2} \right] \quad (iii)$$

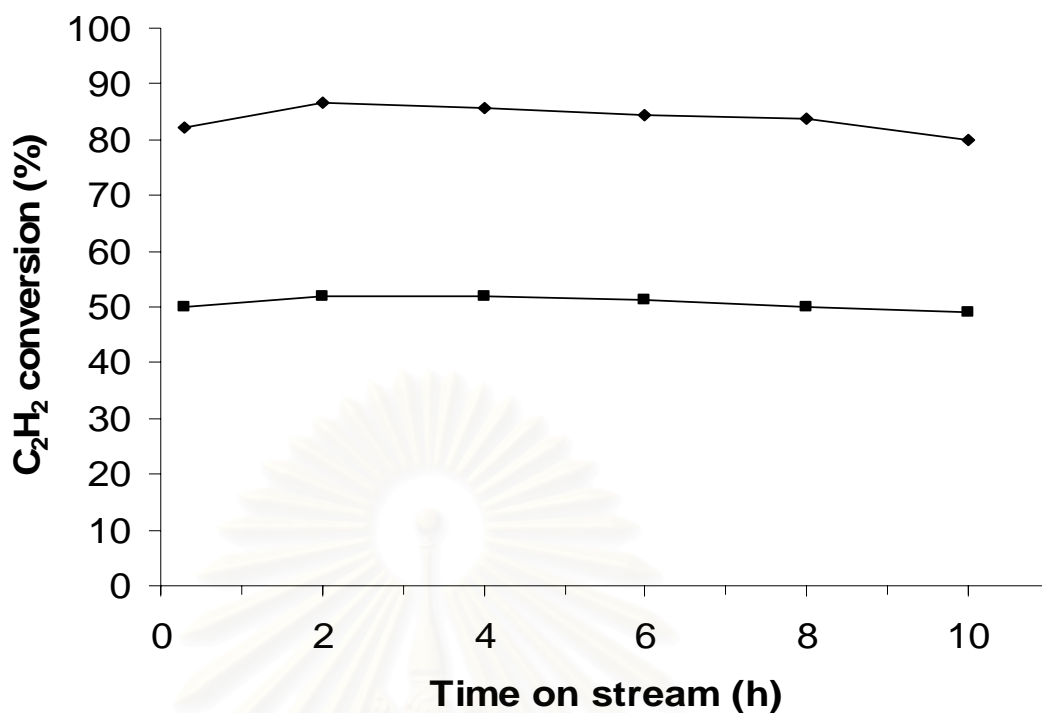
Equation (ii) and (iii) are, of course the same, and ethylene gain discussed in this research is then calculated based on equation (iii). This value is the percentage of the theoretically possible ethylene gain which has been achieved in the operation. A

positive value represents net production of ethylene. When the negative value refers to ethylene loss. However, it should be noted that these calculations can not provide a measure of acetylene polymerization reaction that forms green oil.

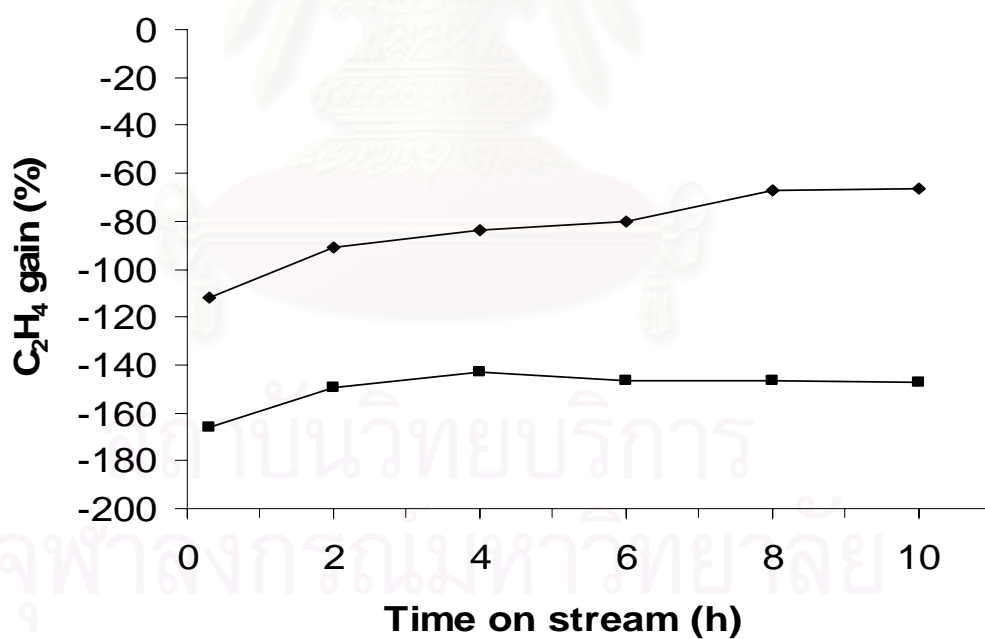
Typically, the normal operating temperature in an acetylene converter lies in the range 65-85°C (Derrien *et al.*, 1986 and Molnár *et al.*, 2001). During start-up, the reaction can proceed at as low as 45°C. After a short period during which the catalyst has stabilized, the reactor temperature would reach the normal operating range and remain constant throughout its life-time. According to the literature, acetylene hydrogenation usually exhibits three distinct phases (Bond *et al.*, 1958; Al-Ammar *et al.*, 1978 and McGown *et al.*, 1978). In a brief initial period (0-2 min on stream), the reaction is rapid, forming both ethylene and ethane. In the second phase (2-60 min on stream), the rates of acetylene consumption, and ethylene and ethane production are all constant. During this period, hydrogenation of acetylene is the primary reaction. The selectivity is usually high, and is the characteristic of changes occurring in the catalyst. The third phase begins when acetylene hydrogenation is nearly complete and in this region approximates to the industrial situation.

In the first study, the performance of the catalysts for acetylene hydrogenation upon aging was measured at 50°C and a space velocity of 28819.36 h⁻¹ for 10 h. Observation of the catalytic behavior was carried out every 2 h as illustrated in Figure 5.11.

It was found that acetylene conversion and ethylene gain were independent of time on stream. For all the catalysts, ethylene gains were below zero. The negative values of ethylene gain indicate that all of the acetylene is converted to ethane and some of the ethylene feed is additionally converted to ethane.



(A)



(B)

Figure 5.11 Reaction result on various catalysts in acetylene hydrogenation after reduction at 500°C (H_2 /acetylene = 2, temperature = 50°C): (A) % C_2H_2 conversion and (B) % C_2H_4 gain; (◆) 1%Pd/TiO₂ (1,4-butanediol), (□) 1%Pd/TiO₂ (toluene).

5.2.2.2 Selective acetylene hydrogenation under the conditions C₂H₂/H₂=1/2 in N₂ balance and total flow 200 cc/min

In the previous section, it was found that over hydrogenation occurred on both TiO₂ supported Pd catalysts under the conditions used (excess ethylene). Pure acetylene in nitrogen balance was used as the reactant gases instead of acetylene in excess ethylene in order to be able to compare the catalyst performances in acetylene hydrogenation.

The performances of the catalysts under these conditions were reported in term of acetylene conversion and ethylene selectivity observed from acetylene and ethylene concentrations as detailed below:

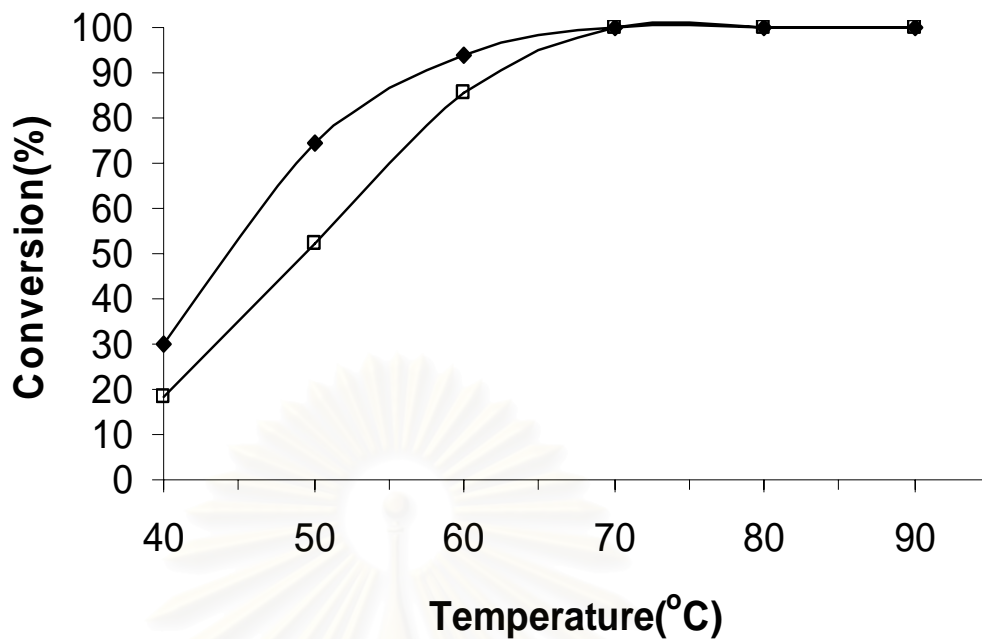
Activity or conversion of acetylene as used herein is defined as moles of acetylene converted with respect to acetylene in feed:

$$\text{C}_2\text{H}_2 \text{ conversion (\%)} = 100 \times \frac{\text{acetylene in feed} - \text{acetylene in product}}{\text{acetylene in feed}}$$

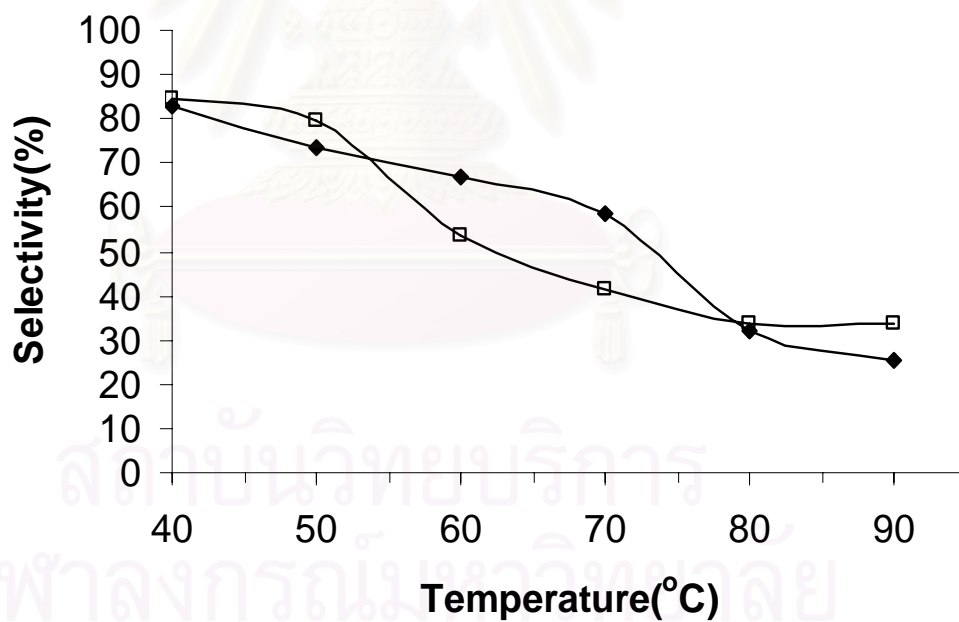
Selectivity of ethylene as used herein is defined as moles of ethylene in product with respect to acetylene converted:

$$\text{C}_2\text{H}_4 \text{ selectivity (\%)} = 100 \times \frac{\text{ethylene in product}}{\text{acetylene in feed} - \text{acetylene in product}}$$

The conversion and selectivity of Pd catalysts supported on TiO₂ synthesized in 1,4-butanediol and TiO₂ synthesized in toluene in selective acetylene hydrogenation as a function of reaction temperature are shown in Figures 5.12. The use of TiO₂ synthesized in 1,4-butanediol as the support for Pd catalysts resulted in higher acetylene conversions than the ones supported on TiO₂ synthesized in toluene. Acetylene conversion of the supported Pd catalysts reached 100% at ca. 70°C. The ethylene selectivity for all the catalysts at the temperature ranges 40-50°C were not significantly difference and were found to be ca. 80-90%. However, at 60-70°C, ethylene selectivity of Pd/TiO₂ synthesized in 1,4-butanediol was much higher than those of Pd/TiO₂ synthesized in toluene.



(A)



(B)

Figure 5.12 Reaction results on various catalysts in acetylene hydrogenation after reduction at 500°C (H_2 /acetylene = 2, balance N_2 , total flow 200 cc/min):

(A) % C_2H_2 conversion and (B) % C_2H_4 selectivity; (◆) 1%Pd/TiO₂ (1,4-butanediol), (□) 1%Pd/TiO₂(toluene).

5.2.3 Catalyst Characterization (spent catalyst)

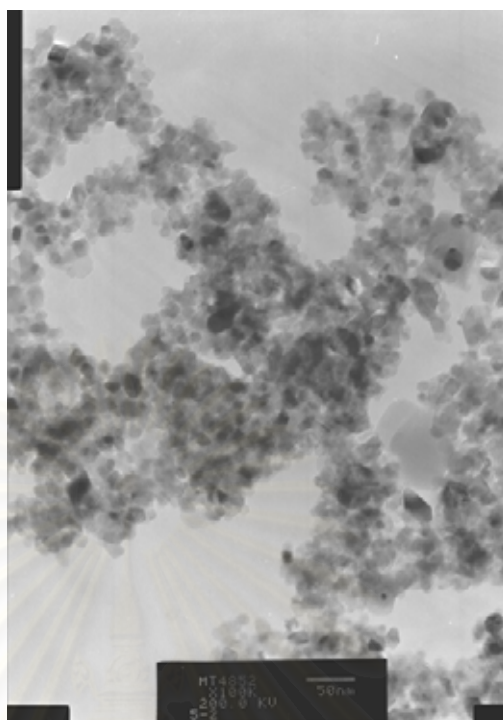
5.2.3.1 Transmission Electron Microscopy (TEM)

TEM micrographs were taken for all the spent titania supported palladium catalysts after the selective acetylene hydrogenation reaction in order to physically observe any change in the size of palladium oxide particles after the reaction. The TEM images of the used catalysts were taken after carbon deposits have been removed by calcination at 500°C for 2 h. The TEM micrographs for the spent titania supported palladium catalysts are shown in Figure 5.13. Table 5.5 also shows the average palladium oxide crystallite sizes that are measured from TEM micrographs. TEM images of the spent catalysts show slightly larger palladium oxide particle sizes than those of the fresh titania supported palladium catalysts suggesting that there was some metal sintering during reduction and reaction.

Table 5.5 Average palladium oxide crystallite sizes of 1%Pd/TiO₂ synthesized in 1,4-butanediol and toluene measured by TEM.

Catalyst	Average particle size by TEM (nm)	
	fresh	spent
1%Pd/TiO ₂ (1,4-butanediol)	10.5	13.5
1%Pd/TiO ₂ (toluene)	13.2	13.9

(A)



(B)

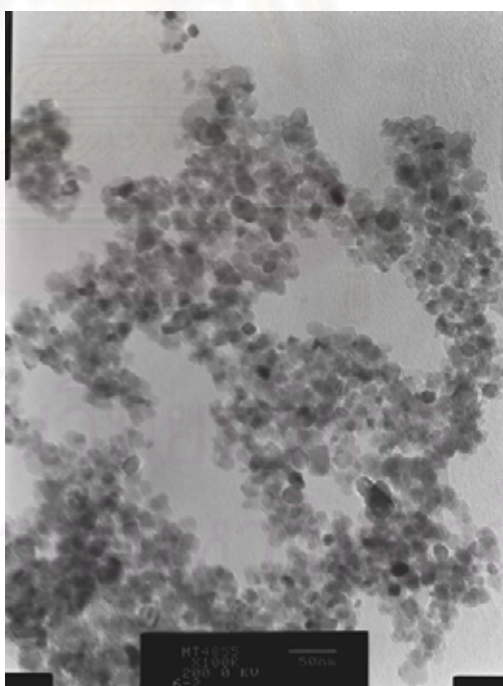


Figure 5.13 TEM micrographs of 1%Pd spent catalysts supported on TiO_2 synthesized in (A) 1,4-butanediol and (B) toluene (reaction conditions were $\text{C}_2\text{H}_2/\text{H}_2=1/2$ and N_2 balance).

5.2.3.2 Temperature Programmed Oxidation (TPO)

The amount of carbonaceous deposits on the spent catalysts were characterized by temperature programmed oxidation (TPO) technique. After reaction test, coke may deposit on the catalyst surface resulting in deactivation of the catalyst which can decrease the activity, selectivity and life time of the catalysts (Kim, *et al.*, 2003, Kang *et al.*, 2002 and Kim *et al.*, 2004). Figure 5.14 shows the comparison of carbon deposits on 1%Pd catalysts supported on titania synthesized in 1,4-butanediol and toluene. It was found that use of titania synthesized in toluene resulted in lower amount of carbonaceous deposits than the one synthesized in 1,4-butanediol. The difference in the amount of carbonaceous deposits of Pd catalysts supported on titania synthesized in different solvents may be induced by their different catalytic activities.

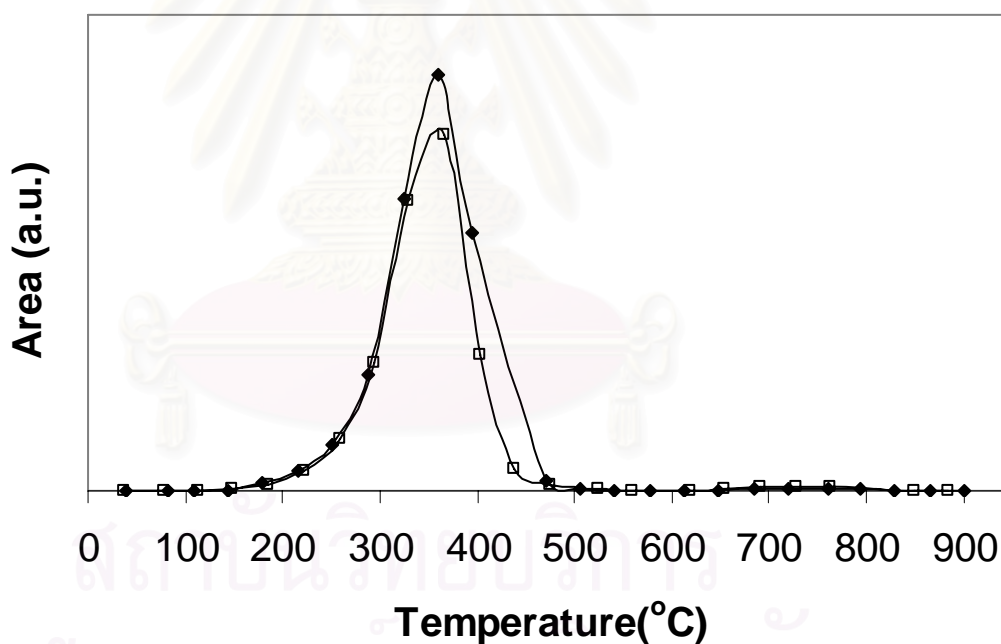


Figure 5.14 Temperature programmed oxidation profiles of; (◆) 1%Pd/TiO₂ (1,4-butanediol) and (□) 1%Pd/TiO₂(toluene).

5.3 1%Pd -3%Ag over Titanium (IV) oxide catalyst

5.3.1 Catalyst Characterization (fresh catalyst)

5.3.1.1 Specific Surface Area

The results of BET surface area of 1%Pd-3%Ag/TiO₂ catalysts analyzed by N₂ adsorption are summarized in Table 5.5.

The data in Table 5.3 and 5.6 indicated that impregnation of palladium onto the titania supports decreased the surface area of titania support. Moreover, when the Pd/TiO₂ catalysts were re-impregnated with Ag, the surface area was further decreased, suggesting that some of the pores of titania support were blocked by the metal.

The BET surface areas of the titania supports, titania supported palladium catalysts and titania supported palladium-silver catalysts which synthesized in the different solvents were found to be in the order of titania supports > titania supported Pd catalysts > titania supported Pd-Ag catalysts. The Pd-Ag catalyst prepared with TiO₂ synthesized in 1,4-butanediol were slightly less than the one prepared with TiO₂ synthesized in toluene. However, the difference in BET surface areas of the catalysts prepared in different solvents was not significant.

Table 5.6 BET Surface area

sample	surface area (m ² /g)
1%Pd-3%Ag/TiO ₂ (1,4-butanediol)	42.1
1%Pd-3%Ag/TiO ₂ (toluene)	47.0

5.3.1.2 Catalyst Structure and Particle Size Distribution

X-ray diffraction analysis was used to determine the bulk crystalline phase in the catalysts. The XRD patterns of 1%Pd-3%Ag/TiO₂ catalysts are depicted in Figure 5.15.

From the XRD results of 1%Pd-3%Ag/TiO₂ catalysts, diffraction peaks for palladium oxide (PdO) were detectable at 33.8°2θ. However, no XRD peaks for AgO were observed. This suggests that the Ag or AgO may be highly dispersed. No structural changes of the titania supports were found during the palladium-silver impregnations and calcination since the XRD analysis only exhibited the anatase TiO₂ phase for both catalysts.

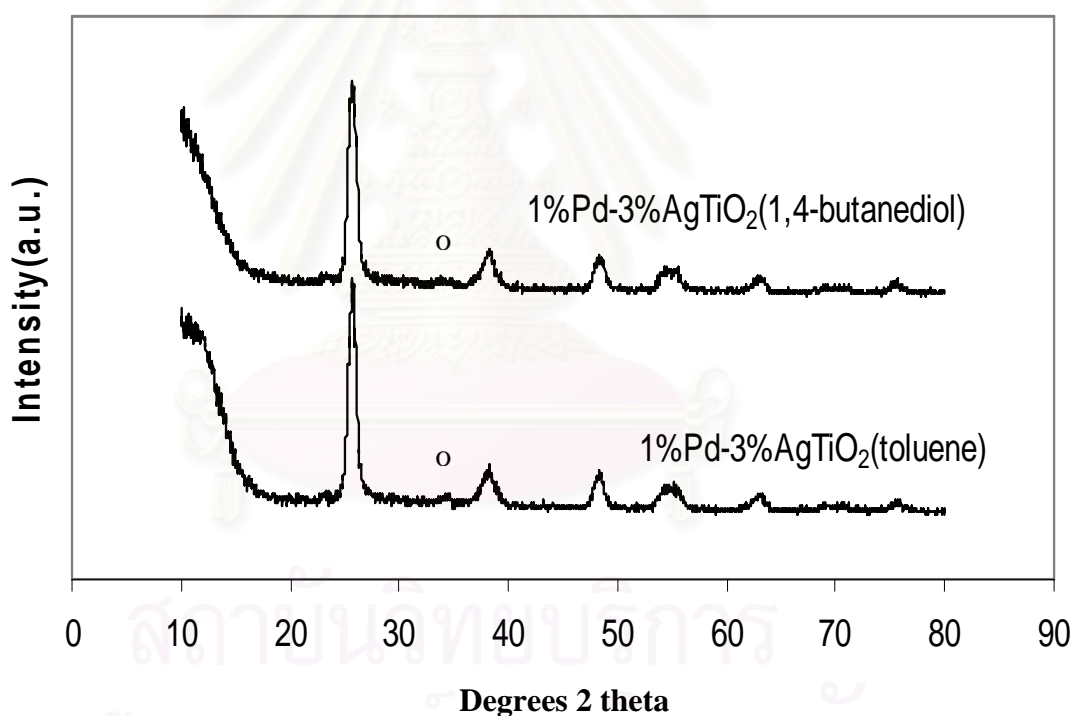


Figure 5.15 XRD patterns of 1%Pd3%Ag/TiO₂ products synthesized in 1,4-butanediol and toluene at 320°C for 6 h.

5.3.1.3 Metal Active Sites

CO chemisorption technique provides the information on the number of palladium active sites and percentages of metal dispersion. The total CO uptakes and the percentages of palladium metal dispersion are reported in Table 5.7.

It is obvious that addition of Ag to Pd/TiO₂ catalysts resulted in lower amount of active surface Pd since CO did not adsorbed on Ag metal. However, the bimetallic Pd-Ag catalyst has been reported to show many beneficial effects in selective hydrogenation of acetylene to ethylene, for examples, suppression of oligomers formation and improvement of ethylene selectivity (Huang *et al.*, 1998). These beneficial effects are due to the altered surface arrangement of Ag atoms on the Pd surface. Roder *et al.* (1993) suggested that Ag atoms are likely to stay at the surface in segregated form with Pd rather than forming an alloy. It was found that Pd-Ag/TiO₂ synthesized in 1,4-butanediol exhibited slightly higher amount of CO chemisorption than Pd-Ag/TiO₂ synthesized in toluene. The results were similar to those of the single metal catalysts.

Table 5.7 Results from Pulse CO Chemisorption

Sample	Active sites (sites/g cat)	%Pd dispersion
1%Pd-3%Ag/TiO ₂ (1,4-butanediol)	1.05x10 ¹⁸	3.8
1%Pd-3%Ag/TiO ₂ (toluene)	0.79x10 ¹⁸	3.6

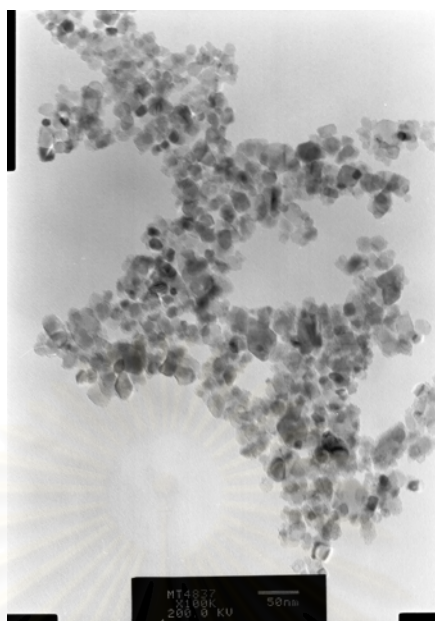
5.3.1.4 Transmission Electron Microscopy (TEM)

The study of morphology of the Pd-Ag catalysts was also carried out using Transmission Electron Microscope (TEM). Figure 5.16 (A) and (B) depict TEM micrographs of Pd-Ag catalysts supported on titania synthesized in 1,4-butanediol and toluene, respectively. The average particle sizes for both metal and support observed from TEM for Pd-Ag catalysts synthesized in 1,4-butanediol and toluene were found to be not different to the single metal catalysts. However, it is difficult to distinguish Pd from Ag based on TEM micrographs. The different solvents used in the synthesis of TiO₂ also have no effect on the bulk structure of the Pd-Ag catalysts.



สถาบันวิทยบริการ
จุฬาลงกรณ์มหาวิทยาลัย

(A)



(B)

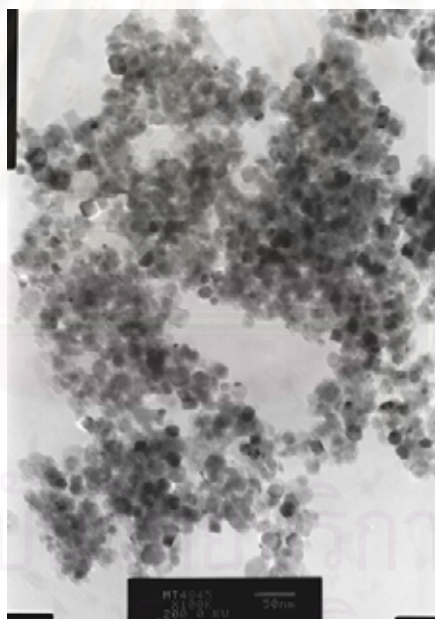


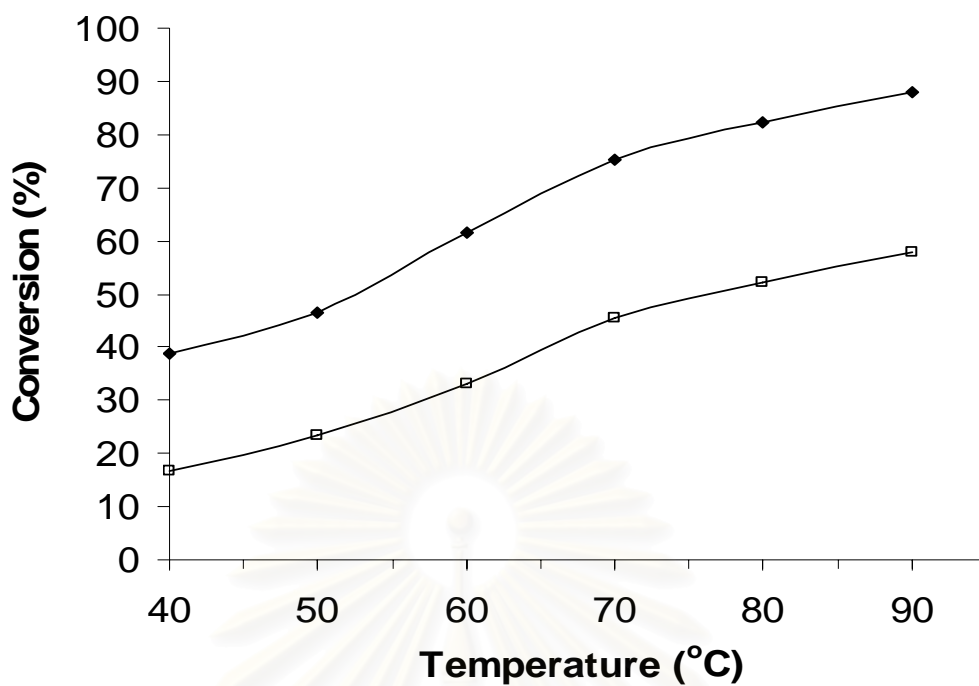
Figure 5.16 TEM micrograph of 1%Pd-3%Ag supported TiO₂ synthesized in (A) 1,4-butanediol and (B) toluene.

5.3.2 Reaction Study in the Selective Acetylene Hydrogenation

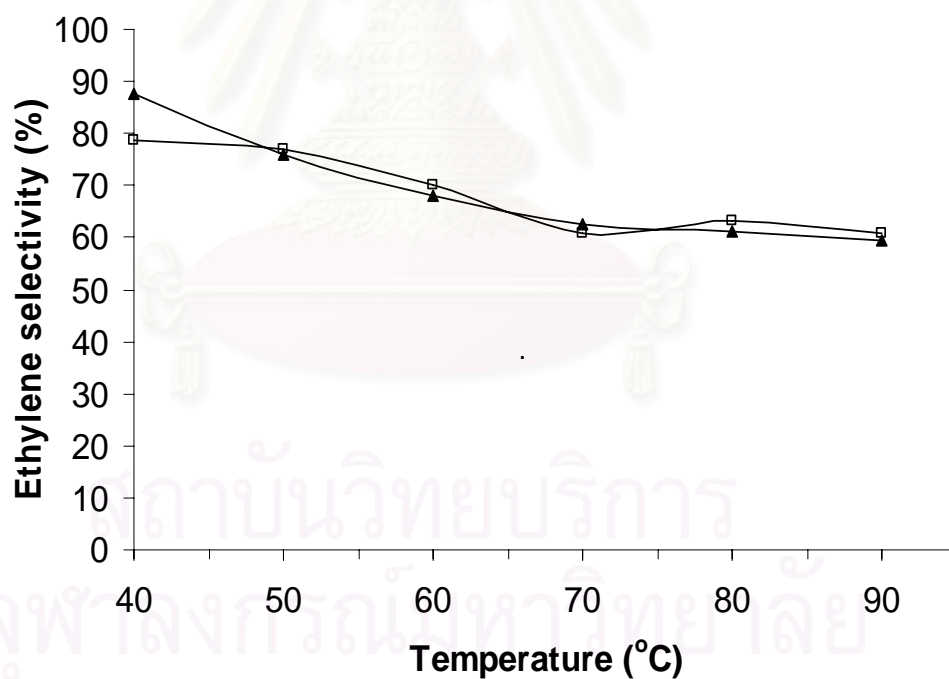
The performance of 1%Pd-3%Ag catalysts supported on TiO₂ catalysts synthesized in the different solvents in acetylene hydrogenation was evaluated in the temperature ranges between 40-90°C at a space velocity 2,8819 h⁻¹. The pure acetylene gas in N₂ balance was used for the selective hydrogenation of acetylene.

Figure 5.17 illustrates the performances of 1%Pd-3%Ag/TiO₂ synthesized in the different solvents. As shown in Figure 5.17(A), the activity of all the catalysts increased with increasing temperature. However, the titania supported Pd-Ag catalyst synthesized in 1,4-butanediol showed higher acetylene conversion than the ones synthesized in toluene for all temperatures used. The selectivity of ethylene (Figure 5.17(B)) for all the catalysts declined when the reaction temperature increased.

Figure 5.18 summarizes the conversion and selectivity of Pd and Pd-Ag catalysts supported on TiO₂-1,4-butanediol and TiO₂-toluene in selective acetylene hydrogenation as a function of reaction temperature. The use of TiO₂ synthesized in 1,4-butanediol as the supports for Pd or Pd-Ag catalysts resulted in higher acetylene conversions than the ones supported on TiO₂ synthesized in toluene. Acetylene conversion of the single metal catalysts reached 100% at ca. 70°C while those for the bimetallic catalysts showed only 40% (for Pd-Ag/TiO₂ synthesized in toluene) and 80% (for Pd-Ag/TiO₂ synthesized in 1,4-butanediol) conversions at 90°C. The ethylene selectivity for all the catalysts at the temperature ranges 40-50°C was not significantly different and was found to be ca. 80-90%. However, at 60-70°C, ethylene selectivity of Pd/TiO₂ synthesized in 1,4-butanediol was much higher than those of Pd/TiO₂ synthesized in toluene. Ethylene selectivity for the Ag-promoted catalysts was similar for all the reaction temperatures used in this study and was higher than those of the non-promoted ones. In this study we have found that use of TiO₂ with higher amount of Ti³⁺ defective sites as a support for Pd catalyst resulted in lower acetylene conversion and selectivity for ethylene after reduction at 500°C. The effect was probably suppressed by Ag promotion since no difference in ethylene selectivity was observed for the Pd-Ag/TiO₂ catalysts.

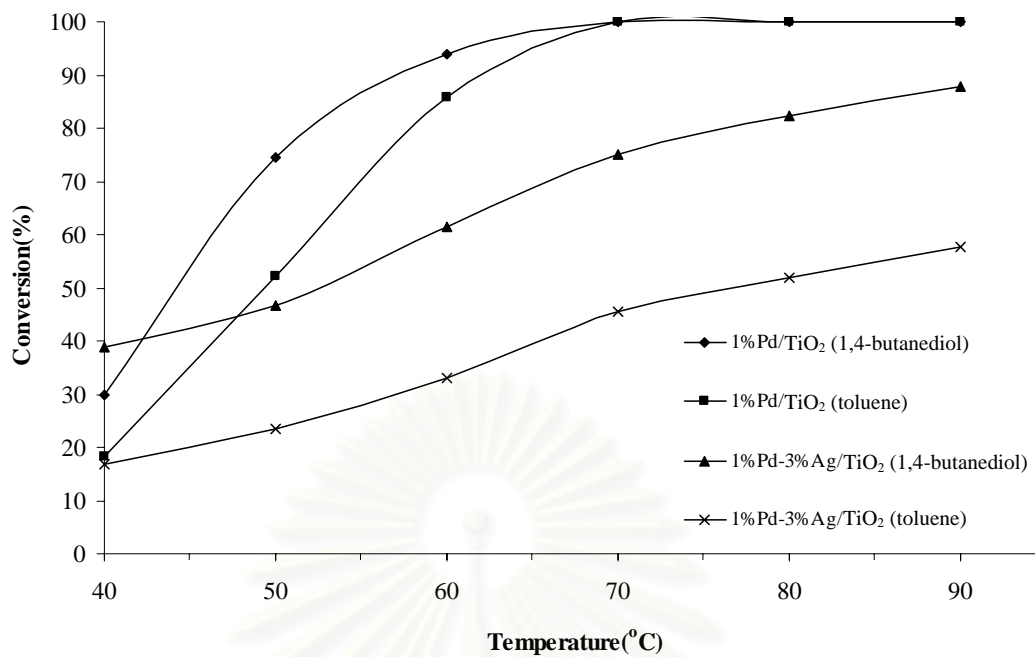


(A)

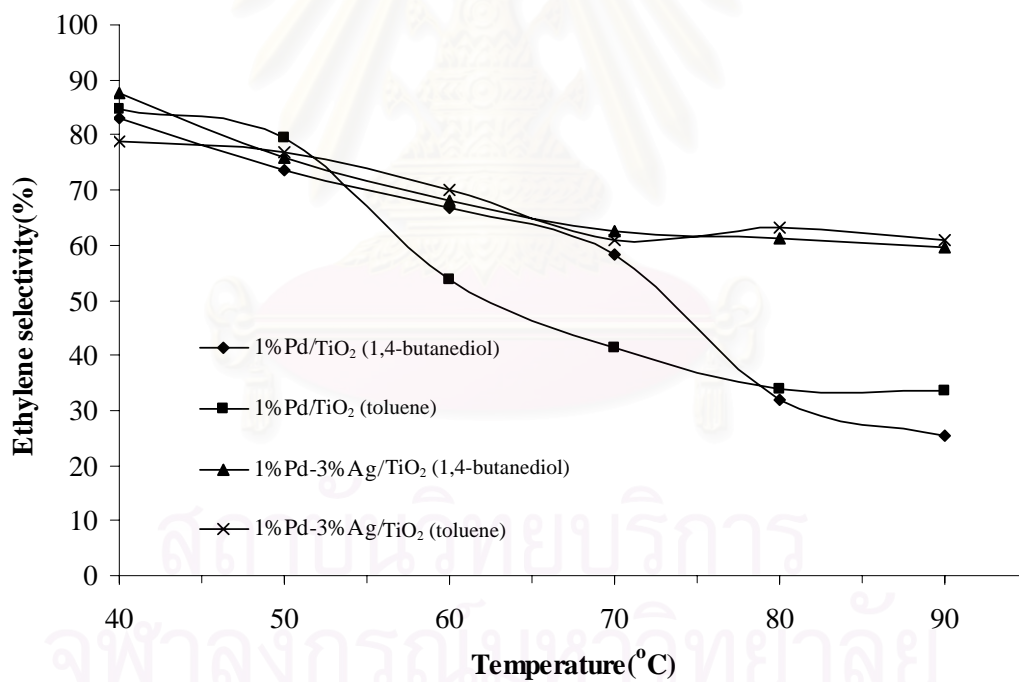


(B)

Figure 5.17 Reaction results on the Pd-Ag/TiO₂ catalysts in acetylene hydrogenation after reduction at 500°C (H₂/acetylene = 2, balance N₂, total flow 200 cc/min): (A) %C₂H₂ conversion and (B) %C₂H₄ selectivity; (◆) 1%Pd-3%Ag/TiO₂ (1,4-butanediol), (□) 1%Pd-3%Ag/TiO₂ (toluene).



(A)



(B)

Figure 5.18 Reaction results on various catalysts in acetylene hydrogenation after reduction at 500°C (H_2 /acetylene = 2 and N_2 balance, total flow 200 cc/min): (A) % C_2H_2 conversion and (B) % C_2H_4 selectivity.

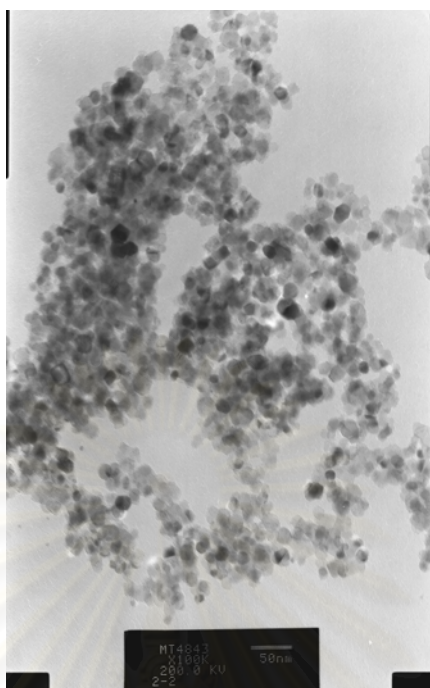
5.3.3 Catalyst Characterization (spent catalyst)

5.3.3.1 Transmission Electron Microscopy (TEM)

TEM micrographs were taken for all the spent titania supported palladium-silver catalysts after the selective acetylene hydrogenation reaction in order to physically observe any change in the size of metal oxide particles after the reaction. The TEM micrographs for spent titania supported palladium-silver catalysts are shown in Figure 5.19. Sintering of metal oxide particles was observed for all the Pd-Ag catalysts, however, the difference between PdO and AgO particles could not be detected by TEM.



A)



B)

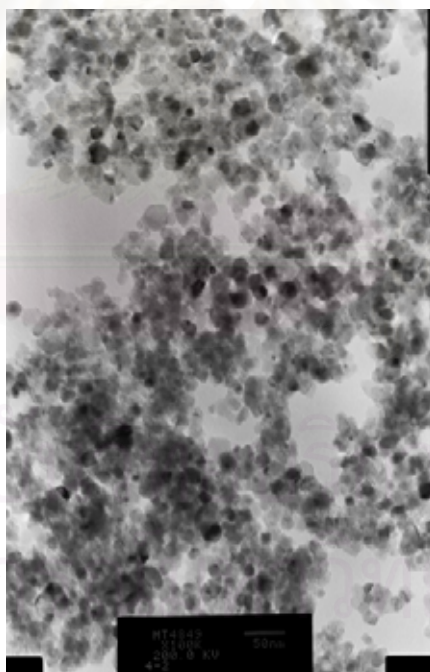


Figure 5.19 TEM micrograph of 1%Pd-3%Ag spent catalysts supported on TiO₂ synthesized in (A) 1,4-butanediol and (B) toluene (reaction conditions were C₂H₂/H₂=1/2 and N₂ balance).

5.4 Temperature Programmed Study

5.4.1 Temperature programmed desorption after ethylene adsorption for 3 h

Temperature programmed desorption (TPD) was performed in order to obtain an information about ethylene adsorption behavior on the catalyst samples. TPD from 35-800°C was carried out after the samples were reduced in H₂ at 500°C, and purged with He at the same adsorption temperature. TPD study was carried out for both the TiO₂ supported and the supported Pd and Pd-Ag catalyst. All the TPD profiles were shown in Figure 5.20. TPD profiles were found to be very different, suggesting that adsorption behavior of ethylene on the supports and on the catalyst were not the same. For example, high desorption peaks were observed for the TiO₂ supports whereas the peaks shifted to lower temperature when Pd or Pd Ag was loaded.

It was found that titania synthesized in toluene support exhibit two main desorption peaks at ca. 460°C and 680°C while the TiO₂-1,4-butanediol showed only one desorption peak at 680°C. The results suggest that there were two different active sites on the TiO₂ synthesized in toluene support, probably Ti³⁺ and Ti⁴⁺ sites. The high temperature peak for both TiO₂ supports disappeared after Pd loading as shown in the profiles of the Pd catalysts. However, desorption peak at ca. 460°C was still apparent for Pd/TiO₂-toluene. Since lower ethylene selectivity was found for Pd/TiO₂ synthesized in toluene than Pd/TiO₂ synthesized in 1,4-butanediol for similar acetylene conversion, this peak can be assigned to the sites for ethylene hydrogenation to ethane. Ethylene hydrogenation is usually believed to take place on the support by means of a hydrogen transfer mechanism (Aplund *et al.*, 1996). Ethylene hydrogenation could take place on the titania support probably Ti³⁺ defective sites resulting in lower acetylene conversion and selectivity for ethylene as observed in the case of Pd/TiO₂-toluene in this study. Moreover, 1% Pd/TiO₂ synthesized in toluene had lower carbon deposits than the one synthesized in 1,4-butanediol as shown previously in the TPO profile of the spent catalysts. It is suggested that higher hydrogen spill-over occurred on such catalyst. This is in a good agreement with the reaction results that higher ethane formation was found for 1%Pd/TiO₂ synthesized in toluene than 1%Pd/TiO₂ synthesized in 1,4-butanediol.

The Ag-promoted Pd catalysts exhibited only one ethylene desorption peak. The peak seemed to be shifted from ca. 460°C to ca. 400°C suggesting that the Pd catalyst surface on both TiO₂ supports was modified by Ag atoms. The presence of Ag probably blocked the sites for ethylene hydrogenation to ethane for both catalysts thus a significant improvement in ethylene selectivity was observed especially for high acetylene conversions at high temperatures. It has been reported that silver addition not only decreases the site that produce direct ethane formation but also reduces the sites of hydrogen spillover migrating from the metal to the support (Hodnett *et al.*, 1986).



สถาบันวิทยบริการ
จุฬาลงกรณ์มหาวิทยาลัย

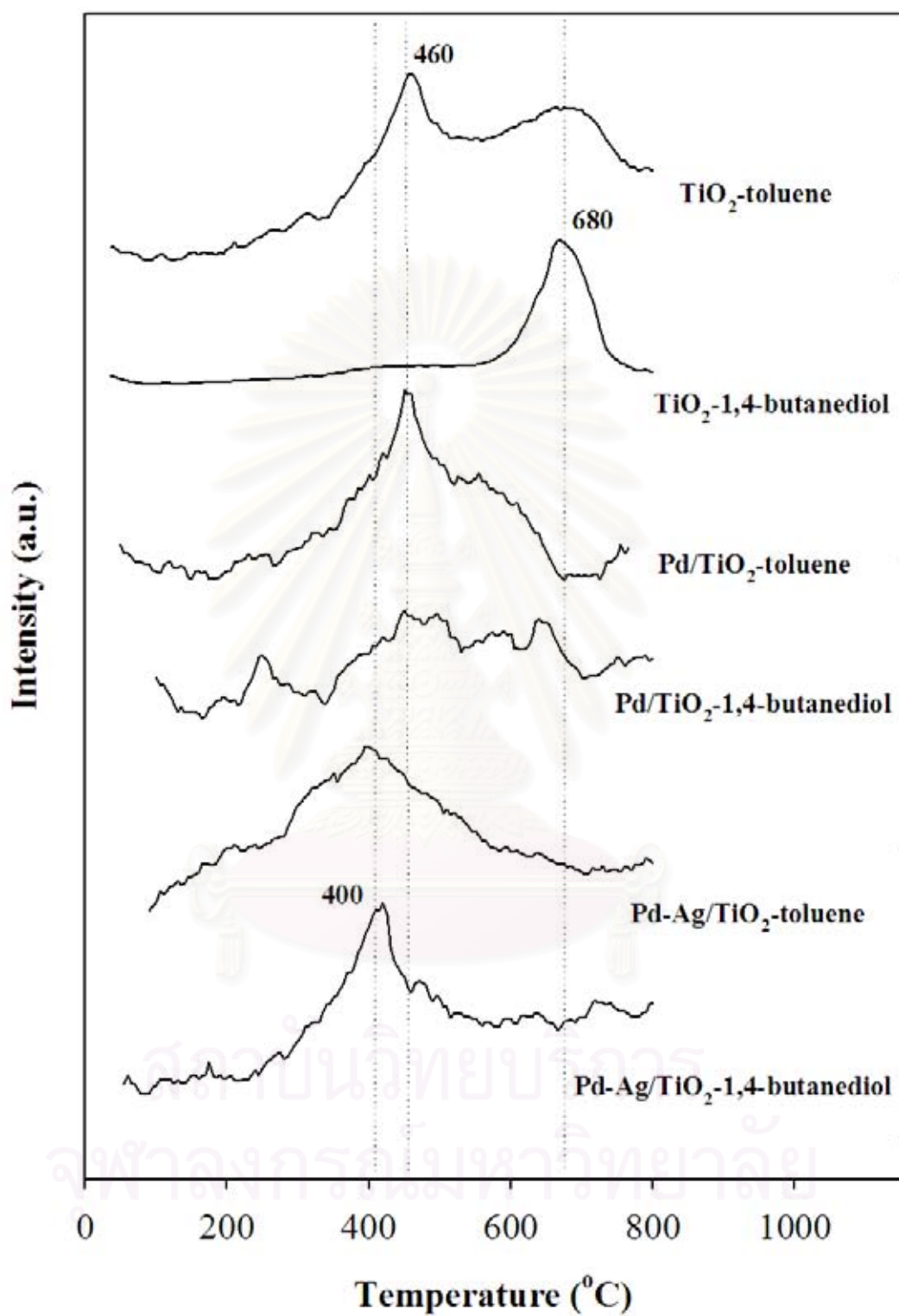


Figure 5.20 Temperature programmed desorption study.

5.4.2 Determination of the effluent gases during temperature programmed desorption

In order to gain the information about species of the effluent gases during the temperature programmed desorption study shown in the previous section(5.4.1), the temperature programmed desorption of ethylene was repeated using the temperature programmed oxidation (TPO) line in which the effluent gases were detected using a gas chromatograph equipped with a FID detector. It was found that the effluent gases from TPD were not ethylene but composed of methane and carbon dioxide. Decomposition of ethylene to methane and carbon dioxide was probably due to O₂ leakage to the system. However, no ethylene hydrogenation to ethane was observed during TPD study. The results of temperature programmed profiles of carbon dioxide and methane desorbed from 1%Pd/TiO₂ synthesized in 1,4-butanediol and toluene are illustrated in Figure 5.21 and 5.22, respectively. The TPD peaks of methane and CO₂ for 1%Pd/TiO₂ synthesized in toluene and TiO₂ synthesized in 1,4-butanediol were not significantly different. However, the results provide confirmation that the TPD study of ethylene in section 5.4.1 can be used to study ethylene adsorption behavior on the catalysts since no ethane formation was found.

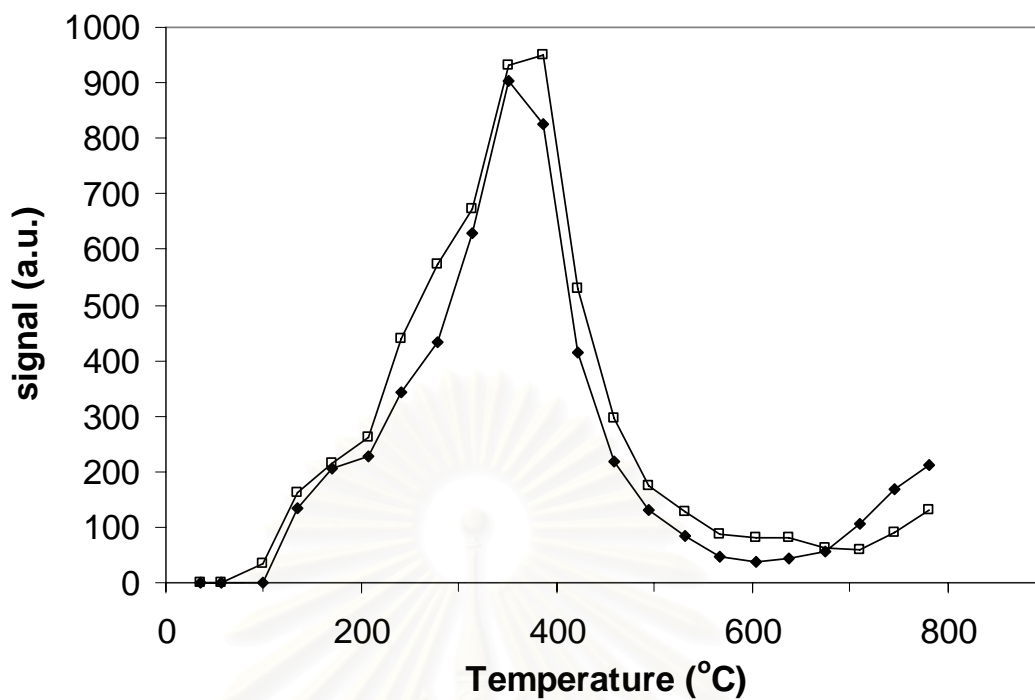


Figure 5.21 Temperature programmed profile of carbon dioxide; (◆) 1%Pd/TiO₂ (1,4-butanediol) and (□) 1%Pd /TiO₂ (toluene).

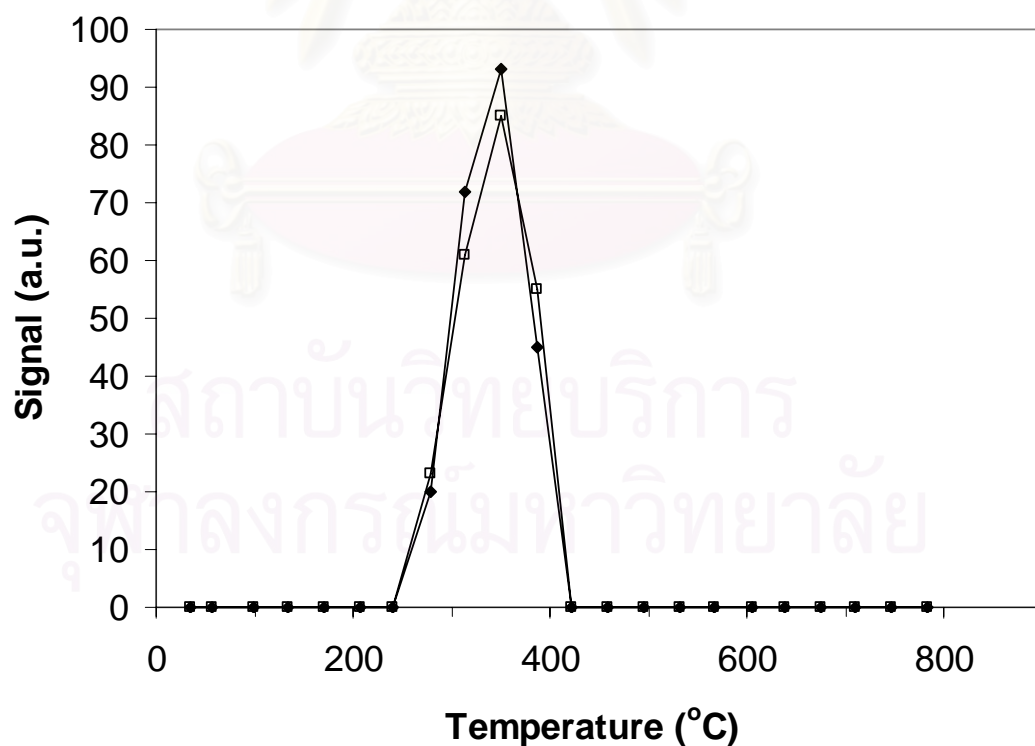


Figure 5.22 Temperature programmed profile of methane; (◆) 1%Pd/TiO₂ (1,4-butanediol) and (□) 1%Pd /TiO₂ (toluene).

5.4.3 Proposed mechanism for selective acetylene hydrogenation on the solvothermal TiO₂ supported Pd and Pd-Ag catalysts

The mechanism of the selective hydrogenation of acetylene to ethylene on the different TiO₂ supported Pd and Pd-Ag catalysts are illustrated in Figure 5.23. The titania support synthesized in 1,4-butanediol had less Ti³⁺ defective site than the one synthesized in toluene. Both TiO₂ supports were found to adsorb ethylene but there was no activity for acetylene hydrogenation under the reaction condition used. Thus, in order that ethylene hydrogenation could take place on the support, a H₂ spill-over from the metal is needed. From the reaction test, using palladium catalysts supported on the titania synthesized in 1,4-butanediol and toluene not only produced ethylene but also produce ethane. However, more ethane was produced for the one supported on TiO₂ synthesized in toluene than that of 1,4-butanediol supported. TPD study reveals that there was two ethylene adsorption sites probably Ti³⁺ and Ti⁴⁺ on TiO₂ synthesized in toluene supported with one site (Ti³⁺) attributed to ethane formation from hydrogenation of ethylene. These Ti³⁺ sites appeared to be blocked by Ag addition.

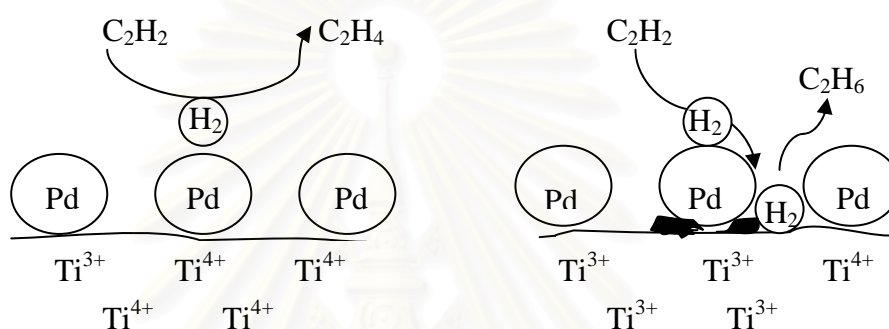
1,4-butanediol

toluene

(A)



(B)



(C)

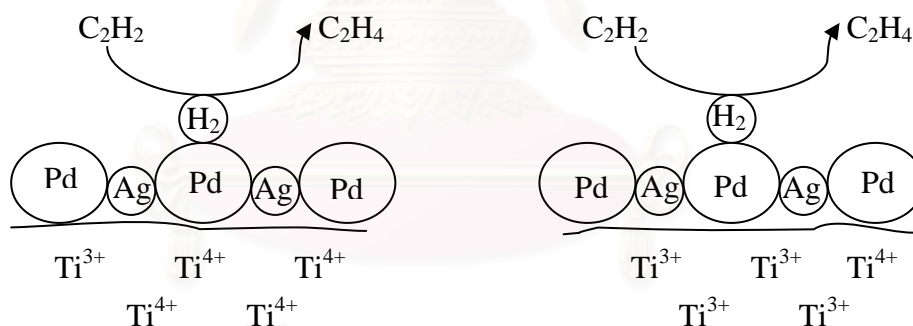


Figure 5.23 The proposal mechanisms of the selective hydrogenation of acetylene to ethylene on (A) TiO_2 , (B) Pd/TiO_2 and (C) $\text{Pd-Ag}/\text{TiO}_2$.

CHAPTER VI

CONCLUSIONS AND RECOMMENDATION

In this chapter, section 6.1 provides the conclusions obtained from the experimental results of the titania supports, the titania supported palladium catalysts, and the silver promoted titania supported palladium catalysts. Additionally, recommendations for further study are given in section 6.2.

6.1 Conclusions

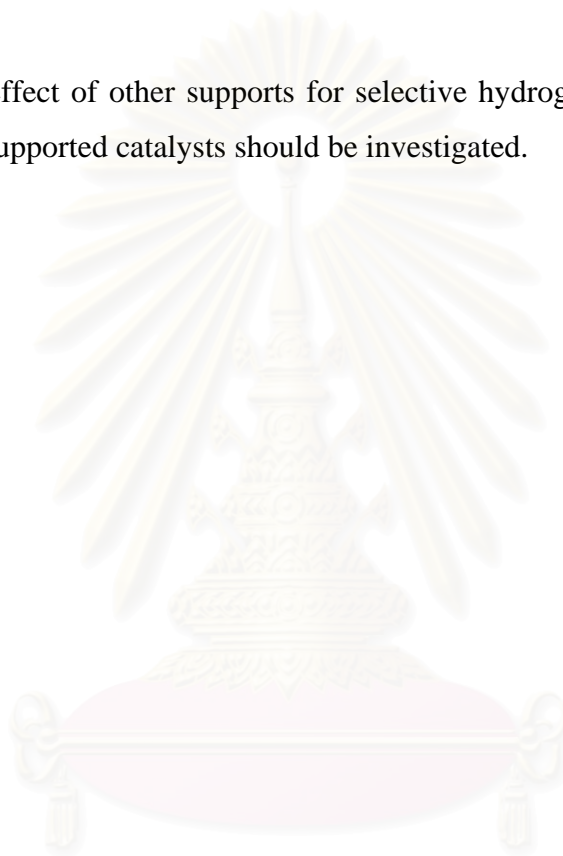
1. Nanocrystalline titania prepared by the solvothermal method using 1,4-butanediol and toluene as the solvents showed only anatase phase with similar crystallite sizes and BET surface areas. However, the titania particles synthesized in toluene possess higher amount of Ti^{3+} defective sites than the one synthesized in 1,4-butanediol.

2. Palladium catalysts supported on titania synthesized in 1,4-butanediol exhibited higher activity and selectivity for selective acetylene hydrogenation than the ones supported on titania synthesized in toluene. The differences in the performances of the catalysts were probably induced by the different ethylene adsorption behaviors as revealed by temperature programmed study.

3. The effect of solvothermal-derived TiO_2 support was not observed for the Ag promoted Pd catalysts. Thus, all the Ti^{3+} sites may be blocked by promotion of Pd/ TiO_2 with Ag metal. In all cases, Ag promoted Pd catalysts showed higher ethylene selectivity than the single metal (Pd) catalysts.

6.2 Recommendation

1. Further study on the titanium defective sites is needed.
2. The effect of pretreatment with oxygen and oxygen-containing compounds on the characteristics and catalytic properties for selective hydrogenation of acetylene over Pd/TiO₂ should be investigated.
3. The effect of other supports for selective hydrogenation of acetylene over Pd and Pd-Ag supported catalysts should be investigated.



สถาบันวิทยบริการ
จุฬาลงกรณ์มหาวิทยาลัย

REFERENCES

- Ali, S. H. and Goodwin, J. G. Jr. SSITKA Investigation of Palladium Precursor and Support Effects on CO Hydrogenation over Supported Pd Catalysts. J. of Catal. **176** (1998): 3–13.
- Al-Ammar, A. S. and Webb, G. Hydrogenation of acetylene over supported metal catalysts Part 2.-Adsorption of [¹⁴C] tracer study of deactivation phenomena. J. Chem. Soc. Faraday. **175** (1978): 657-664.
- Anderson, A. B. and Onwood, D. P. Why carbon monoxide is stable lying down on a negatively charged Ru(001) surface but not on Pt(111). Surface Science Letters **154** (1985): L261-L267.
- Asplund, S. Coke Formation and Its Effect on Internal Mass Transfer and Selectivity in Pd-Catalysed Acetylene Hydrogenation. J. of Catal. **158** (1996): 267-278.
- Boitiaux, J.-P.; Cosyns, J.; Derrien, M. and Leger, G. Newest hydrogenation catalysts. Hydrocarbon Processing (1985): 51-59.
- Bond, G. C; Dowden, D. A. and Mackenzie, N. The selective hydrogenation of acetylene. Trans. Faraday Soc. **54** (1958): 1597-1546.
- Bongkot Ngamsom. Effects of pretreatment with oxygen and oxygen-containing compounds on the catalytic behaviour of Pd-Ag catalyst for the selective hydrogenation of acetylene. Doctor's thesis, Department of Chemical Engineering, Graduated School, Chulalongkorn University, 2002.
- Chou, P. and Vannice, M. A. Calorimetric heat of adsorption measurements on palladium : I. Influence of crystallite size and support on hydrogen adsorption. J. Catal. **104** (1987): 1-16.
- Chu, W.; Chen, M.; Qin, W. and Dai, X. Support effect of palladium catalysts for acetylene hydrogenation to ethylene. Proceeding of the 13th International Congress on Catalysis, Paris, July (2004)
- Cosyns, J. and Boitiaux, J.-P. Process for selective hydrogenating acetylene in a mixture of acetylene and ethylene. US Patent 4,571,442 (Institut Francais du Petrole), 1984

- Dean, J. A. Lange's Handbook of Chemistry. 5 th ed. United State of America: McGraw-Hill, 1999.
- Derrien, M. L. Selective hydrogenation applied to the refining of petrochemical raw materials produced by steam cracking. Stud. Surf. Sci. Catal. 27 (1986):613-666.
- Fujishima, A.; Hashimoto, K. and Watanabe, T., TiO₂ photocatalysis: fundamental and applications. 1 st ed. Tokyo: BKC, 1999.
- Guimon, C.; Auroux, A.; Romero, E. and Monzon A. Acetylene hydrogenation over Ni-Si-Al mixed oxides prepared by sol-gel technique. Appl. Catal. A 251 (2003): 199-214.
- Herrmann, J. M.; Gravelle-Rumeau-Maillot, M. and Gravelle, P. C. A microcalorimetric study of metal-support interaction in the Pt/TiO₂ system. J. Catal. 104 (1987): 136-146.
- Hodnett, B. K. and Delmon, B. Catalytic Hydrogenation (Cerveny, L. ed.), Studies in surface science and catalysis, Elsevier, Amsterdam, 27 (1986):53.
- How, R. F. and Gratzel, M. EPR Observation of Trapped Electrons in Colloidal TiO₂. J. Phys. Chem. 89 (1985): 4495-4499.
- Huang, D. C.; Chang, W. F.; Pong W. F.; Tsang, P.K.; Hung, K. J. and Huang, W. F. Effect of Ag-promotion on Pd catalysts by XANES. Catal. Lett. 53 (1998): 155-159.
- Ikeda, S.; Sugiyama, N.; Murakami, S.; Kominami, H.; Kera, Y.; Noguchi, H.; Uosaki, K.; Torimoto, T. and Ohtani, B. Quantity analysis of defective sites in titanium (IV) oxide photocatalyst powders. Phys. Chem. Chem. Phys. 5 (2003): 778-783.
- Inoue, M.; Kominami, H. and Inui, T. Novel synthetic method for the catalytic use of thermally stable zirconia: thermal decomposition of zirconium alkoxides in organic media. Appl. Catal. A 97 (1993): L25-L30.
- Inoue, M.; Kondo, Y. and Inui, T. An Ethylene Glycol Derivative of Boehmite. Inorg. Chem. 27 (1988): 215-221.
- Iwamoto, S.; Saito, K.; Inoue, M. and Kagawa, K. Preparation of the Xerogels of Nanocrystalline Titanias by the Removal of the Glycol at the Glycothermal Method and Their Enhanced Photocatalytic Activities. Nano. Lett. 1, 8 (2001): 417 – 421.

- Kang, J. H.; Shin, E. W.; Kim, W. J.; Park, J. D. and Moon, S. H., Selective hydrogenation of acetylene on Pd/SiO₂ catalysts promoted with Ti, Nb and Ce oxides. Catal. Today **63** (2000): 183-188.
- Kang, J. H.; Shin, E. W.; Kim, W. J.; Park, J. D. and Moon S. H. Selective Hydrogenation of Acetylene on TiO₂-Added Pd Catalysts. J. Catal. **208** (2002) 310-320.
- Kim, C. S.; Moon, B. K.; Park, J. H.; Chung, S. T. and Son, S. M. Synthesis of nanocrystalline TiO₂ in toluene by a solvothermal route. J. Crystal Growth **254** (2003): 405–410.
- Kim, W. J.; Kang, J. H.; Ahn, I. Y. and Moon, S. H.; Deactivation behavior of a TiO₂-added Pd catalyst in acetylene hydrogenation. J. Catal. **226** (2004): 226-229.
- Kim, W. J.; Kang, J. H.; Ahn, I. Y. and Moon, S. H. Effect of potassium addition on the properties of a TiO₂-modified Pd catalyst for the selective hydrogenation of acetylene. Appl. Catal. A. **268** (2004): 77-82.
- Kim, W. J.; Shin, E. W.; Kang, J. H. and Moon, S. H. Performance of Si-modified Pd catalyst in acetylene hydrogenation: catalyst deactivation behavior. Appl. Catal. A. **251** (2003): 305-313.
- Kominami, H.; Kato, J.-I; Murakami, S.-Y; Kera, Y.; Inoue, M.; Inui, T. and Ohtani B. Synthesis of titanium (IV) oxide of ultra-high photocatalytic activity: high-temperature hydrolysis of titanium alkoxides with water liberated homogeneously from solvent alcohols. J. Mol. Catal.A: Chemical **144** (1999): 165–171.
- Kominami, H.; Kato, J.; Murakami, S.; Ishii, Y.; Kohno, M.; Yabutani, K.; Yamamoto, T.; Kera, Y.; Inoue, M.; Inui, T. and Ohtani, B. Solvothermal syntheses of semiconductor photocatalysts of ultra-high activities. Catal. Today **84** (2003): 181-189.
- Kominami, H.; Kato. J.; Takada, Y.; Doushi, Y. and Ohtani, B. Novel Synthesis of Microcrystalline Titanium (IV) Oxide having High Thermal Stability and Ultra-High Photocatalytic Activity: Thermal Decomposition of Titanium (IV) Alkoxide. Catal. Lett. **46** (1997): 235-240.
- Kominami, H.; Kohno, M.; Takada, Y.; Inoue, M.; Inui, T. and Kera, Y. Hydrothermal of Titanium Alkoxide in Organic Solvent at High

- Temperatures: A New Synthetic Method for Nanosized, Thermally Stable Titanium (IV) Oxide. Ind. Eng. Chem. Res. **38** (1999): 3925-3931.
- Kominami, H.; Murakami, S. Y.; Kohno, M.; Kera, Y.; Okada, K.; and Ohtani, B. Stoichiometric decomposition of water by titanium (IV) oxide photocatalyst synthesized in organic media: Effect of synthesis and irradiation conditions on photocatalytic activity. Phys. Chem. Chem. Phys. **3** (2001): 4102-4106.
- Kongwudthiti, S.; Praserttham, P.; Silveston P. and Inoue M. Influence of synthesis conditions on the preparation of zirconia powder by the glycothermal method. Ceram. Int. **29** (2003): 807-814.
- Lamb, R. N.; Ngamsom, B.; Trimm, D. L.; Gong, B.; Silveston, P. L. and Praserttham, P. Surface characterisation of Pd-Ag/Al₂O₃ catalysts for acetylene hydrogenation using an improved XPS procedure. Appl. Catal. A. **268** (2004): 43-50.
- Lee, D. C.; Kim, H.; Kim, W. J.; Kang, J. H. and Moon, S. H., Selective hydrogenation of 1,3-butadiene on TiO₂-modified Pd/SiO₂ catalysts. Appl. Catal. A. **244** (2003): 83-91.
- Li, Y.; Fan, Y.; Yang, H.; Xu, B.; Feng, L.; Yang, M. and Chen, Y. Strong metal-support interaction and catalytic properties of anatase and rutile supported palladium catalyst Pd/TiO₂. Chem. Phys. Lett. **372** (2003): 160-165.
- Li, Y.; Xu, B.; Fan, Y.; Feng, N.; Qiu, A.; He, J. M. J.; Yang H. and Chen Y. The effect of titania polymorph on the strong metal-support interaction of Pd/TiO₂ catalysts and their application in the liquid phase selective hydrogenation of long chain alkadienes. J. Mol. Catal. A: Chemical **216** (2004): 107-114.
- Mahata, N. and Vishwanathan, V. Influence of Palladium Precursors on Structural Properties and Phenol Hydrogenation Characteristics of Supported Palladium Catalysts. J. of Catal. **196** (2000): 262-270.
- McGown, W. T.; Kemball, C. and Whan, D. A. Hydrogenation of acetylene in excess ethylene on an alumina supported palladium catalyst at atmospheric pressure in a spinning basket reactor. J. Catal. **51** (1978): 173-184.
- Mekasuwandumrong, O.; Silveston, P.L. ; Praserttham, P. ; Inoue, M. ; Pavarajarn, V. and Tanakulrungsank, W. Synthesis of thermally stable micro spherical

- v-alumina by thermal decomposition of aluminum isopropoxide in mineral oil. Inorg. Chem. Commun. **6** (2003): 930–934.
- Molnár, Á.; Sárkány, A.; and Varga, M. Hydrogenation of carbon-carbon multiple bonds: chemo-, region- and stereo-selectivity. J. Mol. Catal. **173** (2001): 185-221.
- Ngamsom, B.; Bogdanchikova, N.; Borja, M. A. and Praserttham P. Characterisations of Pd–Ag/Al₂O₃ catalysts for selective acetylene hydrogenation: effect of pretreatment with NO and N₂O. Catal. Commun. **5** (2004): 243-248
- Othmer, K. Encyclopedia of chemical technology. Vol. 6. 4 th ed. New York: A Wiley-Interscience Publication, John Wiley&Son, 1991.
- Park, H.K.; Kim, D.K. and Kim, C.H. Effect of Solvent on Titania Particle Formation and Morphology in Thermal Hydrolysis of TiCl₄. J. Am. Ceram. Soc. **80**, 3 (1997): 743 – 749.
- Payakgul, W.; Mekasuwandumrong, O.; Pavarajarn, V. and Praserttham, P. Effects of reaction medium on the synthesis of TiO₂ nanocrystals by thermal decomposition of titanium (IV) n-butoxide. Ceram. Int. **31** (2005): 391–397.
- Praserttham P.; Ngamsom B.; Bogdanchikova N.; Phatanasri S. and Pramotthana M., Effect of the pretreatment with oxygen and/or oxygen-containing compounds on the catalytic performance of Pd-Ag/Al₂O₃ for acetylene hydrogenation. Appl. Catal. A. **230** (2002): 41-51.
- Praserttham, P.; Phatanasri, S. and Meksikarin, J. Activation of acetylene selective hydrogenation catalysts using oxygen containing compounds. Catal. Today **63** (2000): 209-213.
- Raupp, G. B. and Dumesic J. A. Effect of varying titania surface coverage on the chemisorptive behavior of nickel. J. Catal. **95** (1985): 587-601.
- Roder, H.; Schuster, R.; Brune, H. and Kern, K. Monolayer-confined mixing at the Ag-Pt (111) interface. Phys. Rev. Lett. **71** (1993): 2086-2089.
- Santos, J.; Phillips, J. and Dumesic, J. A. Metal-support interactions between iron and titania for catalysts prepared by thermal decomposition of iron pentacarbonyl and by impregnation. J. Catal. **81** (1983): 147-167.

- Sárkány, A.; Beck, A.; Horvath, A.; Revay, Zs. and Guzzi L. Acetylene hydrogenation on sol-derived Pd/SiO₂. Appl. Catal. A. 253 (2003): 283-292.
- Sárkány, A.; GuzziAlvin, L. and Weiss, H. On the aging phenomenon in palladium catalysed acetylene hydrogenation. App. Catal. 10 (1984): 369-388.
- Sárkány, A.; Horvath, A. and Beck, A. Hydrogenation of acetylene over low loaded Pd and Pd-Au/SiO₂ catalysts. Appl. Catal. A. 229 (2002): 117-125.
- Shin, E. W.; Choi, C. H.; Chang, K. S.; Na, Y. H. and Moon, S. H. Properties of Si-modified Pd catalyst for selective hydrogenation of acetylene. Catal. Today 44 (1998): 137-143.
- Shin, E. W.; Kang, J. H.; Kim, W. J.; Park, J. D. and Moon, S. H. Performance of Si-modified Pd catalyst in acetylene hydrogenation: the origin of the ethylene selectivity improvement. Appl. Catal. A. 223 (2002): 161-172.
- Sornnarong Theinkeaw. Synthesis of Large-Surface Area Silica Modified Titanium (IV) Oxide Ultra Fine Particles. Master's thesis, Department of Chemical Engineering, Graduated School, Chulalongkorn University, 2000.
- Taylor, G.F.; Thomson, S.J. and Webb, G. The adsorption and retention of hydrocarbons by alumina-supported palladium catalyst. J.Catal.12(1968): 150-156.
- Vannice, M. A.; Wang, S-Y. and Moon, S. H. The effect of SMSI (strong metal-support interaction) behavior on CO adsorption and hydrogenation on Pd catalysts: I. IR spectra of adsorbed CO prior to and during reaction conditions. J. of Catal 71 (1981): 152-166.
- Yang, J.; Mei, S.; Ferreira, M. F. Hydrothermal Synthesis of Nanosized Titania Powders: Influence of Tetraalkyl Ammonium Hydroxides on particle Characteristic. J. Am. Ceram. Soc. 84, 8 (2001): 1696 – 1702.
- Zhang, Q.; Li, J.; Liu, X. and Zhu, Q. Synergetic effect of Pd and Ag dispersed on Al₂O₃ in the selective hydrogenation of acetylene. Appl. Catal. A. 197 (2000): 221-228.



APPENDICES

สถาบันวิทยบริการ
จุฬาลงกรณ์มหาวิทยาลัย

APPENDIX A

CALCULATION FOR CATALYST PREPARATION

Preparation of 1%Pd/TiO₂ with and with promoted Ag catalysts by the incipient wetness impregnation method are shown as follows:

- Reagent:
- Palladium (II) nitrate hexahydrate (Pd (NO₃)₂ · 6H₂O)
Molecular weight = 230.41
 - Silver (III) nitrate (Ag (NO₃))
Molecular weight = 169.87
 - Support: - Titania [TiO₂]

Calculation for the preparation of unpromoted catalyst (1%Pd/TiO₂)

Based on 100 g of catalyst used, the composition of the catalyst will be as follows:

$$\begin{aligned} \text{Palladium} &= 1 \text{ g} \\ \text{Titania} &= 100-1 = 99 \text{ g} \end{aligned}$$

For 2 g of titania

$$\text{Palladium required} = 2 \times (1/99) = 0.02 \text{ g}$$

Palladium 0.02 g was prepared from Pd (NO₃)₂ · 6H₂O and molecular weight of Pd is 106.42

$$\begin{aligned} \text{Pd (NO}_3)_2 \cdot 6\text{H}_2\text{O required} &= \frac{\text{MW of Pd(NO}_3)_2 \cdot 6\text{H}_2\text{O} \times \text{palladium required}}{\text{MW of Pd}} \\ &= (230.41/106.42) \times 0.02 = 0.0437 \text{ g} \end{aligned}$$

Since the pore volume of the titania support is 0.2 ml/g. Thus, the total volume of impregnation solution which must be used is 0.4 ml for titania by the requirement of incipient wetness impregnation method, the de-ionized water is added until equal pore volume for dissolve Palladium (II) nitrate hexahydrate.

Calculation for the preparation of Ag-promoted catalyst (1%Pd-3%Ag/TiO₂)

Based on 100 g of catalyst used, the composition of the catalyst will be as follows:

$$\begin{aligned} \text{Palladium} &= 1 \text{ g} \\ \text{Silver} &= 3 \text{ g} \\ \text{Titania} &= 100-(1+3) = 96 \text{ g} \end{aligned}$$

For 2 g of titania

$$\begin{aligned} \text{Palladium required} &= 2 \times (1/96) = 0.021 \text{ g} \\ \text{Silver required} &= 2 \times (3/96) = 0.063 \text{ g} \end{aligned}$$

Palladium 0.021 g was prepared from Pd (NO₃)₂ · 6H₂O and molecular weight of Pd is 106.42.

$$\begin{aligned} \text{Pd (NO}_3)_2 \cdot 6\text{H}_2\text{O required} &= \frac{\text{MW of Pd (NO}_3)_2 \cdot 6\text{H}_2\text{O} \times \text{palladium required}}{\text{MW of Pd}} \\ &= (230.41/106.42) \times 0.021 = 0.045 \text{ g} \end{aligned}$$

Silver 0.063 g was prepared from (Ag (NO₃)₂) and molecular weight of Ag is 169.87.

$$\begin{aligned} \text{Ag (NO}_3)_3 \text{ required} &= \frac{\text{MW of (Ag (NO}_3)_3) \times \text{silver required}}{\text{MW of Ag}} \\ &= (169.87/107.868) \times 0.063 = 0.098 \text{ g} \end{aligned}$$

Dissolve of palladium (II) nitrate hexahydrate, silver nitrate and volume of de-ionized water like preparation of unpromoted catalyst.

สถาบันวิทยบริการ
จุฬาลงกรณ์มหาวิทยาลัย

APPENDIX B

CALCULATION OF THE CRYSTALLITE SIZE

Calculation of the crystallite size by Debye-Scherrer equation

The crystallite size was calculated from the half-height width of the diffraction peak of XRD pattern using the Debye-Scherrer equation.

From Scherrer equation:

$$D = \frac{K\lambda}{\beta \cos \theta} \quad (\text{B.1})$$

- where
- D = Crystallite size, Å
 - K = Crystallite-shape factor = 0.9
 - λ = X-ray wavelength, 1.5418 Å for CuK α
 - θ = Observed peak angle, degree
 - β = X-ray diffraction broadening, radian

The X-ray diffraction broadening (β) is the pure width of a powder diffraction free of all broadening due to the experimental equipment. Standard α -alumina is used to observe the instrumental broadening since its crystallite size is larger than 2000 Å. The X-ray diffraction broadening (β) can be obtained by using Warren's formula.

From Warren's formula:

$$\beta^2 = B_M^2 - B_S^2 \quad (\text{B.2})$$
$$\beta = \sqrt{B_M^2 - B_S^2}$$

- Where
- B_M = The measured peak width in radians at half peak height.
 - B_S = The corresponding width of a standard material.

Example: Calculation of the crystallite size of titania

$$\begin{aligned} \text{The half-height width of 101 diffraction peak} &= 0.93125^\circ \\ &= 0.01625 \text{ radian} \end{aligned}$$

$$\text{The corresponding half-height width of peak of } \alpha\text{-alumina} = 0.004 \text{ radian}$$

$$\begin{aligned} \text{The pure width} &= \sqrt{B_M^2 - B_S^2} \\ &= \sqrt{0.01625^2 - 0.004^2} \\ &= 0.01577 \text{ radian} \end{aligned}$$

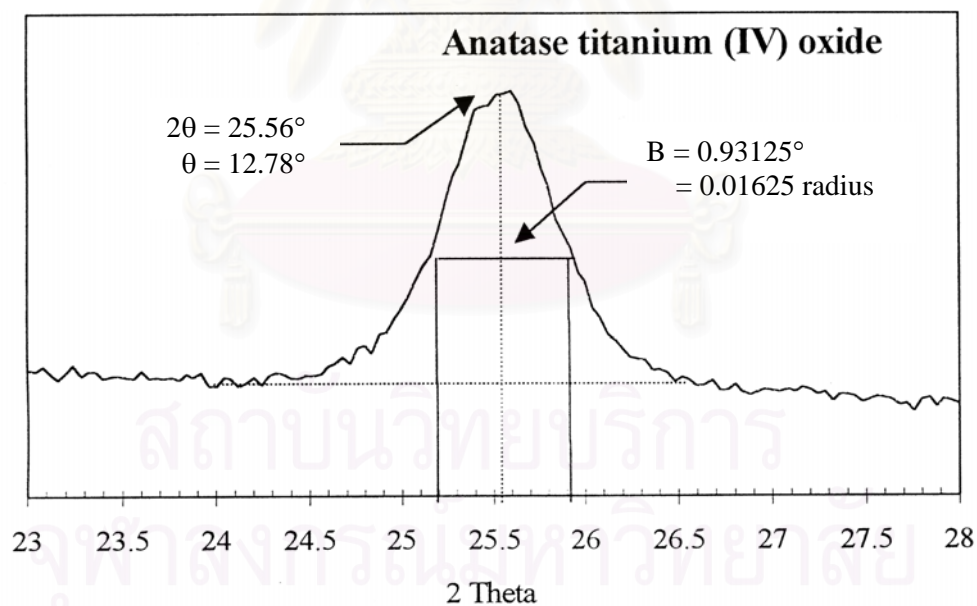
$$B = 0.01577 \text{ radian}$$

$$2\theta = 25.56^\circ$$

$$\theta = 12.78^\circ$$

$$\lambda = 1.5418 \text{ \AA}$$

$$\begin{aligned} \text{The crystallite size} &= \frac{0.9 \times 1.5418}{0.0157 \cos 12.78} = 90.15 \text{ \AA} \\ &= 9 \text{ nm} \end{aligned}$$

**Figure B.1** The 101 diffraction peak of titania for calculation of the crystallite size

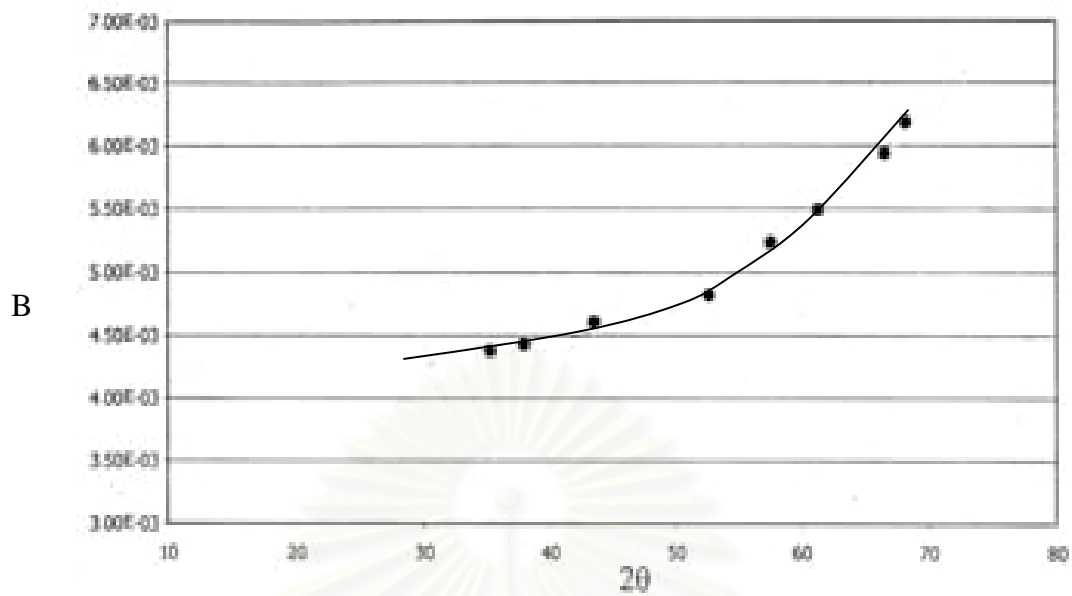


Figure B.2 The plot indicating the value of line broadening due to the equipment. The data were obtained by using α -alumina as standard

สถาบันวิทยบริการ
จุฬาลงกรณ์มหาวิทยาลัย

APPENDIX C

CALCULATION FOR METAL ACTIVE SITES AND DISPERSION

Calculation of the metal active sites and metal dispersion of the catalyst measured by CO adsorption is as follows:

Let the weight of catalyst used	= W	g
Integral area of CO peak after adsorption	= A	unit
Integral area of 50 μ l of standard CO peak	= B	unit
Amounts of CO adsorbed on catalyst	= B-A	unit
Volume of CO adsorbed on catalyst	= $50 \times [(B-A)/B]$	μ l
Volume of 1 mole of CO at 30°C	= 24.86×10^6	μ l
Mole of CO adsorbed on catalyst	= $[(B-A)/B] \times [50/24.86 \times 10^6]$	mole
Molecule of CO adsorbed on catalyst	= $[1.61 \times 10^{-6}] \times [6.02 \times 10^{23}] \times [(B-A)/B]$	molecules
Metal active sites	= $9.68 \times 10^{17} \times [(B-A)/B] \times [1/W]$	molecules of CO/g of catalyst
Molecules of Pd loaded	= $[\% \text{ wt of Pd}] \times [6.02 \times 10^{23}] / [\text{MW of Pd}]$	molecules/g of catalyst
Metal dispersion (%)	= $100 \times [\text{molecules of Pd from CO adsorption} / \text{molecules of Pd loaded}]$	

สถาบันวิทยบริการ
จุฬาลงกรณ์มหาวิทยาลัย

APPENDIX D

CALIBRATION CURVES

This appendix showed the calibration curves for calculation of composition of reactant and products in selective acetylene hydrogenation reaction. The reactant is C_2H_2 and the desired product is ethylene. The other product is ethane.

The thermal conductivity detector, gas chromatography Shimadzu model 8A was used to analyze the concentration of H_2 by using Molecular sieve 5A column.

The carbosieve S-II column is used with a gas chromatography equipped with a flame ionization detector, Shimadzu model 9A, to analyze the concentration of products including of methane, ethane, acetylene and ethylene.

Mole of reagent in y-axis and area reported by gas chromatography in x-axis are exhibited in the curves. The calibration curves of acetylene, ethylene, and hydrogen are illustrated in the following figures.

สถาบันวิทยบริการ
จุฬาลงกรณ์มหาวิทยาลัย

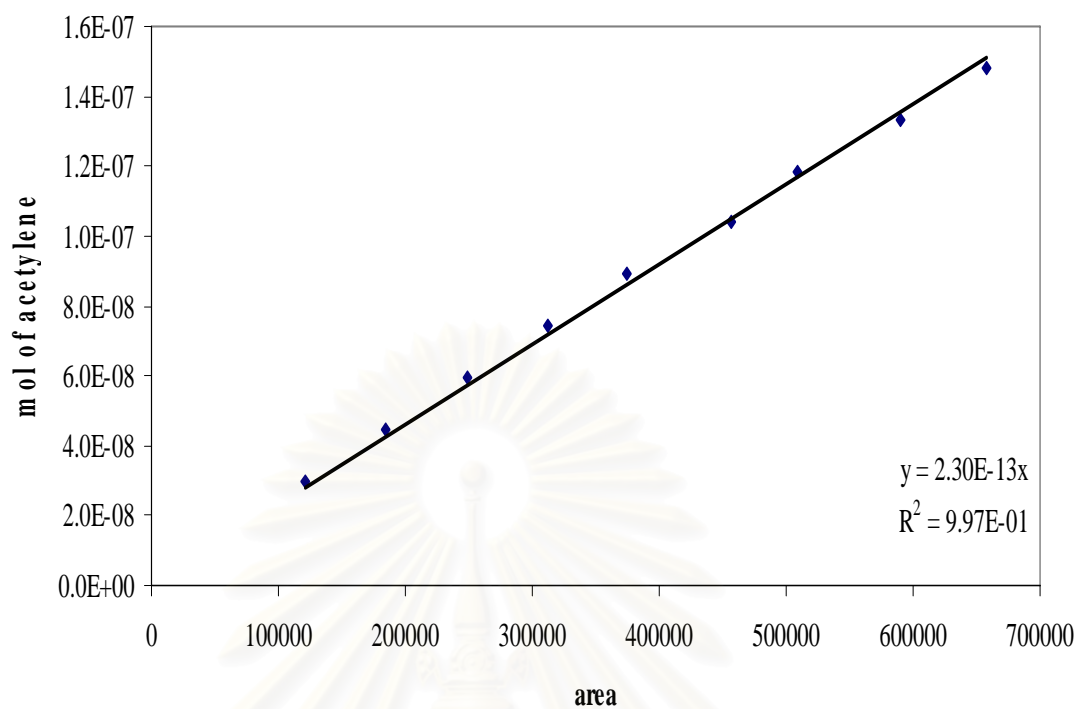


Figure D.1 The calibration curve of acetylene.

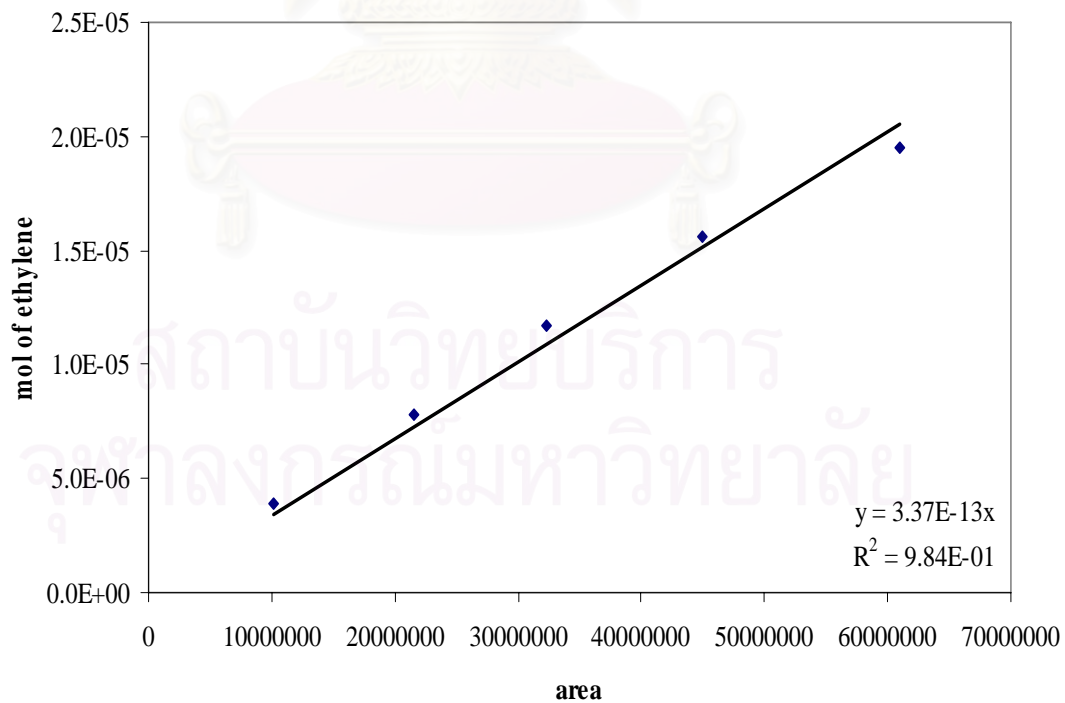


Figure D.2 The calibration curve of ethylene.

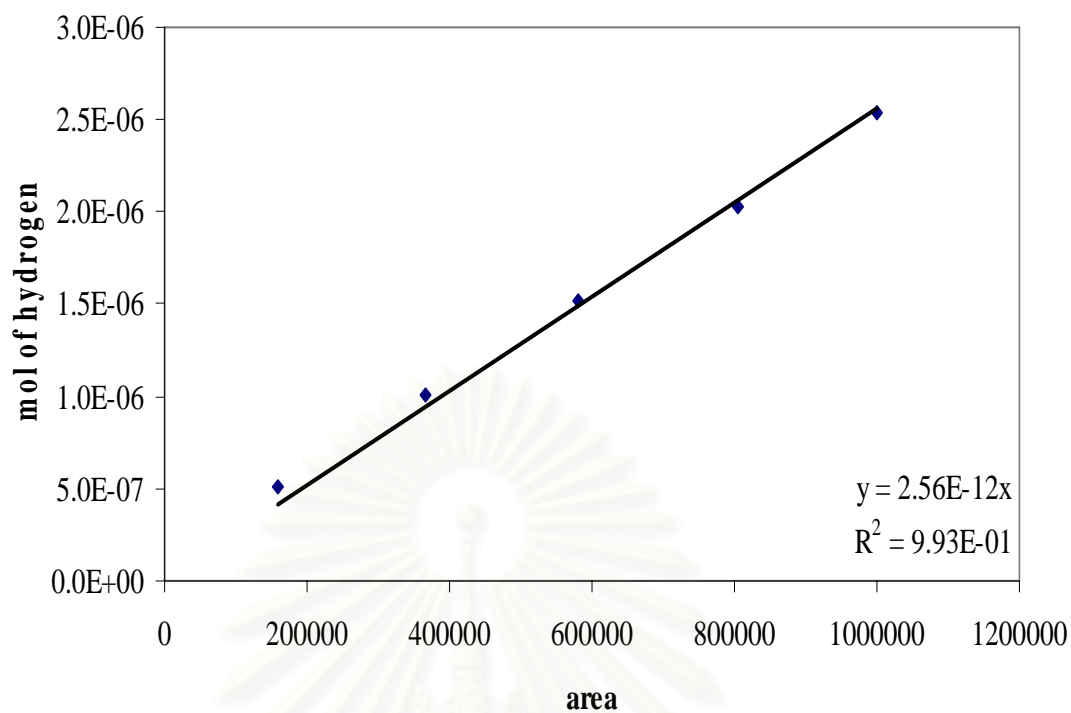


Figure D.3 The calibration curve of hydrogen.

สถาบันวิทยบริการ
จุฬาลงกรณ์มหาวิทยาลัย

APPENDIX E

CALCULATION OF CONVERSION AND SELECTIVITY

The catalyst performance for the selective hydrogenation of acetylene was evaluated in terms of activity for acetylene conversion and selectivity base on the following equation.

Activity of the catalyst performed in term of acetylene conversion is defined as moles of acetylene converted with respect to acetylene in feed:

$$\text{C}_2\text{H}_2 \text{ conversion (\%)} = \frac{100 \times [\text{mole of C}_2\text{H}_2 \text{ in feed} - \text{mole of C}_2\text{H}_2 \text{ in product}]}{\text{mole of C}_2\text{H}_2 \text{ in feed}} \quad (\text{i})$$

where mole of C_2H_2 can be measured employing the calibration curve of C_2H_2 in Figure D.1, Appendix D., i.e.,

$$\text{mole of C}_2\text{H}_2 = (\text{area of C}_2\text{H}_2 \text{ peak from integrator plot on GC-9A}) \times 2.3 \times 10^{-13} \quad (\text{ii})$$

Selectivity of ethylene is defined as moles of ethylene in product with respect to acetylene converted:

$$\text{Selectivity of C}_2\text{H}_4 \text{ (\%)} = 100 \times \frac{\text{mole of C}_2\text{H}_4 \text{ in product}}{\text{mole of C}_2\text{H}_2 \text{ converted}} \quad (\text{iii})$$

where mole of C_2H_4 can be measured employing the calibration curve of C_2H_4 in Figure D.2, Appendix D., i.e.,

$$\text{mole of C}_2\text{H}_4 = (\text{area of C}_2\text{H}_4 \text{ peak from integrator plot on GC-9A}) \times 3.37 \times 10^{-13} \quad (\text{iv})$$

APPENDIX F

LIST OF PUBLICATIONS

1. Nakkararuang, L.; Panpranot, J.; Ngamsom, B. and Praserthdam, P. Selective hydrogenation of acetylene on Pd catalysts supported on solvothermal-derived TiO₂. Proceeding of the Regional Symposium on Chemical Engineering , December 1-3 (2004), Bangkok, Thailand.
2. Panpranot, J.; Nakkararuang, L.; Ngamsom, B. and Praserthdam, P. Synthesis, Characterization, and Catalytic Properties of Pd and Pd-Ag Catalysts Supported on Nanocrystalline TiO₂ Prepared by the Solvothermal Method. Catalysis Letter (2005), in press.



สถาบันวิทยบริการ
จุฬาลงกรณ์มหาวิทยาลัย

**Synthesis, Characterization, and Catalytic Properties of Pd and Pd-Ag Catalysts
Supported on Nanocrystalline TiO₂ Prepared by the Solvothermal Method**

Joongjai Panpranot^{*,1}, Lakkana Nakkararuang¹, Bongkot Ngamsom², and Piyasan
Praserthdam¹

¹Center of Excellence on Catalysis and Catalytic Reaction Engineering
Department of Chemical Engineering, Chulalongkorn University, Bangkok, 10330,
Thailand

²Department of Chemical Engineering, King Mongkut Institute of Technology,
Ladkrabang, Bangkok, Thailand

Submitted to: *Catalysis Letters*

Date: 17 February 2005

Keywords: nanocrystalline titania, solvothermal method, acetylene hydrogenation,
supported Pd catalysts

*To whom correspondence should be addressed.

E-mail: joongjai.p@eng.chula.ac.th, Phone: +66 (02)-218-6859, Fax: +66 (02)-218-6877.

Abstract

Nanocrystalline titania have been prepared by thermal decomposition of titanium (IV) *n*-butoxide in two different solvents (toluene and 1,4-butanediol) at 320°C and employed as supports for Pd and Pd-Ag catalysts for selective acetylene hydrogenation for the first time. The titania products obtained from both solvents were pure anatase phase with relatively the same crystallite sizes and BET surface areas. However, due to different crystallization pathways, the number of Ti³⁺ defective sites as shown by ESR results of the titania prepared in toluene was much higher than the ones prepared in 1,4-butanediol. It was found that the use of anatase titania with higher defective sites as a support for Pd catalysts resulted in lower activity and selectivity in selective acetylene hydrogenation. However, this effect was suppressed by Ag promotion.



สถาบันวิทยบริการ
จุฬาลงกรณ์มหาวิทยาลัย

1. Introduction

The solvothermal method has been used to successfully synthesize various types of nanosized metal oxides with large surface area, high crystallinity, and high thermal stability [1- 7]. For example, thermal decomposition of titanium (IV) *n*-butoxide in organic solvents yields nano-sized pure anatase titania without bothersome procedures such as purification of the reactants or handling in an inert atmosphere. These nanocrystalline titanias have been shown to exhibit high photocatalytic activities [8-9]. However, the thermal stability as well as photocatalytic activity of the solvothermal-derived titania were found to be strongly dependent on the organic solvent used as the reaction medium during crystallization [7]. The titania products synthesized in toluene showed lower thermal stability and lower photocatalytic activities than the ones synthesized in 1,4-butanediol. The authors suggested that the amount of defect structures in the titania prepared by this method was different depending on the solvent used due to the different crystallization pathways.

Due to their unique properties, it is interesting to investigate the characteristics and catalytic properties of the solvothermal-derived nanocrystalline titania supported noble metal as another exploitation of such materials. It is well known that metal catalyst supported on titania exhibits “the strong metal-support interaction” (SMSI) phenomenon after reduction at high temperatures due to the decoration of the metal surface by partially reducible metal oxides [10-11] or by an electron transfer between the support and the metals [12-13]. In selective hydrogenation of acetylene to ethylene on Pd/TiO₂ catalysts, the charge transfer from Ti species to Pd weakened the adsorption strength of ethylene on the Pd surface hence higher ethylene selectivity was obtained [14].

In this study, nanocrystalline titanias were synthesized by the solvothermal method in two different solvents (1,4-butanediol and toluene) and employed as supports for Pd and Pd-Ag catalysts for selective hydrogenation of acetylene for the first time. The physicochemical properties of the titania and the titania supported catalysts were analyzed by means of X-ray diffraction (XRD), N₂ physisorption, scanning electron microscopy (SEM), electron spin resonance (ESR), and CO chemisorption. Moreover, the effect of defective structures in titania on the catalytic performance of the titania supported Pd and Pd-Ag catalysts in acetylene hydrogenation was investigated.

2. Experimental

2.1 Preparation of TiO₂ by the Solvothermal Method

TiO₂ was prepared according to the method described in ref. [7] using 25 g of titanium(IV) *n*-butoxide (TNB) 97% from Aldrich. The starting material was suspended in 100 ml of solvent (1,4-butanediol or toluene) in a test tube and then set up in an autoclave. In the gap between the test tube and autoclave wall, 30 ml of solvent was added. After the autoclave was completely purged with nitrogen, the autoclave was heated to 320°C at 2.5°C/min and held at that temperature for 6 h. Autogenous pressure during the reaction gradually increased as the temperature was raised. After the reaction, the autoclave was cooled to room temperature. The resulting powders were collected after repeated washing with methanol by centrifugation. They were then air-dried at room temperature.

2.2 Preparation of TiO₂ Supported Pd and Pd-Ag Catalysts

1% Pd/TiO₂ were prepared by the incipient wetness impregnation technique using an aqueous solution of the desired amount of Pd(NO₃)₂ (Wako). The catalysts were dried overnight at 110°C and then calcined in N₂ flow 60 cc/min with a heating rate of 10°C/min until the temperature reached 500°C and then in air flow 100 cc/min at 500°C for 2 h. 1%Pd-3%Ag/TiO₂ catalysts were prepared by sequential impregnation of the 1%Pd/TiO₂ with an aqueous solution of Ag(NO₃) (Aldrich) and were calcined using the same calcination procedure as for 1%Pd/TiO₂.

2.3 Catalyst Characterization

The BET surface areas of the samples were determined by N₂ physisorption using a Micromeritics ASAP 2000 automated system. Each sample was degassed under vacuum at < 10 μm Hg in the Micromeritics ASAP 2000 at 150°C for 4 h prior to N₂ physisorption. The XRD spectra of the catalyst samples were measured from 20-80°2θ using a SIEMENS D5000 X-ray diffractometer and Cu K_α radiation with a Ni filter. Electron spin resonance (ESR) spectra were taken at -150°C using a JEOL JES-RE2X spectrometer. Relative percentages of palladium dispersion were determined by pulsing carbon monoxide over the reduced catalyst. Approximately 0.2 g of catalyst was placed in a quartz tube in a temperature-controlled oven. CO adsorption was determined by a thermal conductivity detector (TCD) at the exit. Prior to chemisorption, the catalyst was reduced in a flow of hydrogen (50 cc/min) at room temperature for 2 h. Then the sample was purged at this temperature with helium for 1 h. Carbon monoxide was pulsed at room temperature over the reduced catalyst until the TCD signal from a pulse was constant.

The ethylene-TPD profiles of supported palladium catalysts were obtained by temperature programmed desorption from 35 to 800°C. Approximately 0.05 g of a calcined catalyst was placed in a quartz tube in a temperature-controlled oven and connected to a thermal conductivity detector (TCD). The catalyst was first reduced in H₂ flow 100 cc/min for 1 h at 500°C (using a ramp rate of 10°C/min) and cooled down to room temperature before ramping up again to 70°C in helium flow. The catalyst surface was saturated with ethylene by applying a high purity grade ethylene from the Thai Industrial Gas, Co., Ltd. at 60 ml/min for 3 h. Then the samples were flushed with helium while cooling down to room temperature for about 1 h. The temperature-programmed desorption was performed with a constant heating rate of ca. 10°C/min from 35°C to 800°C. The amount of desorbed ethylene was measured by analyzing the effluent gas with a thermal conductivity detector.

2.4 Selective Hydrogenation of Acetylene

Approximately 0.2 gram of catalyst was packed in a quartz tubular reactor in a temperature-controlled furnace. Prior to reaction, the catalyst was reduced in H₂ at 500°C for 2 h. The reactor was then cooled down to 40°C and the reactant gas composed of C₂H₂/H₂ = 1:2 (2 cc/4 cc) balance with N₂ total flow of 200 ml/min was fed to the reactor to start the reaction. The product samples were taken at 30 min intervals and analyzed by GC.

3. Results and discussion

3.1 Physicochemical properties of the solvothermal-derived TiO₂

Figure 1 shows the XRD patterns of the TiO₂ particles prepared by thermal decomposition of titanium *n*-butoxide in organic solvents. It was found that nanosized anatase titania was produced without any contamination of other phases. The crystallite sizes (*d*) and BET surface areas of the TiO₂ products synthesized in 1,4-butanediol and toluene were found to be essentially the same (*d* = 9-10 nm and BET S.A. 65 m²/g). However, the morphology of the TiO₂ particles was different as shown by SEM micrographs (Figure 2). The products synthesized in toluene agglomerated into spherical micron-sized particles whereas irregular aggregates of nanometer particles were observed for the ones prepared in 1,4-butanediol. The effect of reaction medium on the synthesis of TiO₂ nanocrystals by solvothermal method has recently been reported by Praserttham et al. [7]. It was suggested that anatase titania synthesized in 1,4-butanediol was the result from direct crystallization while titania synthesized in toluene was transformed from precipitated amorphous intermediate.

Due to the different crystallization pathways, degree of crystallinity of the TiO₂ synthesized in 1,4-butanediol and toluene may be different. In this study, the number of defective sites of TiO₂ was determined using electron spin resonance spectroscopy technique and the results are shown in Figure 3. ESR has been shown to be a powerful tool to detect Ti³⁺ species in TiO₂ particles. Such Ti³⁺ species are produced by trapping of electrons at defective sites of TiO₂ and the amount of accumulated electrons may therefore reflect the number of defective sites [15]. The signal of *g* value less than 2 was assigned to Ti³⁺ (3d¹) [16]. Both TiO₂-1,4-butanediol and TiO₂-toluene show Ti³⁺ ESR

signal at $g = 1.9979-1.9980$ with TiO_2 -toluene exhibited much higher intensity. The results clearly show that TiO_2 -toluene possessed more Ti^{3+} defective sites than TiO_2 -1,4-butanediol.

3.2 Characteristics of Pd/TiO₂ and Pd-Ag/TiO₂ catalysts

Table 1 shows the physicochemical properties of the Pd/TiO₂ and Pd-Ag/TiO₂ catalysts. It was found that BET surface areas of the TiO₂ were slightly decreased after impregnation Pd and Pd-Ag suggesting that the metals were deposited in some of the pores of TiO₂. The pulse CO chemisorption technique was based on the assumption that one carbon monoxide molecule adsorbs on one palladium site [17-19]. It was found that Pd/TiO₂-1,4-butanediol exhibited higher amount of CO chemisorption than Pd/TiO₂-toluene. Since both TiO₂ supports possess similar BET surface areas and crystallite sizes, the differences in the amount of active surface Pd were probably induced by the different degrees of crystallinity of the TiO₂ particles.

Addition of Ag to Pd/TiO₂ catalysts resulted in lower amount of active surface Pd. The bimetallic Pd-Ag catalyst has been reported to show many beneficial effects in selective hydrogenation of acetylene to ethylene, for examples, suppression of oligomers formation and improvement of ethylene selectivity [20]. These beneficial effects are due to the altered surface arrangement of Ag atoms on the Pd surface. Roder et al. [21] suggested that Ag atoms are likely to stay at the surface in segregated form with Pd rather than forming an alloy.

3.3 Catalytic performance in selective acetylene hydrogenation

The conversion and selectivity of Pd and Pd-Ag catalysts supported on TiO₂-1,4-butanediol and TiO₂-toluene in selective acetylene hydrogenation as a function of reaction temperature are shown in Figures 4 and 5, respectively. The use of TiO₂-1,4-butanediol as the supports for Pd or Pd-Ag catalysts resulted in higher acetylene conversions than the ones supported on TiO₂-toluene. Acetylene conversion of the single metal catalysts reached 100% at ca. 70°C while those for the bimetallic catalysts showed only 40% (for Pd-Ag/TiO₂-toluene) and 80% (for Pd-Ag/TiO₂-1,4-butanediol) conversions at 90°C. The ethylene selectivity for all the catalysts at the temperature ranges 40-50°C were not significantly difference and were found to be ca. 80-90%. However, at 60-70°C, ethylene selectivity of Pd/TiO₂-1,4-butanediol was much higher than those of Pd/TiO₂-toluene. Ethylene selectivity for the Ag-promoted catalysts were similar for all the reaction temperature used in this study and were higher than those of the non-promoted ones. It was reported that SMSI effect occurs for Pd/TiO₂ catalysts after reduction at high temperature lowering the adsorption strength of ethylene on catalyst surface thus high ethylene selectivity is obtained [10]. Recently, Fan et al. [22] reported that diffusion of Ti³⁺ from the lattice of anatase TiO₂ to surface Pd particle can lower the temperature to induce SMSI. However, in this study we have found that use of TiO₂ with higher concentration of Ti³⁺ as a support for Pd catalyst resulted in lower acetylene conversion and selectivity for ethylene after reduction at 500°C.

The surface active sites of the catalysts were studied by means of the temperature programmed desorption of ethylene from 30-800°C. The results are shown in Figure 6. The TiO₂-toluene support was found to exhibit two main desorption peaks at

ca. 460°C and 680°C while the TiO₂-1,4-butanediol showed only one desorption peak at 680°C. The results suggest that there were two different active sites on the TiO₂-toluene support, probably Ti³⁺ and Ti⁴⁺ sites. The high temperature peak for both TiO₂ supports disappeared after Pd loading as shown in the profiles of the Pd catalysts. However, desorption peak at ca. 460°C was still apparent for Pd/TiO₂-toluene. Since lower ethylene selectivity was found for Pd/TiO₂-toluene than Pd/TiO₂-1,4-butanediol for similar acetylene conversion, this peak can be assigned to the sites for ethylene hydrogenation to ethane. Ethylene hydrogenation is usually believed to take place on the support by means of a hydrogen transfer mechanism [23]. Since only Ti³⁺ species that were in contact with palladium surface promoted SMSI effect [22], ethylene hydrogenation could take place on the Ti³⁺ defective sites that were not in contact with palladium resulting in lower acetylene conversion and selectivity for ethylene as observed in the case of Pd/TiO₂-toluene in this study. The Ag-promoted Pd catalysts exhibited only one ethylene desorption peak at ca. 400°C suggesting that the Pd catalyst surface on both TiO₂ supports was modified by Ag atoms. The presence of Ag probably blocked the sites for ethylene hydrogenation to ethane for both catalysts thus a significant improvement in ethylene selectivity was observed especially for high acetylene conversion at high temperature.

4. Conclusions

Nanocrystalline anatase titania prepared by the solvothermal method were successfully used as supports for Pd and Pd-Ag catalysts for selective hydrogenation of acetylene to ethylene. However, Pd supported on titania synthesized in toluene (higher defective sites) exhibited lower activity and selectivity for selective acetylene hydrogenation than the ones supported on titania synthesized in 1,4-butanediol (lower defective sites). Ethylene hydrogenation probably took place on the Ti^{3+} defective sites that were not in contact with palladium surface. These sites were blocked by promotion of Pd/TiO₂ with Ag metal.

Acknowledgement

The financial supports from the Thailand Japan Technology Transfer Project (TJTTP-JBIC) and the Thailand Research Fund are gratefully acknowledged.

สถาบันวิทยบริการ
จุฬาลงกรณ์มหาวิทยาลัย

Table 1. Characteristics of Pd and Pd-Ag catalysts supported on solvothermal-derived TiO₂ prepared in different solvents

Catalyst	BET S.A. ^a (m ² /g)	CO chemisorption ^b (molecule CO x10 ¹⁸ /g cat.)	%Pd dispersion	d _p Pd ⁰ (nm) ^c
1%Pd/TiO ₂ (1,4-butanediol)	52	5.65	10.0	11.2
1%Pd/TiO ₂ (toluene)	60	4.69	8.3	13.5
1%Pd-3%Ag/TiO ₂ (1,4-butanediol)	42	2.18	3.8	29.1
1%Pd-3%Ag/TiO ₂ (toluene)	47	2.05	3.6	30.9

^aError of measurement = +/- 10 %.

^bError of measurement = +/- 5 %.

^cBased on $d = 1.12/D$ (nm), where D = fractional metal dispersion [17].

สถาบันวิทยบริการ
จุฬาลงกรณ์มหาวิทยาลัย

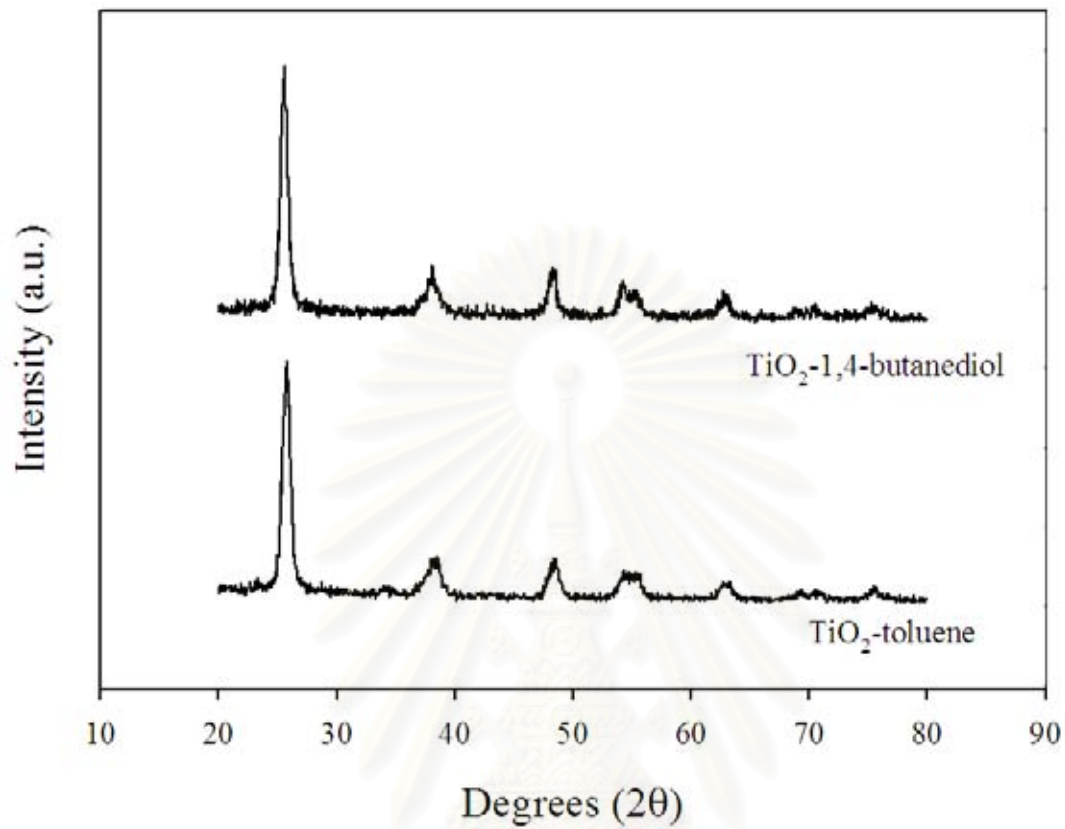
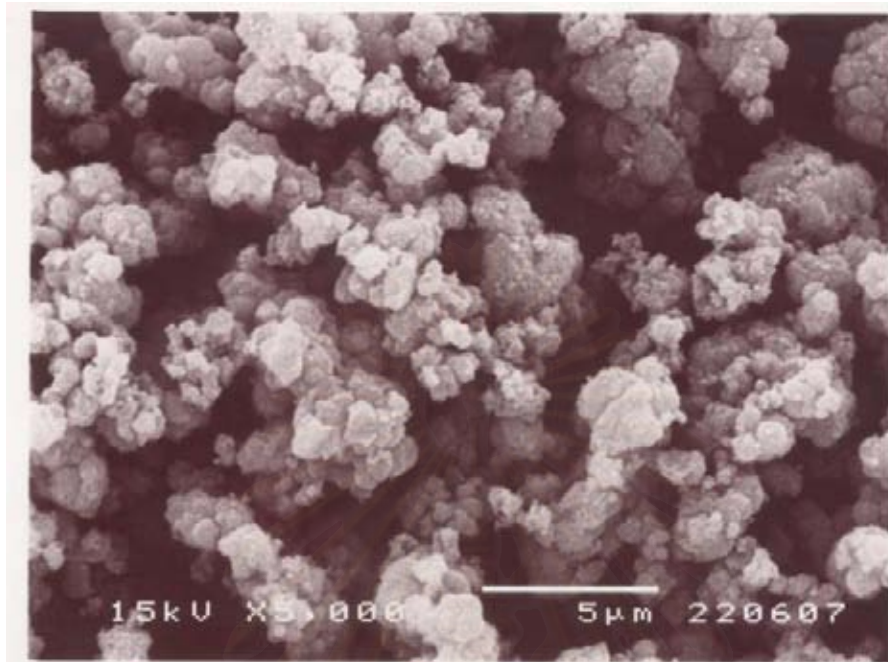
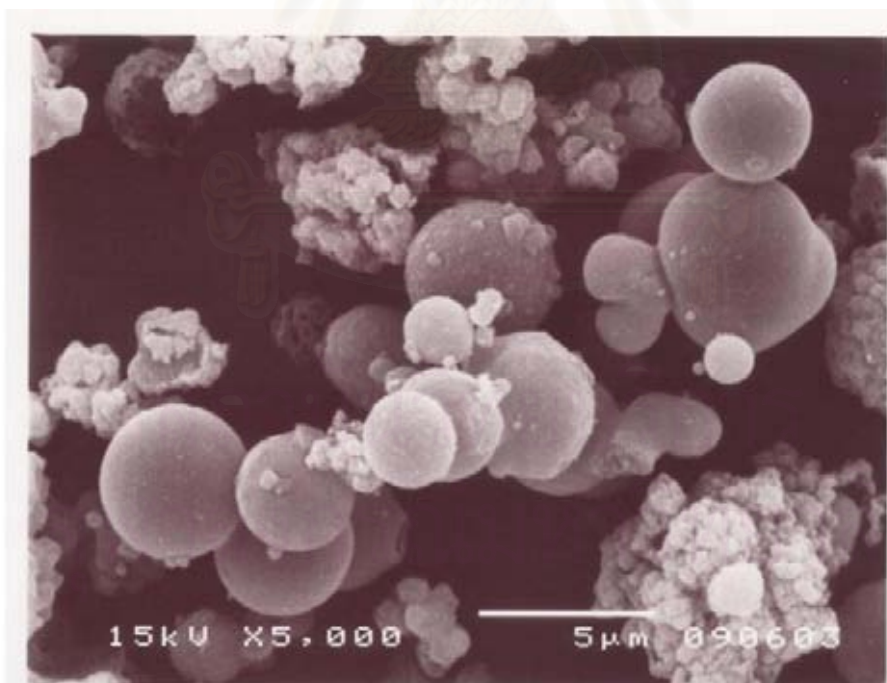


Figure 1. XRD patterns of the solvothermal-derived TiO₂ prepared in two different solvents.

สถาบันวิทยบริการ
จุฬาลงกรณ์มหาวิทยาลัย

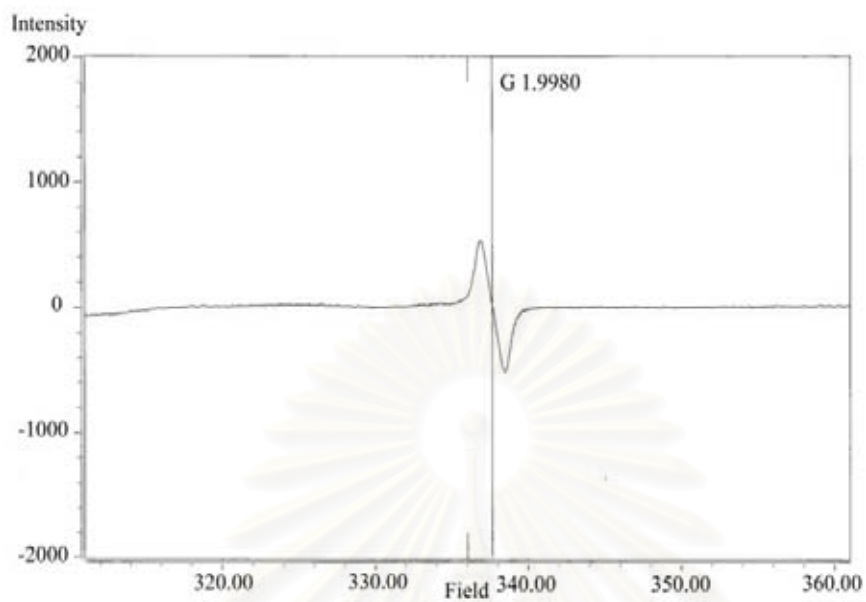


(a)

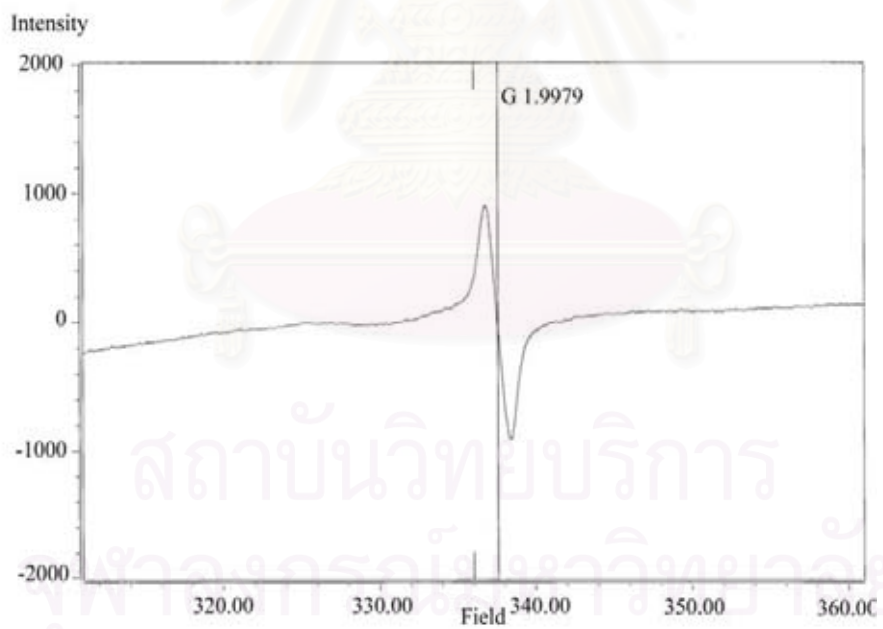


(b)

Figure 2. SEM micrographs of (a) TiO₂-1,4-butanediol and (b) TiO₂-toluene



(a)



(b)

Figure 3. ESR results of (a) TiO_2 -1,4-butanediol and (b) TiO_2 -toluene

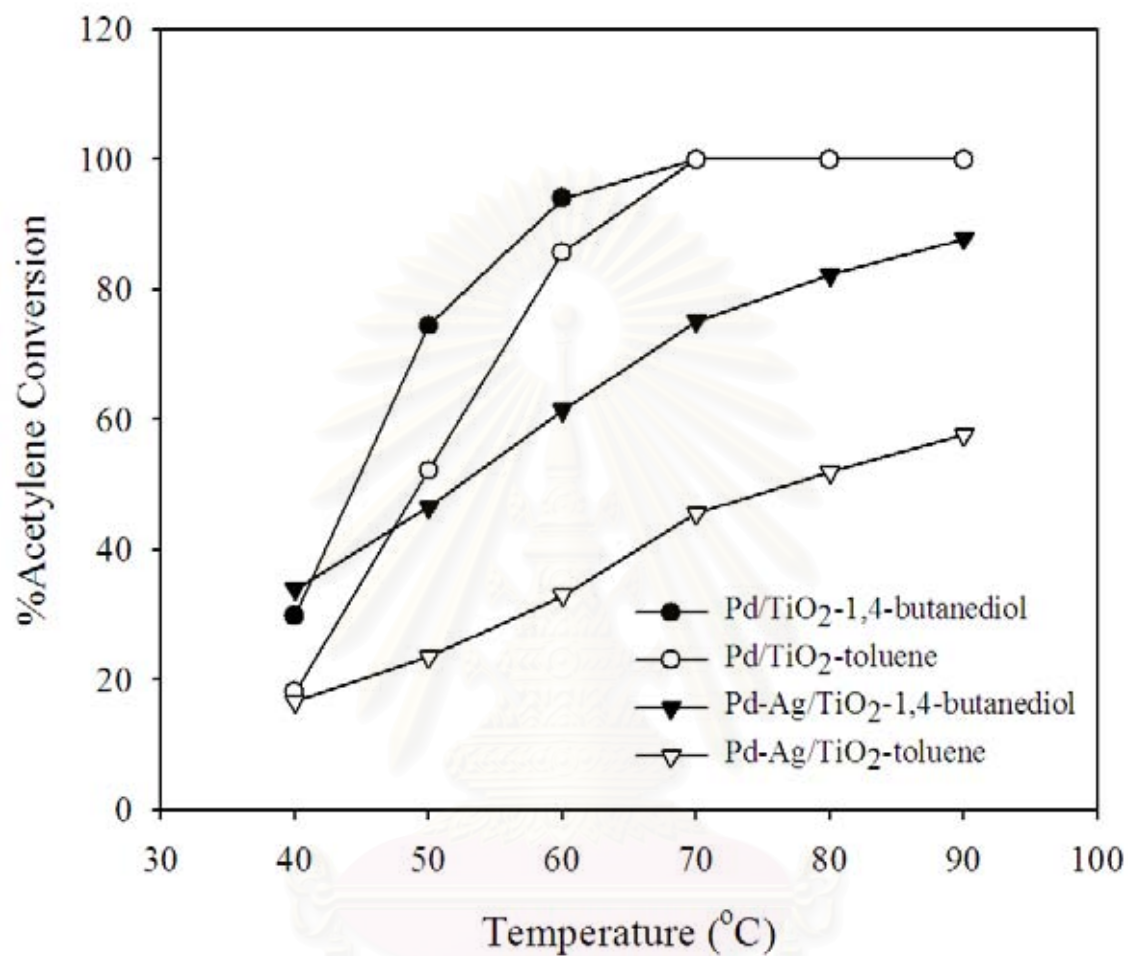


Figure 4. Acetylene conversion as a function of temperature for various TiO₂ supported catalysts

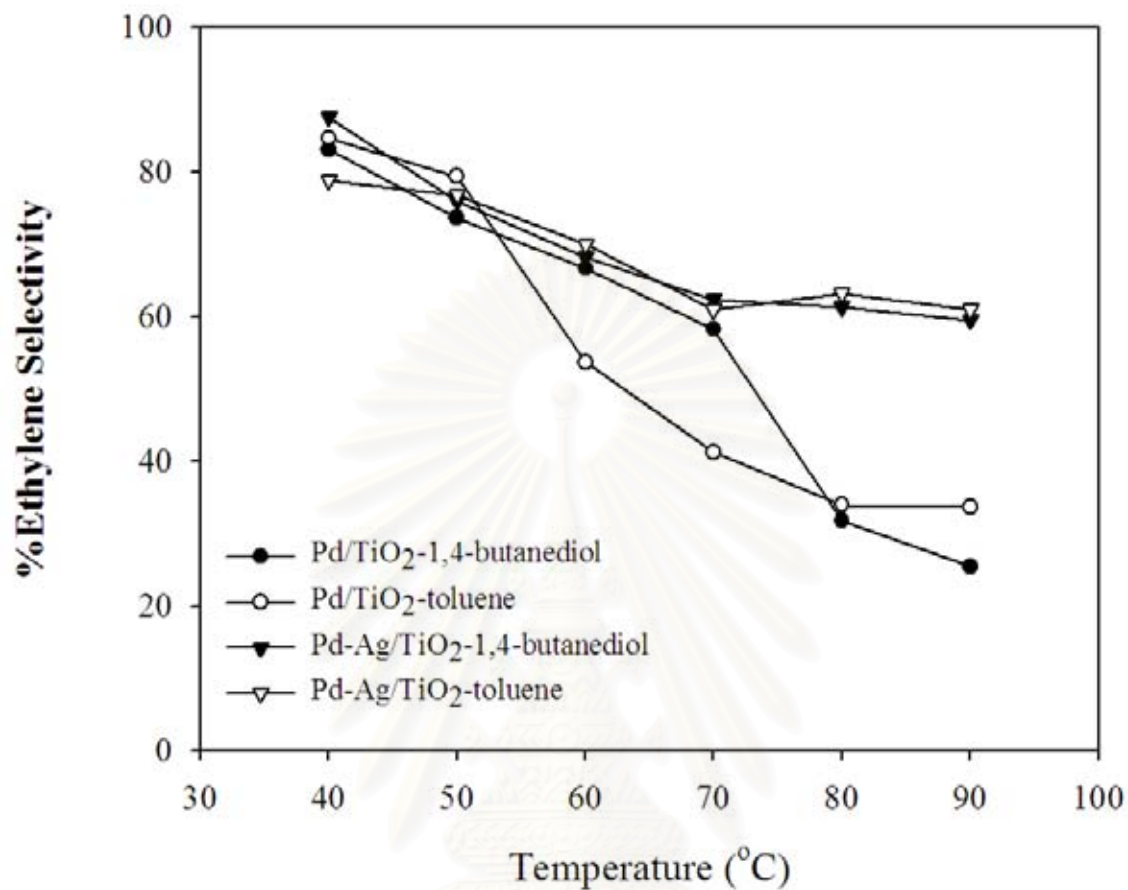


Figure 5. Ethylene selectivity as a function of temperature for various TiO₂ supported catalysts

สถาบันวิทยบริการ
จุฬาลงกรณ์มหาวิทยาลัย

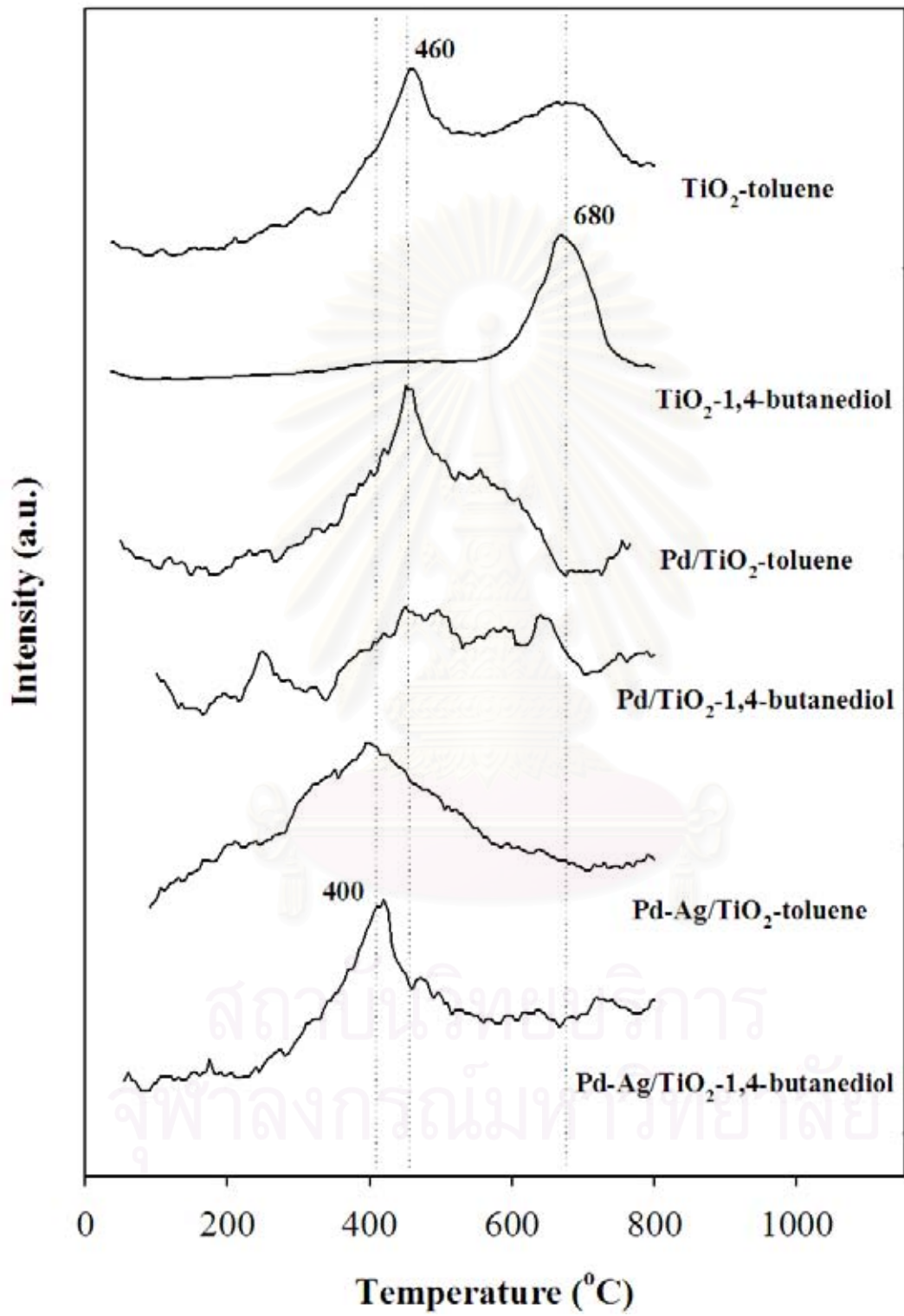


Figure 6. Ethylene-TPD results

Reference

- [1] M. Inoue, Y. Kondo, T. Inui, *Inorg. Chem.* 27 (1988) 215.
- [2] M. Inoue, H. Kominami, T. Inui, *J. Am. Ceram. Soc.* 75 (1992) 2597.
- [3] M. Inoue, H. Kominami, T. Inui, *Appl. Catal. A* 97 (1993) 125.
- [4] H. Kominami, J.-I. Kato, S.-Y. Murakami, Y. Kera, M. Inoue, T. Inui, B. Ohtani, J. *Mol. Catal. A* 144 (1999) 165.
- [5] S. Kongwudthiti, P. Praserthdam, P. L. Silveston, M. Inoue, *Ceram. Int.* 29 (2003) 807.
- [6] O. Mekasuwandumrong, P. L. Silveston, P. Praserthdam, M. Inoue, V. Pavrajarn, W. Tanakulrungsank, *Inorg. Chem. Commun.* 6 (2003) 930.
- [7] W. Payakgul, O. Mekasuwandumrong, V. Pavrajarn, P. Praserthdam, *Ceram. Int.* (2004) in press.
- [8] H. Kominami, S.-Y. Murakami, M. Kohno, Y. Kera, K. Okada, B. Ohtani, *Phys. Chem. Chem. Phys.* 3 (2001) 4102.
- [9] B. Ohtani, K. Tennon, S.-I. Nishimoto, T. Inui, *J. Photosci.* 2 (1995) 7.
- [10] J. Santos, J. Phillips, J. A. Dumesic *J. Catal.* 81 (1983) 147.
- [11] G. B. Raupp, J. A. Dumesic *J. Catal.* 95 (1985) 587.
- [12] J. M. Herrmann, M. Gravelle-Rumeau-Maillot, P. C. Gravelle *J. Catal.* 104 (1987) 136.
- [13] P. Chou, M. A. Vannice *J. Catal.* 104 (1987) 1.
- [14] J. H. Kang, E. W. Shin, W. J. Kim, J. D. Park, S. H. Moon, *J. Catal.* 208 (2002) 310.
- [15] S. Ikeda, N. Sugiyama, S. Murakami, H. Kominami, Y. Kera, H. Noguchi, K.

Uosaki, T. Torimoto, B. Ohtani, *Phys. Chem. Chem. Phys.* 5 (2003) 778.

[16] T. M. Salama, H. Hattori, H. Kita, K. Ebitani, T. Tanaka, *J. Chem. Soc. Faraday Trans.* 89 (1993) 2067.

[17] N. Mahata, V. Vishwanathan, *J. Catal.* 196 (2000) 262.

[18] S. H. Ali, J. G. Goodwin, Jr., *J. Catal.* 176 (1998) 3.

[19] E. A. Sales, G. Bugli, A. Ensuque, M.J. Mendes, F. Bozon-Verduraz, *Phys. Chem. Chem. Phys.* 1 (1999) 491.

[20] D. C. Huang, K. H. Chang, W. F. Pong, P. K. Tseng, K. J. Hung, W. F. Huang, *Catal. Lett.* 53 (1998) 155.

[21] H. Roder, R. Schuster, H. Brune, K. Kern, *Phys. Rev. Lett.* 71 (1993) 2086.

[22] Y. Li, B. Xu, Y. Fan, N. Feng, A. Qiu, J. Miao, J. He, H. Yang, Y. Chen *J. Mol. Catal. A* 216 (2004) 107.

[23] S. Aplund, *J. Catal.* 158 (1996) 267.

สถาบันวิทยบริการ
จุฬาลงกรณ์มหาวิทยาลัย

VITA

Miss Lakkana Nakkharuang was born in July 2nd, 1980 in Songkhla, Thailand. She finished high school from Hadyaiwittayalai School, Songkhal in 1999, and received bachelor's degree in Chemical Engineering from the department of Chemical Engineering, Faculty of Engineering, King Mongkut's Institute of Technology Ladkrabang, Bangkok, Thailand in March 2003. She continued her Master study in the same major at Chulalongkorn University, Bangkok, Thailand in June 2003.



สถาบันวิทยบริการ
จุฬาลงกรณ์มหาวิทยาลัย